AN ABSTRACT OF THE THESIS OF

Sean P. Conway for the degree of Master of Science in Environmental Engineering presented on June 7, 2022.

Title: Aerobic Cometabolism of 1,4-Dioxane and *cis*-Dichloroethylene by Gellan Gum and Polyvinyl Alcohol/Sodium Alginate Hydrogel Beads Co-Encapsulated with *Rhodococcus rhodochrous* Strain ATCC 21198 and Slow-Release Growth Substrates: Batch, Column, and Toxicity Studies.

Abstract approved:

_____

Lewis Semprini

1,4-Dioxane (dioxane) and *cis*-dichloroethylene (*c*DCE) are compounds commonly found in industrial cleaning and degreasing agents that are frequently present as groundwater contaminants. In an effort to develop a more effective treatment method for these compounds, hydrogel beads were fabricated with either gellan gum or a combination of polyvinyl alcohol (PVA) and sodium alginate (SA) co-encapsulated with *Rhodococcus rhodochrous* Strain ATCC 21198 (21198) and a slow-release growth substrate (SRS). The hydrogel beads were investigated in batch reactors and column systems to determine the long-term ability of these beads to successfully transform dioxane and *c*DCE through aerobic cometabolism. Tetra-butylorthosilicate (TBOS) and tetra-s-butylorthosilicate (T2BOS) were used to slowly release 1-butanol and 2-butanol, respectively, as growth substrates for 21198.

The batch reactor studies conducted using gellan gum hydrogel beads co-encapsulated with 21198 and either TBOS or T2BOS demonstrated an ability to

transform essentially all (>99%) of the added dioxane at a range of ~250-1000 µg/L and the added *c*DCE at ~250 µg/L throughout several additions. The beads containing TBOS showed significantly faster rates of transformation for both contaminants. An embryonic zebrafish toxicity study completed using the TBOS gellan gum beads showed no significant toxicity was generated after the complete transformation of *c*DCE.

A column study was completed by packing a glass column with gellan gum beads co-encapsulated with 21198 and T2BOS. The influent media was composed of 10x diluted phosphate buffer mineral salt media (MSM) and added contaminants. Hydrogen peroxide (H_2O_2) was added to the influent media at concentrations of 25-100 mg/L to meet oxygen demands. The column had a hydraulic retention time (HRT) of 26 hours. This column initially demonstrated the ability to transform essentially all (>99%) influent *c*DCE (~300 µg/L) from 52 to 75 pore volumes (PV), while showing no evidence of transforming influent dioxane (~200 µg/L). A high-flow study was completed in which the influent flow rate was increased from 1 mL/hr to 90 mL/hr. This study provided evidence that cometabolism of *c*DCE was occurring due to the presence of *c*DCE epoxide in the effluent, but it also exposed the entire bead pack to the epoxide. This epoxide likely damaged the health of the column, and the column was unable to recover from this high-flow transient test and a subsequent stop-flow study. This was evidenced by a decrease in *c*DCE transformation. By the end of the column's operation at 118 PV, a mass balance determined that a total of 71.5% of the influent *c*DCE was transformed. However, none of the influent dioxane was transformed.

A column study was also completed by packing a glass column with side sampling ports with PVA/SA beads co-encapsulated with 21198 and TBOS. The influent media was made using a synthetic groundwater formulation and 200x diluted phosphate buffer MSM for additional nutrients. H_2O_2 was added at increasing concentrations (50-250 mg/L) over the operating period to meet oxygen demands. The influent pH was increased from 7.0 to 7.5 to 7.9 during the operating period in an effort to lower the rate of TBOS hydrolysis to 1-butanol. The column initially had an HRT of 28 hours from 0 to 7 PV. The flow rate was then doubled and the column had an HRT of 14 hours for the final 90 PV. The column demonstrated the ability to transform >95% of influent *c*DCE (~200 µg/L) when the influent media contained 250 mg/L H_2O_2 and was at a pH of 7.5. Side port sampling showed the presence of *c*DCE epoxide throughout the column, signifying the aerobic cometabolism of *c*DCE. There was evidence that nearly all of the transformation occurred directly at the influent end of the column. A visual orange tint, representing significant 21198 biostimulation in the bead, was evident mainly in that end of the column. By the end of the column's operating period, samples from the lower side sampling port located near the influent also measured nearly equal in *c*DCE concentration to the column effluent, indicating that the majority of cometabolic transformation was occurring where visual biomass growth was observed. 1-butanol remained >50 mg/L in the effluent throughout the column's operating period, indicating biostimulation did not occur throughout the column. Embryonic zebrafish toxicity studies demonstrated that the column effluent was significantly toxic when 1-butanol levels were ~120 mg/L and not significantly toxic when ~60 mg/L, suggesting that 1-butanol was the source

of toxicity. More detailed studies are needed to establish factors causing the observed toxicity in the column effluent.

Aerobic Cometabolism of 1,4-Dioxane and *cis*-Dichloroethylene by Gellan Gum and Polyvinyl Alcohol/Sodium Alginate Hydrogel Beads Co-Encapsulated with *Rhodococcus rhodochrous* Strain ATCC 21198 and Slow-Release Growth Substrates: Batch, Column, and Toxicity Studies

by
Sean P. Conway

A THESIS

submitted to

Oregon State University

in partial fulfillment of
the requirements for the
degree of

Master of Science

Presented June 7, 2022
Commencement June 2023

Master of Science thesis of Sean P. Conway presented on June 7, 2022

APPROVED:

Major Professor, representing Environmental Engineering

Head of the Department of Chemical, Biological, and Environmental Engineering

Dean of the Graduate School

I understand that my thesis will become part of the permanent collection of Oregon State University libraries. My signature below authorizes release of my thesis to any reader upon request.

Sean P. Conway, Author

ACKNOWLEDGEMENTS

I would like to start out by thanking Dr. Lew Semprini and Dr. Mohammad Azizian for their guidance and assistance throughout this past year and a half. Lew, thank you for allowing me to enter your research group and being so encouraging when there were bumps in the road. Thank you as well for working with me and the graduate school to ensure I was funded. Mohammad, thank you for constant assistance in the analytical room. It would not be possible to do the research that we do without your knowledge and willingness to help us out.

I would also like to thank the other members of the Semprini group, Hannah, Alisa, Juliana, Conor, and Jacob, for your mentorship and friendship. Hannah and Alisa especially, thank you for your guidance when I first joined the lab. I know I asked way too many questions, but you were always willing to answer them. Thank you as well to those who trained me on different instruments and methods. Conor, thank you for all the work you put in developing beads for me to use. Jacob, Clint, Derek, and the rest of my CBEE friends, thank you for making these past couple years a lot more fun.

Lastly, I would like to thank my parents and brother, Eileen, Neal, and Ryan, for supporting me these last two years. Moving across the country given the circumstances was not easy, but I knew I could always call you when I needed. Your encouragement was greatly appreciated throughout this whole process.

This research was funded in part by the National Institute of Environmental Health Sciences (grant P0527A) and in part by Oregon State University's Environmental Health Sciences Center (grant P0508P).

TABLE OF CONTENTS

LIST OF FIGURES

Figure Page

LIST OF FIGURES (Continued)

LIST OF FIGURES (Continued)

LIST OF FIGURES (Continued)

LIST OF TABLES

LIST OF TABLES (Continued)

LIST OF APPENDICES

LIST OF APPENDIX FIGURES

Figure Page

ABBREVIATIONS

1,1,1-TCA	1,1,1-Trichloroethane
21198	*Rhodococcus rhodochrous* strain ATCC 21198
*c*DCE	cis-Dichloroethylene
COC	Contaminant of Concern
DI	Deionized
Dioxane	1,4-Dioxane
DO	Dissolved Oxygen
EC50	Half Maximal Effective Concentration
ECD	Electron Capture Detector
EDTA	Ethylenediaminetetraacetic Acid
FID	Flame Ionization Detector
GC	Gas Chromatograph
H_2O_2	Hydrogen Peroxide
hpf	Hours Post Fertilization
IC	Ion Chromatograph
m/z	Mass-to-Charge
MS	Mass Selective Detector
MSM	Mineral Salt Media
N_2	Nitrogen
O_2	Oxygen
ORC	Oxygen Releasing Compound
PCE	Perchloroethylene
PRB	Permeable Reactive Barrier
PTFE	Polytetrafluoroethylene
PV	Pore Volumes
PVA	Polyvinyl Alcohol
rcf	Relative Centrifugal Force
rpm	Revolutions Per Minute
SA	Sodium Alginate
SRS	Slow-Release Substrate
T2BOS	Tetra-s-butyl orthosilicate
TBOS	Tetrabutyl orthosilicate
TCD	Thermal Conductivity Detector
TCE	Trichloroethylene
TSGA	Tryptic Soy Glucose Agar
TSS	Total Suspended Solids
v/v	Volume Per Volume
VC	Vinyl Chloride
VOA	Volatile Organic Analysis
w/v	Weight Per Volume

CHAPTER 1 – INTRODUCTION

Contamination of the subsurface, especially groundwater, is a global issue that is currently being addressed through a variety of methods. The pathways these contaminants follow to enter the environment often include industrial spills or accidents that occur during transport, waste site leaks, or direct releases from facilities.[1] Chlorinated ethenes are some of the most common and widespread contaminants, with compounds such as trichloroethylene (TCE) and cis-dichloroethylene (*c*DCE) being released due to being contained within cleaning solvents used in degreasing and dry-cleaning.[2] As it is commonly used as a stabilizer for these chlorinated solvents, 1,4-dioxane (dioxane) is often a co-contaminant in the environment.[3] *c*DCE is considered hazardous in large part due to its tendency to degrade into vinyl chloride, which is highly toxic.[4] Dioxane is classified as a probable human carcinogen.[5] For these reasons, determining methods for treatment of these compounds that are effective and affordable is necessary.

Environmental remediation involves the treatment or removal of contaminants such as these from the environment. This is a field that has been around for decades, and there are a variety of remediation techniques that have shown success. Success of a remediation technique depends largely on the subsurface conditions, and some remediation projects can take many years to reach contaminant levels below the acceptable concentration limits. A non-exhaustive list of treatment technologies includes air sparging, bioremediation, chemical reduction, chemical oxidation, permeable reactive barriers, phytotechnology, soil vapor extraction, and thermal treatment.[6]

Bioremediation and permeable reactive barriers (PRBs) are most relevant to this thesis. Bioremediation is the process of degrading contaminants through biological methods, usually

through the use of microorganisms.[7] Generally this involves stimulating microorganisms already present in the subsurface by the addition of nutrients, electron acceptors, or oxygen. Certain microorganisms possess the ability to reduce contaminants. Previous studies have shown that *Rhodococcus rhodochrous* strain ATCC 21198 is able to biologically transform contaminants including *c*DCE and dioxane.[8,9] As part of an endeavor to determine additional technologies for environmental remediation, the use of PRBs constructed from entrapped microorganisms is at the center of this study. PRBs are barriers of reactive media that are able to passively transform contaminants that pass through, which should be possible using these entrapped microorganisms.[10] One method of entrapping microorganisms is to use hydrogel beads fabricated from compounds such as gellan gum or sodium alginate. Earlier work provided evidence of beads with encapsulated microorganisms being effective in contaminant transformation via the process of cometabolism.[11] These beads were made of gellan gum, and the fundamental component was a slow-release substrate (SRS), in this case tetrabutyl orthosilicate (TBOS) and tetra-s-butyl orthosilicate (T2BOS). These compounds hydrolyzed over time to release 1-butanol and 2-butanol, respectively. These studies were conducted using batch reactors.

The goal for this study was to investigate the possibility of these beads as an *in situ* remediation technique. The goals for this study involved verifying the contaminant transformation efficacy of these beads in batch systems and measuring potential toxicity generated through their use. Other goals included testing these beads in column settings to simulate permeable reactive barriers and investigating the potential of beads made with a different formulation.

The objectives created to meet these goals were as follows:

1. Assess the long-term contaminant transformation efficacy of *Rhodococcus rhodochrous* strain ATCC 21198 co-encapsulated with SRSs in gellan gum beads in batch and column systems.
2. Determine rates for contaminant transformation and oxygen consumption in batch systems to be able to more effectively compare SRSs.
3. Assess the long-term contaminant transformation efficacy of *Rhodococcus rhodochrous* strain ATCC 21198 co-encapsulated with SRSs in polyvinyl alcohol/sodium alginate beads in a column system.
4. Measure potential toxicity generated through bead use and contaminant transformation by conducting embryonic zebrafish toxicity tests.
5. Determine long-term bead durability through qualitative and quantitative tests.

CHAPTER 2 – LITERATURE REVIEW

2.1 Contaminants

There are a wide variety of contaminants that have made their way into the soil, groundwater, surface water, and air. These contaminants commonly enter the environment through industrial spills or accidents that occur during transport, waste site leaks, and direct releases from facilities.[1] Other contaminant sources include industrial and municipal wastewater treatment plants as well as agricultural sources such as livestock and crop production.[12] In many cases, previously ignored or underestimated chemical compounds have moved to the forefront of contaminant remediation following discoveries made from years of studies. These are termed contaminants of emerging concern and include chemicals from pharmaceuticals, personal care products, nanomaterials, microplastics, non-stick surfaces, and firefighting foam.[13–15]

The contaminants most relevant to the scope of this thesis are *c*DCE and dioxane. *c*DCE is a pertinent contaminant of concern (COC) because it is produced as part of the anaerobic degradation pathway of perchloroethylene (PCE) and TCE. PCE and TCE are two of the most common contaminants found in the environment. These contaminants are regularly contained within cleaning solvents used for degreasing, dry-cleaning, and semiconductor production.[2] As such, PCE and TCE are frequently present in the subsurface of both industrial and commercial zones. PCE is transformed to TCE and subsequently *c*DCE through reductive dechlorination.[16] In reductive dechlorination, a chlorine atom is replaced with a hydrogen atom in the molecule. Bacteria conducting this process use chlorinated compound as an electron acceptor in respiration.[17] These same anaerobic conditions may then also lead to the transformation of *c*DCE into vinyl chloride (VC) and eventually ethene.[16] These final two steps are typically the slowest

in the process, potentially leading to sites that have a buildup of *c*DCE and VC. It is important that complete transformation of the contaminants occurs, because VC is a known carcinogen.[4]

Alternatively, aerobic cometabolism has been shown to be the key process for transforming many contaminants in the environment. In aerobic cometabolism, enzymes in microorganisms transform contaminants despite these compounds not being used as carbon or energy sources.[18] Because of this, the presence of a growth substrate is necessary to grow cells and provide an energy source. The aerobic biodegradation of cDCE and its epoxide is attributed to aerobic cometabolism by a class of enzymes known as monooxygenases. Monooxygenases are a class of enzymes that catalyze the insertion of oxygen atoms in place of atoms like hydrogen.[19] The *c*DCE epoxide is produced when an oxygen is inserted across the double bond of *c*DCE. Oxygen is consumed for these reactions to take place, so oxygen demand can be significant. Methane and butane monooxygenases have previously been shown to transform *c*DCE and *c*DCE epoxide through this oxidative dechlorination reaction.[20,21] It is likely that the same monooxygenase enzyme is responsible for the transformation of both *c*DCE and *c*DCE epoxide. Chlorinated ethenes like *c*DCE produce epoxides when transformed with this process.[21,22] *c*DCE epoxide has a 72-hour half-life in aqueous solutions. Disappearance of this epoxide at a faster rate can potentially be ascribed to biotic transformation.[23] The *c*DCE transformation process can cause significant toxicity to the cells conducting it due to the production of the previously mentioned epoxide.[20] One of the issues with the transformation of chlorinated ethenes is that the original chlorinated ethenes may not be toxic to the cells, but they often yield transformation products that are toxic. This can inhibit treatment overall or lead to byproducts that must then be transformed as well, possibly by different bacteria.[24]

Dioxane is a stabilizer for chlorinated solvents like PCE, TCE, and 1,1,1-trichloroethane (1,1,1-TCA), meaning that it is often present alongside these contaminants in the environment. It is also a wetting agent in paper and textile processing and in organic chemical manufacturing.[3] Dioxane is listed as a probable human carcinogen.[5] This increases the importance of its treatment, especially because dioxane has been commonly found in surface and groundwater systems.[25–27] A recent study in the United States found dioxane present in 21% of public water systems, with 6.9% exceeding the health-based reference concentration of 0.35 µg/L.[26] In general, there are several issues with the treatment of dioxane. When dioxane ends up in water it becomes difficult to remove as it is fully miscible in water, non-volatile, not easily adsorbed by activated carbon, not readily biodegraded in normal environments to safe levels, and it is not readily oxidized by common oxidants.[28–30] Current *ex situ* treatment methods using oxidation techniques, such as ozone, hydrogen peroxide, ultraviolet light, sonication, and other chemicals, are generally expensive.[31–36] Dioxane also may not be effectively treated using pump-and-treat as low permeability zones will often release dioxane long after treatment has been completed in the higher permeability zones.[37] This is known as a diffusion matrix, where contaminants diffuse in and out of lower permeability zones in a heterogeneous subsurface.[38] This diffusion back into higher permeability zones can mean that detectable contamination remains even if the source has been completely treated.[37,39] For these reasons, there is a desire for long-term *in situ* treatment techniques that are more effective and cheaper.

Evidence of monooxygenase degradation of dioxane has been found in a variety of genera of bacteria induced with growth substrates such as methane, propane, tetrahydrofuran, or toluene.[40] A recent study found evidence of dioxane degradation with *Rhodococcus rhodochrous* Strain ATCC 21198.[9] A proposed pathway for the degradation of dioxane by monooxygenases

is: dioxane to 2-hydroxy-1,4-dioxane to 2-hydroxyethoxyacetic acid (HEAA) to dihydroxyethoacetic acid (with ortho- or para- hydroxyl groups) to ethylene glycol/glycolate/glyoxalate/oxalate to carbon dioxide. The intermediates formed during this process are not expected to lead to toxic accumulation in the environment.[41]

2.2 Remediation and Bioremediation

For environmental contaminants in general, traditional treatment methods are relatively simple. These tend to focus on capping the site and allowing for natural attenuation, excavating the site and moving the contaminated material to a more well-contained location, or conducting a pump-and-treat operation for removing contaminated groundwater.[42,43] These technologies have been in use for decades and are proven to be effective under certain site conditions. However, these methods are not without issues. Capping still usually requires long-term monitoring and maintaining the contaminants' isolation using methods like barriers. It also does not typically treat the source of the contamination, which means that there is still long-term potential for problems.[44] Likewise, excavation does not typically treat the contamination in most cases and has the added risks of exposure and accidents during the excavation and transportation processes.[44] There is an extensive list of *in situ* and *ex situ* remediation technologies that range from relatively cheap and simple to considerably expensive and challenging. A partial list of treatment technologies includes air sparging, bioremediation, chemical reduction, chemical oxidation, permeable reactive barriers, phytotechnology, soil vapor extraction, and thermal treatment.[6]

Bioremediation is most relevant to this thesis. This is defined as "the process whereby organic wastes are biologically degraded under controlled conditions to an innocuous state, or to levels below concentration limits established by regulatory authorities."[7] Nutrients are key to

stimulating the growth of the microorganisms that perform this biological degradation. Biostimulation of microorganisms typically involves adding nutrients, electron acceptors, and/or oxygen to foster microbial growth. These nutrients generally include nitrogen, phosphorous, and a carbon source.[44,45] As discussed previously, cometabolism is often the process that transforms the contaminants. These additional nutrients are necessary to stimulate microbial growth as the transformation of the contaminant does not provide the cells with an energy source.[18] It is often necessary to stimulate microbial growth because the low levels of organic matter within subsurface soils and groundwater do not foster microbe activity or diversity.[46] An underrealized limitation of bioremediation, especially when it involves cell immobilization, is that it requires expertise from numerous fields that are generally not closely related. Successful bioremediation projects can involve expertise in microbiology, engineering, geology, hydrogeology, soil science, material science, and project management.[47] Bioremediation techniques can be either *in situ* or *ex situ*. *In situ* techniques include bioventing, biosparging, phytoremediation, and permeable reactive barriers (PRB). *Ex situ* techniques include biopiles, windrows, and bioreactors.[48]

PRBs are particularly relevant to this thesis. A PRB is defined as:

> 'An emplacement of reactive media in the subsurface designed to intercept a contaminated plume, provide a flow path through the reactive media, and transform the contaminant(s) into environmentally acceptable forms to attain remediation concentration goals down-gradient of the barrier.'[10]

PRBs offer a number of advantages. They are passive, meaning they do not require energy input continuously, and *in situ* treatment means it is not necessary to bring contaminants to the surface. An issue with other methods of *in situ* bioremediation is they often necessitate the addition of growth substrates to keep microorganisms from dying out. This is often counteracted by using substrate injection or re-circulation wells, but bioactive PRBs should negate this

problem.[49] Degradation is also preferable to the collection of contaminants in a different form or location (e.g. excavation or granulated activated carbon adsorption). In addition, there are fewer regulatory issues when there is no discharge from a treatment system like there is with pump and treat.[43] The main categories of PRBs are funnel-and-gate and continuous. In funnel-and-gate systems, the contaminant plume is directed to a PRB by impermeable barriers. In a continuous system, a PRB is installed across the entire cross-section of the plume. Funnel-and-gate systems are more expensive in general, so their use is normally reserved for when the material of the PRB itself is costly.[50]

Early era PRBs were generally made for treatment using zero valent iron. This can treat some contaminants, but there are limitations to the types of contaminants that can be degraded or sorbed.[51] Other common PRB materials include activated carbon, zeolite, lime, apatite, sodium dithionite, transformed red mud, and alumina.[52] Biobarriers were thus introduced in an attempt to broaden the scope of contaminants treatable by PRBs. These allowed for cheap material and/or substrate to be used in a PRB as a way to stimulate native or inoculated microorganisms that could degrade the contaminants.[51,53,54] Aerobic biobarriers are desirable because there is a wide variety of contaminants that are efficiently removed by aerobic biodegradation. Petroleum hydrocarbons are one of the primary examples of this.[52] The main issue is that these aerobic biobarriers quickly become oxygen limited, leading to contaminant breakthrough.[55] In an attempt to overcome this, oxygen releasing compounds (ORC) have been added to some aerobic biobarriers. Examples of ORCs include calcium peroxide, hydrogen peroxide, and magnesium peroxide.[52] A commonly used method of incorporating ORCs is by embedding these compounds in cement. Cement-embedded ORCs have shown the ability to adequately meet the oxygen demands of aerobic biobarriers for potentially months to years, but this technique also generally

results in a high pH that can negatively affect microorganisms.[56,57] ORCs within cement may also be an issue at sites with high levels of organic carbon and dissolved iron as these can quickly deplete the released oxygen.[58]

Anaerobic biobarriers are mainly structured around the degradation of nitrates, sulfates, and chlorinated solvents.[52] For nitrates, cheap organic materials such as alfalfa, sewage sludge, manure, sawdust, wood waste, leaves, compost, and peat have been used.[59–62] Sulfates and heavy metals have also been shown to be successfully removed using PRBs composed of woodchips, sawdust, sewage sludge, and leaves, although removal efficiency of sulfate decreased over time.[63] Mulch and compost PRBs have been shown to effectively create bioactive zones and degrade PCE and TCE.[64–66]

2.3 *Rhodococcus rhodochrous* Strain ATCC 21198

Rhodococcus rhodochrous Strain ATCC 21198 (21198) is the strain of microbe used for all experiments presented in this thesis. *Rhodococcus rhodochrous* is a Gram-positive bacterium that has industrial uses, mainly for acrylamide production. It is also used in bioremediation for compounds including hydrocarbons and polychlorinated biphenyls.[67] The genome of 21198 was sequenced in 2014.[68] This strain is well-characterized at this point, and it has long been known to metabolize isobutane.[69] 21198 grown on isobutane has been shown to transform low and high levels of dioxane under aerobic conditions.[8,9,70,71] It has also demonstrated the ability to cometabolically transform low levels of *c*DCE under aerobic conditions.[9,71] A previous batch kinetic study established that 21198 maintains the ability to transform both dioxane and *c*DCE when co-encapsulated within gellan gum beads.[9] Beads of the same material were used for several studies completed for this thesis. The short-chained alkane monooxygenase enzyme of 21198 that transforms contaminants like *c*DCE and dioxane is inactivated when exposed to

acetylene.[72,73] This allows for acetylene controls to be created in which the microorganisms remain alive and retain their ability to consume oxygen and substrates, but they are unable to degrade contaminants. Isobutane grown 21198 has also shown the ability to utilize 1-butanol and 2-butanol as substrates. This is important because the orthosilicates known as tetra-butyl orthosilicate (TBOS) and tetra-s-butyl orthosilicate (T2BOS) have been shown to effectively hydrolyze and release 1-butanol and 2-butanol over time, respectively. Successful cometabolism of 1,1,1-TCA, dioxane, and *c*DCE has been demonstrated using TBOS and T2BOS as slow-release growth substrates for 21198.[9,73] Figure 2.1 presents the structures of TBOS and T2BOS, along with their hydrolysis products.

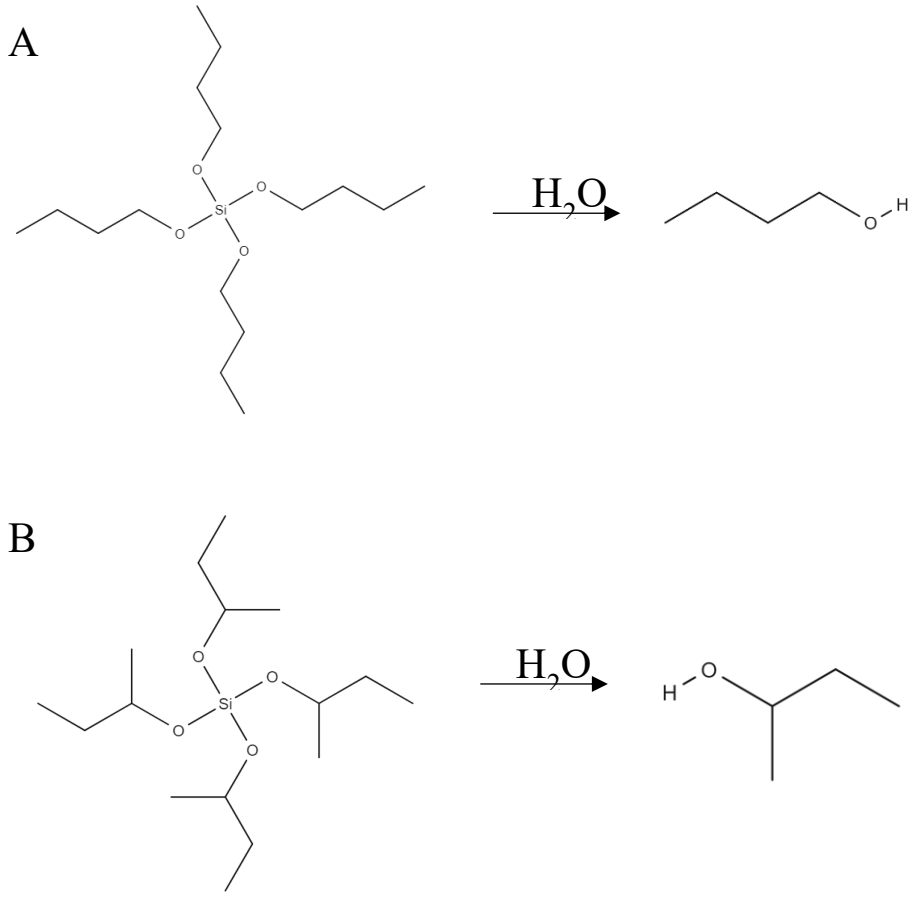

Figure 2.1. Structural diagrams of TBOS (A) and T2BOS (B) demonstrating their hydrolysis into 1-butanol and 2-butanol, respectively.

2.4 Cell Immobilization

In general, cell immobilization involves capturing live cells in a matrix to increase the ability to use the cells for a purpose. Cell immobilization has been explored for a wide variety of cell types and immobilization agents. Immobilization offers a number of benefits compared to free cells. There is evidence that immobilized cells endure less biotic and abiotic stress, experience less toxicity from hazardous compounds, and have increased rates of survival and metabolism.[74–81] These advantages are key as to why it is a beneficial method in bioremediation. Cell immobilization is used for other purposes as well. It is applicable across a variety of industries including food and dairy, pharmaceuticals, bioplastics, and biofuels.[82] Immobilization may also involve enzymes or organelles in the place of cells.[83] For the studies in this thesis, immobilization was primarily used as a way to co-encapsulate cells and a slow-release growth substrate necessary for the cometabolism of contaminants. The slow-release growth substrate was either 1-butanol or 2-butanol, which were slowly hydrolyzed from TBOS and T2BOS over time, respectively.

Bacteria often function differently in natural settings when they are attached to surfaces as opposed to being free cells. Groups of bacteria attached to a surface together are known as a biofilm. Interacting with a solid matrix causes changes in bacterial characteristics, and bacteria in biofilms have behaviors and metabolisms that differ from when they are unattached.[84–87] Other differences are that attached cells may show higher levels of activity and changes in gene expression.[88,89] Microorganisms in biofilms can be viewed as a community that has a metabolism and a homeostasis condition. It has also been determined in a previous study that microorganisms in biofilms are at least 500 times more resistant to antiobiotics.[84] Biofilms are commonly used as the basis of reactors that treat wastewater.[90] In general, some of the benefits

of immobilized cells when compared to suspended cells are continuous utilization, higher cell density, higher activity, protection against acidification, protection against shear forces, and resistance to factors such as heavy metals, solvents, pH, and temperature.[88,91–93] The effectiveness of the cell immobilization and its effects on biodegradation vary based on the bacterial species, carrier agent (gellan gum, alginate, etc.), initial mass of inoculum, and the culture's conditions.[94,95] Ideal carrier agents are non-toxic and light. They should also ideally be cheap, easily produced, and widely accessible.[96,97] It is not always possible to find an agent that meets all of these requirements, but studies conducted in parallel to the work in this thesis focused on determining the ideal hydrogel bead formulation.

Cell immobilization does possess issues. In some cases, decreased growth rate is observed for the immobilized cells. One reason for this is that oxygen and nutrients are not available throughout the entire hydrogel, especially in larger hydrogels. There are often a mass transfer limitations leading to more nutrients and oxygen being available on the edges of the hydrogel, so these are the areas that have the most cell growth.[94,98–100] With cell encapsulated beads specifically, the larger the diameter of the bead, the lower the loading capacity and the higher the risk for cell death, known as necrosis.[98] Smaller diameter beads have a lower resistance to oxygen transport into the bead.[101–103] A previous study using the same gellan gum beads as used in this thesis attempted to create micro-beads of the same structure, but failed to encapsulate both the microorganisms and the slow-release substrates in the micro-beads.[11] Other contributors to decreased growth rate in immobilized cell matrices may include a build-up of toxic byproducts and large cell growth occurring on the outer sections of the carrier, weakening the carrier as a whole.[104]

2.5 Gellan Gum

Gellan gum was the main component of one of the two varieties of hydrogel beads used in this thesis. Gellan gum falls into the category of natural gums. Various natural gums were originally used primarily as food additives, but recent developments have led to their use in the pharmaceutical and medical fields.[105] Gellan gum was first discovered to have commercial potential in 1978 by Kelco during a study of soil and water bacteria. Kelco is also notable for being the first company to commercially produce xanthan gum, a still widely used food additive for thickening and stabilizing.[106] The product that later became known as gellan gum is secreted by the bacteria *Sphingomonos elodea* Strain ATCC 31461.[107] It is a bacterial polysaccharide, and it was soon used as an alternative gelling agent to agar.[108] Structurally, gellan gum is a tetrasaccharide that has a repeating sequence consisting of two ß-D-glucose residues, one ß-D-glucuronate residue, and one α-L-rhamnose residue.[109] Naturally synthesized gellan gum will sometimes have an acetyl group on one of the glucose residues (Figure 2.2), but commercially produced gellan gum is deacylated.[106]

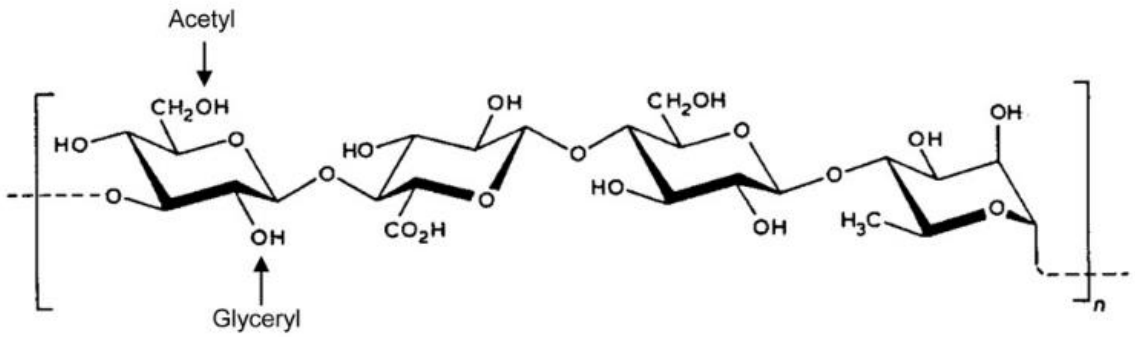

Figure 2.2. Structural diagram of naturally biosynthesized gellan gum showing the location of the acetyl group before being deacylated in the commercial production process.[106]

Gellan gum eventually became a food-grade product when it was approved in Japan in 1988 and later in the US in 1992. This led to an increase in studies on its potential uses.[110] Gellan gum became a relatively common carrier agent for immobilized cells. Gellan gum immobilized microorganisms of various types have been shown to biodegrade contaminants of concern, such as gasoline hydrocarbons, cyanide, carbazole, phenol, 1,1,1-trichloroethane, *c*DCE, and dioxane.[9,111–114]

2.6 Alginate

An alternative carrier agent to gellan gum is alginate, usually sold in the form of sodium alginate. It is a biopolymer and a polyelectrolyte that is biocompatible, non-toxic, and biodegradable, thus having several properties of a suitable carrier agent.[115,116] Commercial alginate is extracted from the outer cell wall of brown algae like kelp and seaweed.[117] Like gellan gum, alginate is a food-grade product with a history of use as a food additive. Alginate is a copolymer made of mannuronic acid (M) and guluronic acid (G). Units within the copolymer vary with subunits of double M blocks, double G blocks, and M and G blocks (Figure 2.3).[118]

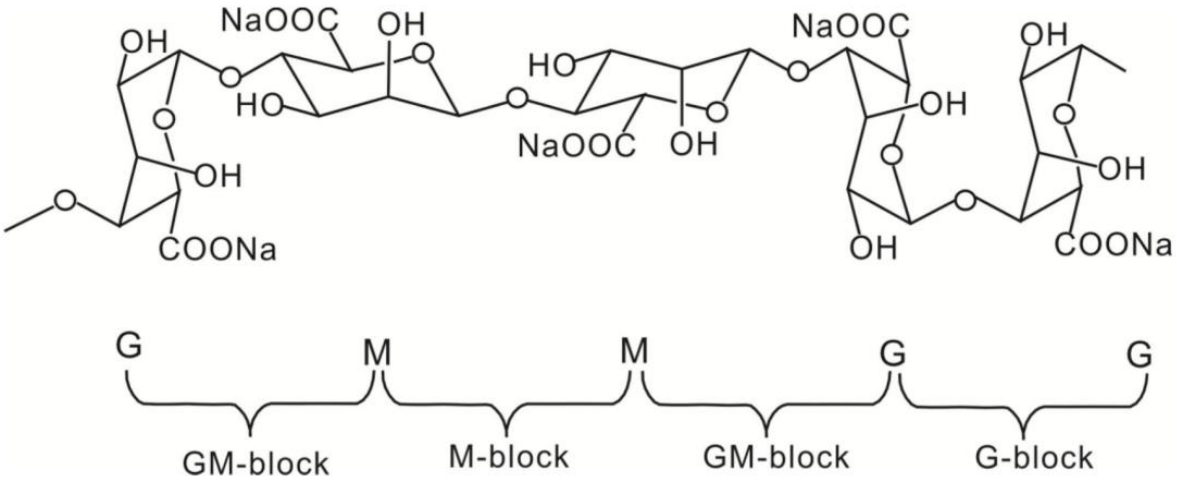

Figure 2.3. Diagram of the alginate copolymer structure illustrating MM, GG, and GM blocks.[119]

The composition of alginate can vary greatly, which affects the pore size of alginate gels. As the ratio of M to G increases, the average pore size decreases.[120,121] Often, alginate is produced and sold in the form of sodium alginate. Sodium alginate has previously been shown to support cell immobilization of a variety of microorganisms. Using sodium alginate as a carrier agent, evidence has been generated supporting biodegradation of contaminants of concern such as pyrene, phenol, di-*n*- octyl phthalate, carbamazepine, atrazine, and cyanide.[122–127] These studies vary between using sodium alginate as the sole carrier agent or using sodium alginate and another compound(s) to create an immobilization matrix.

2.7 Polyvinyl alcohol

Polyvinyl alcohol (PVA) is a vinyl polymer with carbon-carbon linkages. This linkage functions the same as the linkages in common plastics like polyethylene.[128] PVA is produced by the hydrolysis of polyvinyl acetate. As such, PVA falls into two categories: fully hydrolyzed and partially hydrolyzed (Figure 2.4).[129] The majority of hydrogels produced for the purpose of bioremediation, including the research conducted within in this thesis, use fully hydrolyzed PVA. It is water soluble and biodegradable, so it is regularly used in products like fertilizers, pesticides, and herbicides.[128] An advantage of PVA as opposed to other immobilization matrices is that matrices composed of PVA have crystalline regions that act as physical crosslinks, which adds strength.[130,131]

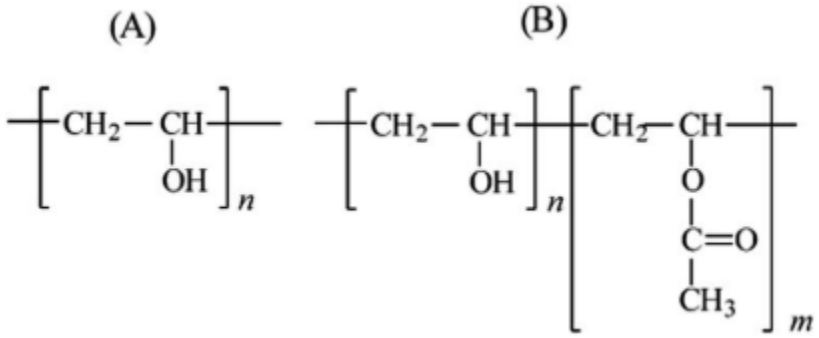

Figure 2.4. Structural diagrams for PVA: (A) fully hydrolyzed; (B) partially hydrolyzed.[129]

Using hydrogel beads made from PVA to immobilize cells is not a novel practice. These beads have a higher flexibility than beads made from natural polymers. Bead elasticity increases as the porosity increases.[132] PVA immobilized microorganisms have been shown to survive the process of immobilization, but there is evidence of an initial loss of cell viability. Respiration rate for these beads increased over time, supporting that the microorganisms are able to grow up within the hydrogel matrix.[133] Similarly to gellan gum and alginate, PVA has been shown to be an effective method for cell immobilization and biodegradation of a variety of contaminants of concern including phenanthrene, phenol, bisphenol A, nitrobenzene, dimethyl sulfoxide, alkanes, atrazine, and carbazole.[134–141]

2.8 PVA/Sodium Alginate

The combination of PVA and sodium alginate has commonly been used in hydrogels outside the realm of cell immobilization. It has been used in conjunction with antibacterial silver nanoparticles, nanohydroxyapatite, Provatex CP, clindamycin, nitrofurazone, graphene oxide, curcumin, and lutein.[142–149] Much of this work is focused on pharmaceuticals rather than environmental remediation. This is because the PVA and alginate complex has been shown to effectively capture antibiotics and vitamins, which can then be released within the system over

time. While it falls under a different field, it is similar to using TBOS and T2BOS within a hydrogel to slowly release 1-butanol and 2-butanol.

There is extensive evidence that the PVA and alginate complex is effective for cell immobilization. In some cases, this combination has been used with cells to produce specific compounds. Microorganisms immobilized in a PVA/alginate matrix have been used to produce ethanol, lactic acid, and glycolic acid.[150–152] It has also been used for the degradation and removal of several compounds. Examples include biotransformation of fumaric acid, the removal of nitrogen from wastewater, the degradation of polycyclic aromatic hydrocarbons, ammonia oxidation, treatment of *N*,*N*-dimethylformamide, penicillin G degradation, and activated sludge immobilization for wastewater treatment.[153–159] Using PVA and alginate can dependably immobilize cells for bioremediation, but it also leads to the production of a better overall hydrogel from a structural standpoint. This is important, as past studies and portions of the research completed within this thesis have demonstrated long-term issues with hydrogel integrity.[11] PVA adds strength and crosslinking capacity to the hydrogel while alginate decreases the tendency of beads to agglomerate.[160]

2.9 Embryonic Zebrafish Testing

Zebrafish, *Danio rerio*, are an accepted biological model for toxicity testing with an extensive history of usage. This species is advantageous for a number of reasons. They are small and cheap, which allows for rapid, large studies to be conducted. They are a model organism because they are complex with metabolic pathways and organ systems that allow for a wide range of toxicological studies.[161] Specifically, embryonic zebrafish testing was implemented as part of this thesis. Embryonic zebrafish assays are valuable as embryo development occurs *ex vivo*: outside of the parent. This allows for effects to be observed both easily and quickly. The

zebrafish only requires months to reach adulthood.[162] Importantly, zebrafish embryos have functioning organs and a circulatory system by the 6th day after fertilization.[163] This is especially relevant to this thesis as the embryonic zebrafish assays conducted were 5 days long. Even with such a short study period, it is possible to measure teratogenic effects.

The developmental process of zebrafish embryos is well understood, and deviations from normal development should be easily discovered.[164] The assay is able to measure lethality, teratogenicity, and phenotypic changes.[161] Despite being a freshwater fish, zebrafish offer an acceptable alternative to mammalian studies that may have cost, time, difficulty, or ethical concerns. Researchers have found that the similarity between zebrafish and mammalian developmental toxicity studies ranges from 55-100%.[165–167] Comparatively, the similarity between rats, mice, and rabbits is 56%.[168] Specific zebrafish embryonic toxicity data for dioxane and *c*DCE, and products produced during their cometabolic treatment, is not readily available, and it is possible the data from this thesis is novel in that respect.

CHAPTER 3 – METHODS

3.1 Chemicals

A summary of the chemical compounds used within the following methods along with their manufacturers and purities is presented in Table 3.1. To use *c*DCE, a saturated stock solution was created. This was done by adding 1 mL of *c*DCE to a 27 mL vial. The vial was filled with DI water and capped with a butyl septum. The vial was allowed to equilibrate, and then the concentration of the aqueous phase was assumed to be the solubility limit for *c*DCE in water. This aqueous phase was used for *c*DCE additions in all experiments.

Table 3.1. Summary of the chemical compounds used for the experiments conducted within this thesis, including manufacturer and purity.

Compound	Manufacturer	Purity
*c*DCE	TCI	>99.00%
Dioxane	Baker	99.00%
Deuterated dioxane	Sigma-Aldrich	>99.00%
Isobutane	Gas Innovations	99.99%
1-butanol	Sigma-Aldrich	99.80%
2-butanol	Sigma-Aldrich	99.00%
TBOS	Gelest Inc.	97.00%
T2BOS	Gelest Inc.	95.00%
Gellan gum	C.P. Kelco	--

3.2 Analytical Methods

3.2.1 Headspace Sample Analysis

Gas chromatographs (GC) were used to measure headspace levels of oxygen, *c*DCE, cis-DCE epoxide, and isobutane. In all cases, a Hamilton 1710 Series Gastight Syringe was used to collect and inject 100 µL of headspace sample into the gas chromatograph. Oxygen (O_2) was measured using a Hewlett Packard 5890 Series Gas Chromatograph with a thermal conductivity detector (GC-TCD) and a Supelco 60/80 Caroboxen 1000 capillary column. Helium was used as

the carrier gas, with a flow rate of 30 mL/min. O_2 was measured using a ratio of the peak areas of O_2 and nitrogen (N_2), which had retention times of 4.1 and 4.3 minutes, respectively. The oven temperature was maintained at 40°C. External standards for gas phase concentrations based on the eluted peak areas were used to determine headspace concentrations.

*c*DCE and *c*DCE epoxide were both measured with a single method using a Hewlett Packard 6890 Series Gas Chromatograph equipped with a micro-electron capture detector (GC-ECD) and an Agilent Technologies DB-624 UI capillary column. The carrier gas used was helium flowing at a rate of 15 mL/min. The isothermal oven temperature was kept at 50°C. *c*DCE and *c*DCE epoxide were eluted with retention times of 2.0 and 2.7 minutes, respectively. The standard used for *c*DCE yielded a limit of detection of 7 peak area, which corresponded to a gas concentration of 0.009 µM. The method was calibrated using external standards.

Isobutane was measured using a Hewlett Packard 6890 Series Gas Chromatograph with a flame-ionization detector (GC-FID) and an Agilent Technologies 115-3432 GS-Q capillary column. Helium flowing at a rate of 15 mL/min was used as the carrier gas, and the oven temperature was 150°C. Isobutane had a retention time of 0.8 minutes. The method was calibrated using external standards.

The method for converting liquid samples into headspace samples will be discussed in a future section. After determining the headspace concentration, liquid phase concentration was calculated using Equation 1:

$$C_L = \frac{C_g}{H_{cc}}, \textit{ where,} \qquad \text{Eqn 1}$$

C_L = *Liquid Phase Concentration*

C_g = *Gas Phase Concentration*

H_{cc} = *Henry's Law Constant*

3.2.2 Liquid Sample Analysis

Liquid phase concentrations of dioxane, 1-butanol, and 2-butanol were determined by first filling a 40 mL volatile organic analysis (VOA) vial with 25 mL of deionized (DI) water. For the dioxane measurement method, deuterated dioxane was used as an internal standard. Deuterated dioxane was added to the VOA vial such that the final concentration would be 5 µg/L. Depending on the estimated dioxane concentration, 125 – 500 µL of batch bottle or column liquid phase sample was added to the VOA vial. For 1-butanol and 2-butanol, external standards were used to calibrate the method. A typical VOA vial in these cases would consist of 50 µL of batch bottle or column sample and 25 mL of DI water.

5 mL were removed from the VOA vials by a Teledyne Tekmar AQUATek100 Autosampler, which then sent the samples to a Teledyne Tekmar Lumin PTC Purge and Trap. The samples were measured using a Hewlett Packard 6890 Gas Chromatograph equipped with a mass selective detector (GC-MS). Chromatographic separation was achieved using a Restk Rtx-VMS capillary column. Single ion mode was used with the GC-MS to isolate the desired compound. Dioxane and deuterated dioxane had mass-to-charge (m/z) values of 88 and 96, respectively, with both peaks having a retention time of 7.1 minutes. 1-butanol and 2-butanol had m/z values of 56 and 45, respectively, with retention times of 5.2 and 5.9 minutes. Liquid concentrations were determined by comparing peak areas from samples to a standard curve of peak areas generated using known concentrations. Dioxane samples were diluted 50-200 times, such that the limit of detection was under 1 µg/L. 1-butanol and 2-butanol were diluted 400 times, such that the limits of detection were 2 µg/L and 1 µg/L, respectively.

Bromide concentrations were measured using a Dionex DX-500 ion chromatograph equipped with an electrical conductivity detector and a Dionex AS14 column. 0.6 mL liquid

samples were loaded into Dionex 0.5 mL PolyVials to ensure all vial space was filled. Dionex PolyVial filter caps were then inserted into the vials. Up to 8 of these vials were placed into a Dionex AS40 Autosampler rack, and the rack was placed on the Dionex AS40 Autosampler. The ion chromatograph was then run using an eluent composed of 0.37 g/L sodium carbonate and 0.084 g/L sodium bicarbonate. The ion chromatograph results displayed bromide as a peak with a retention time of approximately 2 minutes. The peak area was measured to obtain a concentration value based on a calibration curve. Calibration curves were regularly obtained using bromide samples in DI water with known concentrations.

Dissolved oxygen (DO) was initially measured for both the influent and effluent column media for the gellan gum bead packed column. The influent was measured by sampling 2-3 mL from the influent syringe directly into a VOA vial. A Hach sension156 liquid DO probe was used to measure the DO in mg/L. Effluent DO was measured by attaching a 5 mL disposable syringe to the column effluent line. After 2-3 hours, the syringe collected 2-3 mL of sample. This was then injected into a VOA vial and measured using the Hach sension156 liquid DO probe. It is important to note that while effluent DO values were typically in the 3-5 mg/L range, the true values were likely much closer to 0 mg/L. Based on tests with the disposable syringes, 2-3 hours was enough time for significant oxygen to diffuse into the sample. Even when the effluent had a strong sulfur odor, suggesting anaerobic activity, effluent DO levels were in the 3-5 mg/L range, which was determined to be the detection limit for DO when collecting samples for measurement from the gellan gum bead column.

DO was measured using the same method for the PVA/SA bead packed column. Because this column was operated at twice the flow rate for the majority of its run time, the effluent could be collected more quickly prior to DO measurement. This meant there was less time for outside

oxygen to seep into the sample. As such, DO values around 2 mg/L, as opposed to 3-5 mg/L, were obtained in the presence of the sulfur odor, again suggesting anaerobic activity. ~2 mg/L was thus considered the detection limit for the PVA/SA column.

3.3 Cell Culture and Harvest

For the hydrogel beads used in this thesis, it was necessary to grow and harvest cells to use for co-encapsulation with SRSs. All encapsulated beads contained a pure culture of *Rhodococcus rhodochrous* strain ATCC 21198, which was initially obtained from Dr. Michael Hyman of North Carolina State University. Mineral salt media (MSM) plates with an added fungicide, nystatin at 24 mL/L of a 10,000 unit/mL solution, were used to streak plate Strain ATCC 21198. Plates were stored in an airtight canister with isobutane in a 30°C room. Microbial work was always done within a sterile laminar flow hood or biosafety cabinet.

Growth reactors were prepared as the first step toward immobilizing cells. Each growth reactor was created using a 500 mL glass Wheaton bottle. 300 mL of phosphate buffer MSM was used as the base for each reactor (Table 3.2). In the laminar flow hood, a flamed culture loop was then used to transfer a loop of Strain ATCC 21198 from the MSM plate to each growth reactor. The growth reactors were capped, and 50 mL of isobutane was added into the reactor through the septum. The growth reactors were then stored in a 30°C room on a 150 revolutions per minute (rpm) shaker table. After 4-5 days, the growth reactors were opened in the laminar flow hood and a loop of liquid from each the reactors was streaked onto a tryptic soy glucose agar (TSGA) plate. This TSGA plate was divided such that each reactor had an isolated streak. The TSGA plate was sealed with parafilm and stored at 30°C to serve as a check for microbial contamination. The growth reactors were recapped and given an additional 50 mL of isobutane

through the septum, which is known as refreshing the reactors. They were then returned to the shaker table in the 30°C room.

Table 3.2. Chemical composition of the phosphate and carbonate buffered MSM solutions.

Compound	Phosphate MSM Concentration (g/L)	Carbonate MSM Concentration (g/L)
NH_4Cl	2.0	2.0
$MgCl_2*6H_2O$	0.075	0.075
$(NH_4)_2SO4$	0.10	0.10
EDTA	0.010	0.010
$ZnSO_4*7H_2O$	4.4E-03	4.4E-03
$CaCl_2$	1.0E-03	0.60
$MnCl_2*4H_2O$	1.0E-03	1.0E-03
$FeSO_4*7H_2O$	1.0E-03	1.0E-03
$(NH_4)_6Mo_7O_{24}*4H_2O$	2.2E-04	2.2E-04
$CuSO_4*5H_2O$	3.0E-04	3.0E-04
$CoCl_2*6H_2O$	3.4E-04	3.4E-04
$NaHCO_3$	--	1.3
K_2HPO_4	1.6	--
NaH_2PO_4	0.85	--
pH	7.0	7.0

The day after refreshing, the reactors were placed in the laminar flow hood, along with 6 disposable 250 mL centrifuge tubes. The contents of all reactors were poured with an even distribution into the centrifuge tubes. The centrifuge tubes were capped and moved to the centrifuge, where they were centrifuged for 15 minutes at 4000 relative centrifugal force (RCF). When the centrifuge cycle was complete, the supernatant from each tube was poured out as waste. 50 mL of 50 mM NaH_2PO_4 phosphate buffer was poured into each centrifuge bottle, and then the bottles were centrifuged again at the same settings. The supernatant was again poured out as waste, and 10 mL of the phosphate buffer was added to one of the centrifuge bottles. The bottle was shaken to resuspend the cells. This solution was poured into the next bottle, and those cells were then resuspended as well. This process was completed for all 6 bottles. The

concentrated cell solution remaining in the final bottle was then collected in a 50 mL Falcon tube and stored at 4°C.

To determine the total suspended solids (TSS) concentration of the concentrated cell solution, two weigh tins and two 45 µm membrane filter papers were first retrieved. One filter paper was placed in each weigh tin, and the combined mass was recorded for each. An Erlenmeyer vacuum flask and a filter funnel with tubing were then set up so a vacuum was formed with the filter funnel. One of the filter papers was placed on top of the funnel and slightly wetted to secure it. 400 µL of the concentrated cell solution was then pipetted on top of the vacuumed filter paper. The filter paper was then placed in one of the weigh tins and moved to the 103°C drying oven. This process was then repeated for the second filter paper and weigh tin. After 20-30 minutes, both tins were moved to the desiccator and allowed to cool. The mass of each filter paper and weigh tin combination was recorded again, with the difference between the new mass and the original mass all divided by the 400 µL to find the TSS. The two TSS values were averaged to find the TSS of the remaining cell concentrate which was then used for hydrogel bead immobilization.

3.4 Cell Immobilization

3.4.1 Gellan Gum Beads

Gellan gum beads with 21198 co-encapsulated with TBOS and T2BOS used in this study were created by Alisa Bealessio, a former student. The method for bead production of both TBOS and T2BOS gellan gum beads with 21198 is thoroughly described in the 2018 thesis of Mitchell Rasmussen[11]. Beads possessed 0.5 mg TSS/mL bead. The batch of TBOS and T2BOS beads were made 8 months and 3 months prior to their use in this work, respectively. Beads were

stored in the 4°C fridge after their production. All beads were washed 3 times with carbonate buffer media (Table 3.2) before beginning the experiments.

3.4.2 Polyvinyl Alcohol/Sodium Alginate Beads

Bead optimization tests were conducted in parallel to the studies in this thesis. Through this work, a polyvinyl alcohol/sodium alginate (PVA/SA) bead for use in these studies was developed using the following method. This method was obtained through personal communication with Conor Harris, who developed the fabrication method.[169] A 4.6% (w/v) PVA solution was prepared by dissolving the appropriate amount of PVA in autoclaved water at 80°C. A 5.1% (w/v) sodium alginate solution was prepared by dissolving the appropriate amount of SA in autoclaved water at room temperature. The solutions were mixed at a 1:1 ratio with an impeller blade until fully combined. Span80, a nonionic surfactant, was added at a concentration of 0.1% (v/v) and followed by the addition of TBOS at a concentration of 10% (v/v). Once the solution was emulsified and homogeneous, 21198 cells were added at a concentration of 0.5 mg/mL. The final concentration of PVA and SA was 2.0% (w/v) and 2.2% (w/v), respectively. This was selected due to this combination demonstrating bead durability while maintaining the ability for cometabolism of contaminants. The solution was then extruded through a syringe with an 18-gauge needle at 12 mL/hr into a crosslinking solution of boric acid (BA) and calcium chloride ($CaCl_2$) at 3.0% (w/v) and 1.5% (w/v), respectively. The beads were crosslinked for 75 minutes. Finally, beads were removed from the crosslinking solution and washed three times with DI water. The completed beads were stored in DI water at 4°C. The beads used within the column were stored for one night before packing. The beads used for the abiotic hydrolysis tests, described in Section 3.4, were stored for 3 weeks before being added to the batch bottles.

3.5 Batch Bottle Reactor Studies

Batch reactor kinetic studies were completed using the gellan gum beads to confirm the long-term effectiveness of cometabolism and durability. This was done primarily to verify the results of a previous study completed by Mitchell Rasmussen, a former student, and the methods from this study were closely followed, with the primary difference being the mass of beads used.[11] Ten 155mL glass Wheaton bottles with septa lids were originally filled with 100mL of carbonate buffer MSM (Table 3.2). 8 grams each of 5% (w/w) T2BOS beads were added to 7 of the bottles. 3 grams each of 5% (w/w) TBOS beads were added to 2 of the bottles due to there being a limited sample of these beads. The final bottle without beads served as an abiotic control to measure contaminant losses due to the septum or leakage. Two of the T2BOS bottles were made into poison controls by adding sodium azide to create a 0.2% (w/v) solution in the bottle. These would allow for measurement of the abiotic hydrolysis of T2BOS into 2-butanol. 10% of the headspace in 2 of the other T2BOS bottles was filled with acetylene to create controls that would block the monooxygenase enzymes and prohibit cometabolism.[72,73] The final three T2BOS bottles and both TBOS bottles were live to assess metabolism and cometabolism. All construction steps were conducted in the laminar flow hood to avoid contamination.

Controls were allowed to equilibrate for 1 hour before contaminant addition. Dioxane was added to each reactor to create an initial concentrate of ~200 µg/L. O_2, 2-butanol, 1-butanol, and dioxane levels were measured at regular intervals throughout the course of the experiments. For liquid samples, approximately 1 mL of solution was removed from each bottle using a disposable 5 mL syringe. The 1 mL sample was then filtered using a 25 mm 1 µm VWR polytetrafluoroethylene (PTFE) membrane syringe filter into a 2 mL plastic sample tube. 0.2 µm filters were not used because bead particles rapidly clogged these filters and made them

unusable. The sample tubes were stored at 4°C, if they were not immediately used for analysis. *c*DCE at approximately 200 µg/L was added to all the bottles after 13 days of incubation. Once contaminants were depleted, further spikes of dioxane and *c*DCE were added throughout the course of the experiment. After 90 days, the non-control batch bottles were refreshed with media to return the volume to 100 mL in each bottle. The same process was repeated after 188 days, for the TBOS bottles only, in preparation for the zebrafish toxicity testing experiment.

PVA/SA beads were also used to conduct an abiotic hydrolysis test for production of 1-butanol. The setup for this was similar to the poison controls for the gellan gum beads. 100 mL of carbonate buffer MSM each was added to two 155 mL glass Wheaton bottles with septa lids. Two grams of the PVA/SA beads were added to each bottle. Sodium azide was then added to create a 0.2% (w/v) solution in each bottle. The bottles were placed in a 20°C room on a 100-rpm shaker table for the extent of the experiment. Liquid samples of 0.5-1 mL were taken regularly and filtered using 25 mm 0.2 µm VWR PTFE membrane syringe filters. The volume removed was logged in order to calculate the total mass of compounds within the bottles over time. Samples were stored in 2 mL plastic sample tubes. Generally, samples were analyzed immediately upon collection, but in some cases the tubes were stored for a short period of time at 4°C. 1-butanol analysis was completed for the samples as described in the liquid sample analysis section.

3.6 Column Experiments

3.6.1 Gellan Gum Bead Column

A column study was completed using the gellan gum beads to determine the long-term ability to cometabolize contaminants in a situation more similar to that of a PRB. The column study was conducted in a 20.3 cm long Ace Glass Inc. cylindrical glass column with a diameter

of 3.18 cm. The following procedure was used to pack the column and determine the porosity after packing. The column was weighed both empty and filled with water. It was then packed with 5% (w/w) T2BOS gellan gum beads within a laminar flow hood. Beads were rinsed with 10x diluted phosphate buffer MSM (Table 3.2) prior to being added to the column. The bead-filled column was then purged with nitrogen for an hour to drain as much liquid as possible. The column was weighed again before being filled with 10x diluted phosphate buffer MSM and then weighed a final time. These column masses were used to estimate a porosity and an HRT. The difference in the column mass between the column when filled with nitrogen purged beads and the column when filled with beads and media was determined. This difference represented the mass of liquid in the column, which was then divided by the density of liquid media to estimate the pore volume (PV). The mass of liquid was divided by the combined mass of the beads and liquid to estimate the porosity.

The column was then prepared for use in a bromide tracer study to measure retardation of compounds through the bead pack and for use in a study determining the long-term ability of the beads to cometabolize contaminants. The column was covered with aluminum foil and vertically attached to a frame. Plastic tubing was attached to the influent and effluent ends of the column using Swagelok connectors. All connectors were wrapped with Swagelok PTFE thread sealant to prevent leaks. A Hamilton 1000 Series 100 mL gastight glass syringe was attached to the influent line. This syringe was filled with 10x diluted phosphate buffer MSM (Table 3.2) and 30 mg/L bromide to complete a bromide tracer study. The syringe was connected to a ThermoScientific Orion M361 Sage Syringe Pump and operated at the rate of 1 mL/hr. The column effluent was attached to a 2 mL amber glass sample vial using a needle through the vial's septum cap. This

allowed for effluent samples to easily be collected by switching out the glass vial. A diagram of the column set-up is shown in Figure 3.1.

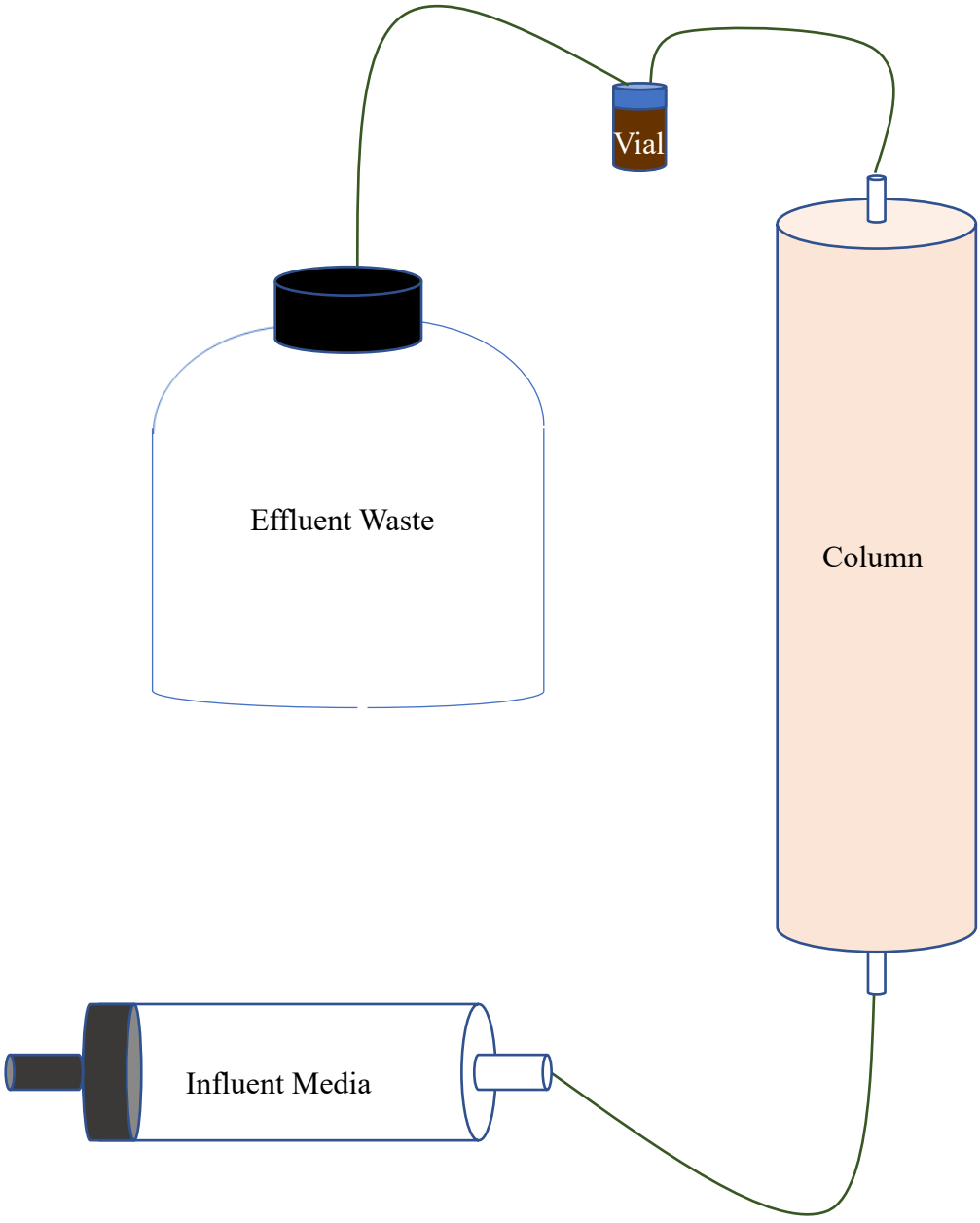

Figure 3.1. Diagram of the T2BOS gellan gum bead column set-up.

The glass vial had another needle and tubing combination driven through its septum that allowed for effluent sample to be transferred from the sample vial to a 500 mL glass Wheaton

bottle once the sample vial was filled. When the effluent collection bottle became full, it was autoclaved and its contents were poured into the proper hazardous waste disposal bin. The entire system was located under a hood operated at a low rate of ventilation.

Initially, the media being fed into the column had no oxygen amendments. To counter a demonstrated oxygen deficiency, oxygen in the influent media was increased by making it saturated with O_2 by purging the media bottle headspace with pure O_2 and then attaching a 1 L gas bag filled with pure O_2 to the bottle at 27 PV. After 34 PV, when it was determined there was still not enough DO to meet the column's demands, the addition of 50 mg/L of hydrogen peroxide (H_2O_2) to the media replaced this method. It was lowered to 25 mg/L at 52 PV into the experiment and returned to 50 mg/L at 58 PV. When the column was paused for a stop-flow test at 88 PV, the H_2O_2 level was raised to 100 mg/L once the column was restarted after 27 days.

Upon start-up of the column, the media being fed into it had approximately 30 mg/L of bromide in addition to the 10x diluted phosphate buffered MSM. Effluent samples were taken regularly to run on the ion chromatograph (IC) to generate a bromide breakthrough curve. Bromide analysis was completed as described in the liquid sample analysis section. This process was continued until the column's effluent bromide level became constant, at which point the bromide was removed from the influent media. Bromide levels continued to be measured in the column effluent until the concentration fell below the detection limit.

Once the bromide tracer test was complete, *c*DCE and dioxane were added to the influent of the column at concentrations of approximately 300 and 200 µg/L, respectively, at 52 PV. Addition was done by pipetting directly into the Hamilton 1000 Series 100 mL gastight glass syringe and was always done within a fume hood. Effluent sample vials were regularly collected to conduct both liquid and gas analysis. From the vials, samples were drawn up using a

disposable syringe and then filtered through a 25 mm 0.2 µm VWR PTFE syringe filter into a 2 mL disposable sample tube. If not prepared for analysis immediately, these samples were stored in the 4°C refrigerator. Samples were ready for dioxane and 2-butanol analysis at this point, which was completed as described in Section 3.1.2. For *c*DCE analysis, 1 mL of each sample was injected into another 2 mL glass vial with a septum cap. These vials were vortexed for 1 minute to allow for equilibration with the headspace and were then measured for *c*DCE as previously describedin Section 3.1.1. *c*DCE was removed from the influent media after the fast-flow test at 78 PV. Dioxane was removed from the influent media when the column was restarted after the stop-flow experiment at 88 PV.

To confirm that *c*DCE epoxide was being produced in the column, a fast-flow test was conducted at 75 PV of the column experiment. The influent media syringe was filled with 80 mL of 10x diluted phosphate buffer MSM, 50 mg/L H_2O_2, 300 µg/L *c*DCE, and 200 µg/L dioxane. This 80 mL was then injected into the column at a rate of 90 mL/hr instead of the regular 1 mL/hr. Effluent media samples were collected in the usual 2 mL glass vials approximately every 10 minutes until the influent syringe was emptied. Samples were analyzed for 2-butanol, dioxane, *c*DCE, and *c*DCE epoxide using the methods described in Section 3.1. The influent flow was then returned to 1 mL/hr. *c*DCE was removed from the column influent at this point, 78 PV, leaving dioxane as the sole contaminant addition.

At 88 PV of the gellan gum column experiment, flow was paused for 27 days. During this time, the column was left at room temperature with no alterations. No sampling occurred during this period. When the flow was resumed, dioxane was removed from the influent media. At that point, the influent feed solution consisted of 10x diluted phosphate buffer MSM and 100 mg/L H_2O_2. Flow was resumed at the normal 1 mL/hr rate. Effluent sampling was resumed for the

measurement of DO, dioxane, *c*DCE, *c*DCE epoxide, and 2-butanol levels. The column study was concluded at 78 PV. All adjustments made to the column are summarized in Table 3.3.

Table 3.3. Summary of the influent feed solution adjustments made to the gellan gum bead column throughout its operation. Flow was paused for 27 days at 88 PV.

Pore Volumes	Flow Rate (mL/hr)	DO/H_2O_2 (mg/L)	*c*DCE (µg/L)	Dioxane (µg/L)
0 – 27	1.0	DO = 8.0	0	0
27 – 34	1.0	DO = 15	0	0
34 – 52	1.0	H_2O_2 = 50	0	0
52 – 58	1.0	H_2O_2 = 25	300	200
58 – 75	1.0	H_2O_2 = 50	300	200
75 – 78	90	H_2O_2 = 50	300	200
78 – 88	1.0	H_2O_2 = 50	0	200
88	0	N/A	N/A	N/A
88 – 117	1.0	H_2O_2 = 100	0	0

3.6.2 PVA/SA Bead Column

A column study was also completed using the PVA/SA beads co-encapsulated with TBOS and 21198 to determine the efficacy of long-term cometabolism of contaminants and to compare results to the gellan gum bead column as well as previous hydrogel bead column studies. This study was also completed to measure possible toxic products generated during cometabolism through the use of embryonic zebrafish toxicity studies. A 10.2 cm long Ace Glass Inc. glass column measuring 3.18 cm in diameter was packed with the beads and the porosity was estimated by weighing the column when filled with media and when filled with beads. The initial set-up of this column was very similar to the set-up of gellan gum bead column described in Section 3.5.1 and diagramed in Figure 3.1. Notable differences include that this column possessed 3 side ports with rubber endcaps from which spatial sampling could be conducted. These side ports protruded from the column such that the column was no longer a perfect cylinder. The influent solution used in this column was also different (Table 3.4) in order to

avoid toxicity to zebrafish embryos in control samples. The media was a combination of a synthetic groundwater formulation plus 200x diluted phosphate MSM supplying added nutrients. This column was packed with glass beads (120 4mm soda lime beads) to enable sampling of biofilms that might develop during column operation and to act as a filter for bead particle to prevent clogging. 50 were packed at the entrance of the column, 20 were spread within the PVA/SA bead pack, and 50 were packed at the end of the column.

Table 3.4. Chemical composition of the initial influent feed solution used in the PVA/SA bead column study prior to the addition of H_2O_2, *c*DCE, and bromide.

Compound	Concentration (mg/L)
$(NH_4)_2SO_4$	0.50
$(NH_4)_6Mo_7O_{24}*4H_2O$	1.1E-03
$CaCl_2$	28
$CaSO_4$	95
$CoCl_2*6H_2O$	1.7E-03
$CuSO_4*5H_2O$	1.5E-03
EDTA	5.0E-02
$FeCl_2*4H_2O$	6.0E-02
$FeSO_4*7H_2O$	5.0E-03
K_2HPO_4	7.8
KCl	1.2
$MgCl_2*6H_2O$	0.38
$MgSO_4$	100
$MnCl_2*4H_2O$	5.1E-03
$MnSO_4*H_2O$	0.11
NaF	0.35
NaH_2PO_4	4.3
$NaH_2PO_4*H_2O$	4.0E-02
$NaHCO_3$	80
$NaNO_2$	0.20
NH_4Cl	10
NH_4NO_3	0.60
$ZnSO_4*7H_2O$	4.4

The column was weighed while filled with dried beads and while filled with beads and media to determine the PV and porosity as described in the previous section. The volume of 1

PV was determined to be 28 mL. Before beginning flow through the column, a constant head test was conducted. This consisted of using a funnel filled with media at a constant head that was connected to tubing that ran through the bottom of the column and out of the top of the column. Effluent was collected in a graduated cylinder and tests were done at varying head differentials (16, 12.5, and 9 inches) in triplicate to determine the length of time for 20 mL to flow through the column. The goal of this was to collect data at column start-up and then to conduct the same test after a period of time running the column to determine changes in permeability. Once this test was completed, the column was started up with 50 mg/L H_2O_2, 200 µg/L cis-DCE, and 50 mg/L bromide in the aforementioned media at a rate of 1 mL/hr. The bromide was added to complete a bromide tracer test and determine the column breakthrough curve. The media solution was added using a 100 mL Hamilton 1000 Series Gastight Syringe attached to a ThermoScientific Orion M361 Sage Syringe Pump. The column setup in terms of the methods for sample collection, influent addition, and general setup of the column and connected tubing was identical to that of the gellan gum bead column. Sampling for DO, cis-DCE and bromide was conducted as described previously in Section 3.5.1. Bromide was removed from the column influent when the effluent bromide levels reached a steady state. Bromide was measured in the column effluent until it fell below the detection level.

In addition to influent and effluent samples, side port samples were also collected. This was done by taking 1 mL of sample, using a plastic 1 mL disposable syringe and needle, from each side port, working from the top port to the bottom port. Samples were filtered with a 25 mm 0.2 µm VWR PTFE syringe filter before conducting sample analysis for *c*DCE, *c*DCE epoxide, and 1-butanol as described in Section 3.1. A summary of the changes made to the column over the course of its operation is presented in Table 3.5.

Table 3.5. Summary of the adjustments made to the PVA/SA bead column throughout its operation. Samples were collected for embryonic zebrafish toxicity testing at 30 PV and 97 PV.

Pore Volumes	Flow Rate (mL/hr)	pH	H_2O_2 (mg/L)	*c*DCE (µg/L)
0 – 6.9	1.0	7.0	50	200
6.9 – 26	1.9	7.0	100	200
26 – 44	1.9	7.0	200	200
44 – 64	1.9	7.5	200	200
64 – 88	1.9	7.5	250	200
88 – 97	1.9	7.9	250	200

3.7 Embryonic Zebrafish Toxicity Testing

Embryonic zebrafish toxicity testing was completed to measure possible toxic compounds generated in the process of aerobic cometabolism of contaminants. This was first done for the TBOS gellan gum batch bottles by taking samples prior, during, and after contaminant transformation. This was done by collecting 2 mL of sample from each of the 2 bottles after a long period of exposure to no contaminants. These samples were collected in 2 mL screw-top glass vials with septum caps to avoid any headspace that could lead to volatilization of compounds. The TBOS bottles were then spiked with ~200 µg/L *c*DCE and samples were collected using the same method. After a significant amount of the *c*DCE had been transformed, samples were collected again. Once nearly all the *c*DCE was transformed but *c*DCE epoxide remained, more samples were collected. Final samples were taken when no *c*DCE or *c*DCE epoxide remained in the bottles.

For the PVA/SA column, samples for embryonic zebrafish toxicity testing were initially collected at 30.1 PV. In an effort to avoid disrupting the column's flow, only samples of 2 mL each were taken from the top and bottom ports as described in Section 3.5.2. 12 mL samples were collected from the influent by disconnecting the influent line from the column and speeding

up the syringe pump. 12 mL were collected from the effluent by replacing the normal 2 mL effluent sample vial with a 12 mL sample vial and allowing it to fill overnight. A second sampling period for the PVA/SA column was conducted at 96.5 PV, collecting only influent and effluent samples using the same method.

Samples were then transported to the Sinnhuber Aquatic Research Laboratory located off the campus of Oregon State University for embryonic zebrafish testing. During transport and storage, samples were kept at 4°C or held on ice. The embryonic zebrafish toxicity testing was conducted by members of the Sinnhuber Aquatic Research Laboratory, and the full method is described thoroughly in Truong, et al. 2017.[170] Embryos were evaluated for the presence or absence of mortality, a curved or bent axis, brain malformations or necrosis, malformed, missing, or smaller than normal eyes, snouts, or jaws, heart or yolk sac malformations, pericardial or yolk sac edema, malformations of the lower trunk, lack of circulation or improper swim bladder formation, notochord distortions, lack of pigmentation, nonresponse to touch, and whether the organism was upright or laying on its side. This information is summarized in Table 3.6. Statistical significance was also determined by the Sinnhuber Lab using Fisher's exact test.

Table 3.6. Summary of embryonic zebrafish toxicity testing endpoints with abbreviations used in results plotting.

Abbreviation	Endpoint	Timepoint (hpf)
MO24	Mortality at 24 hpf	24
SM24	Spontaneous movement	24
MORT	Dies between 24 and 120 hpf	120
AXIS	Curved or bent axis in either direction	120
BRN	Brain malformations or necrosis	120
CRAN	Malformed, missing, or smaller than normal eye, snout, and/or jaw	120
EDEM	Heart and/or yolk sac malformation, pericardial or yolk sac edema (fluid around the heart)	120
LTRK	Malformation of the lower trunk, including caudal fin region	120
MUSC	Lack of circulation, malformation or disorganized/missing somites, and improper swim bladder formation	120
NC_	Notochord distortion	120
PIG_	Lack of pigmentation or overpigmentation	120
TR	Not responsive to touch	120
SIDE	Upright or laying on its side	120

3.8 Bead Compression Testing

Beads were tested for durability by conducting compression tests on individual beads. The method for this test currently not published, but it was obtained from personal communication its developer, Conor Harris.[169] Compressibility of beads was measured for the gellan gum bead column on beads prior to use in the column and on beads taken from the influent and effluent sections of the column after shutdown. The basis of this test was to determine how much compression pressure the beads were able to endure individually as a way

of measuring the strength of the beads. Each bead was compressed between two parallel plates on an ARG2 rheometer. The stress (force/bead area) was measured versus the strain. The compressive modulus was determined as the slope of the linear reversible portion of the resultant data before the bead experienced deformation.

CHAPTER 4 – BATCH REACTOR STUDIES

Batch bottle reactors were created to measure the long-term efficacy of gellan gum beads on the basis of their contaminant transformation potential and durability. These studies were similar to previous studies conducted using gellan gum beads.[9] The main objectives here were to verify the results from these previous studies and to measure for potential toxicity created by the beads using embryonic zebrafish toxicity testing. Batch bottle reactors were created using gellan gum beads containing T2BOS TBOS as an SRS. Abiotic and acetylene controls were created that demonstrated that any significant loss of contaminant mass could be attributed to transformation by the 21198 encapsulated within the beads. The experimental reactors were exposed to several additions of dioxane and *c*DCE to measure the long-term ability to transform the contaminants through aerobic cometabolism. Bead durability was also quantitatively determined through observations. The full results of these batch bottle studies are thoroughly described in the following sections.

4.1 T2BOS Batch Bottle Reactors

Batch bottle reactors were prepared as described in the methods section (3.5), using isobutane grown 21198 coencapsulated with T2BOS in gellan gum hydrogel beads. 8 grams of beads with 0.5 mg TSS / g bead were added to each bottle. Dioxane was added at the time the reactors were created, and *c*DCE was added on day 13. Oxygen within the reactors was measured throughout the course of the study. Results for the mass of oxygen, dioxane, and *c*DCE within the T2BOS batch reactors and the measured *c*DCE peak area within the reactors are displayed in Figure 4.1. Oxygen results illustrate time periods where there may have been insufficient oxygen to transform contaminants. Results for the acetylene controls are displayed in Appendix A.1.

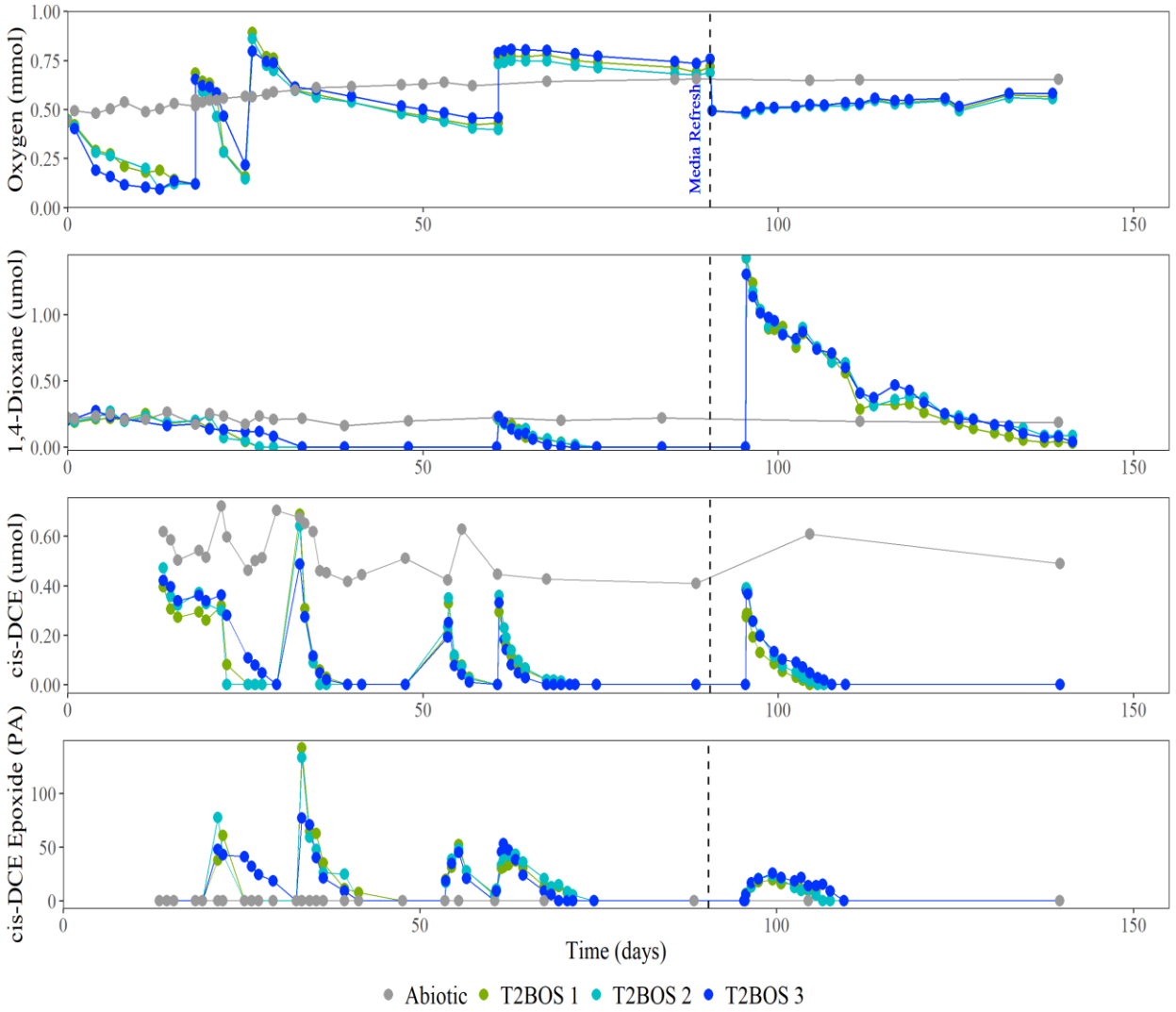

Figure 4.1. Mass of oxygen, dioxane, and *c*DCE, along with *c*DCE epoxide peak area, measured in the T2BOS batch reactors over time. Results from the abiotic control are also displayed. Media was refreshed in the non-control reactors on day 90.

Dioxane did not significantly decrease in the experimental reactors until after the addition of oxygen on day 18. After 33 days of incubation, dioxane fell below detection in the triplicate reactors. A second addition of dioxane on day 60 led to complete depletion in the triplicate reactors on day 74. When the reactors were exposed to approximately 5 times the mass of dioxane on day 95, it took significantly longer to transform it. The reactors were at a low level of oxygen at the time of the first addition of *c*DCE. Significant transformation of *c*DCE did not

occur until additional oxygen was added on day 18. In the reactors T2BOS 1 and T2BOS 2, *c*DCE was transformed to below detection by day 25, while reactor T2BOS 3 reached this point by day 29. This is consistent with the dioxane results, which showed that T2BOS 3 took more time to transform the initial addition. *c*DCE epoxide formation, a transformation product of *c*DCE, was observed once *c*DCE levels began to decrease in the bottles. This supported that *c*DCE depletion was due to aerobic cometabolism from 21198 facilitated by the monooxygenase enzyme. This epoxide rapidly disappeared once the *c*DCE was depleted, which indicates that the 21198 was also able to transform this compound. Peak area given by the GC-ECD was measured due to the lack of a *c*DCE epoxide standard.

The first-order transformation rates for dioxane are summarized in Table 4.1. While the rates for the first two T2BOS reactors stayed relatively the same between the initial spike and the second addition, the rate increased by 8-fold for T2BOS 3. The biomass within this reactor likely increased over time. However, the rate was double in T2BOS 3 for the second addition when compared to T2BOS 1 and T2BOS 2. There was significant variability even between triplicate reactors. It should be noted that the final addition of dioxane was ~6 times as large as the previous two additions, which may have impacted the first-order rates of transformation as well as impacted the health of the biomass.

Table 4.1. First-order dioxane transformation rates for the T2BOS gellan gum batch bottle reactors based on the day the contaminant was added. Rates are normalized to the initial mass of beads.

	T2BOS 1	T2BOS 2	T2BOS 3
Day	Rate (1/d-g bead)	Rate (1/d-g bead)	Rate (1/d-g bead)
0	0.028	0.030	6.9E-03
60	0.034	0.027	0.057
95	9.8E-03	7.2E-03	8.0E-03

All three T2BOS non-control bottles were subjected to five additions of *c*DCE. The first order rates of transformation for these spikes are summarized in Table 4.2, normalized to the mass of beads initially in each reactor. Rates were not obtained for each addition in every bottle due to an insufficient number of data points in some cases.

Table 4.2. First-order *c*DCE transformation rates for the T2BOS gellan gum batch bottle reactors based on the day the contaminant was added. Rates are normalized to the initial mass of beads.

	T2BOS 1	T2BOS 2	T2BOS 3
Day	Rate (1/d-g bead)	Rate (1/d-g bead)	Rate (1/d-g bead)
13	0.028	8.0E-03	0.029
32	0.11	0.13	0.11
53	0.098	0.11	0.13
60	0.048	0.047	0.082
95	0.043	0.043	0.031

As with dioxane, the rate of transformation increased from the first addition to the second addition for each of the three reactors. However, the rates then decreased with successive additions. The final addition of *c*DCE occurred concurrently with the largest addition of dioxane, which could partially explain the lower rates. It is possible this amount of dioxane negatively impacted the microbial biomass or moderately inhibited *c*DCE transformation. However, the media was refreshed on day 90 in these bottles, which should have led to more microbial growth due to an influx of nutrients. This was not evident based on either the *c*DCE or the oxygen results. With this final addition, the peak *c*DCE epoxide was lower than during any of the other additions, further supporting a lower rate of transformation and a smaller microbial community. A greater amount of *c*DCE epoxide would indicate that the *c*DCE was being transformed more rapidly. Conversely, the highest levels of *c*DCE epoxide were measured after the second *c*DCE addition, which is also when the highest rates of transformation were recorded. Oxygen levels

remained fairly constant after the final *c*DCE addition despite cometabolic transformation taking place.

The rates of oxygen consumption for each addition are displayed in Table 4.3. For these batch bottle reactors, oxygen consumption followed a first-order trend. Oxygen consumption increased from the first addition to the second addition, suggesting a higher microbial presence. However, oxygen consumption decreased with successive additions. The rate eventually slowed such that a rate could not be estimated. It is speculated that the rate of oxygen consumption was lower than the rate that oxygen entered the reactors during liquid sampling due to a vacuum that developed and leaks through the septa. The septa had not been replaced and were punctured many times.

Table 4.3. First-order rates for oxygen utilization within the T2BOS gellan gum bead batch bottle reactors normalized to the initial mass of beads.

	T2BOS 1	T2BOS 2	T2BOS 3
Day of Spike	Rate (1/d-g bead)	Rate (1/d-g bead)	Rate (1/d-g bead)
0	9.0E-03	0.010	0.016
18	0.029	0.028	0.020
26	2.7E-03	2.5E-03	2.1E-03
67	6.1E-04	5.6E-04	4.9E-04

Figure 4.2 shows a comparison between the T2BOS 1 gellan gum bead batch bottle reactor at the start of the study and 47 days into batch incubation. In the image from the start date, there are translucent bead particles present. In the later image, the beads appeared as a filmy substance sitting on top of the media. The media itself also became cloudy, suggesting the beads had broken apart. The T2BOS beads used in this study were not structurally strong, and it is possible this affected the long-term effectivity of 21198 within the reactors.

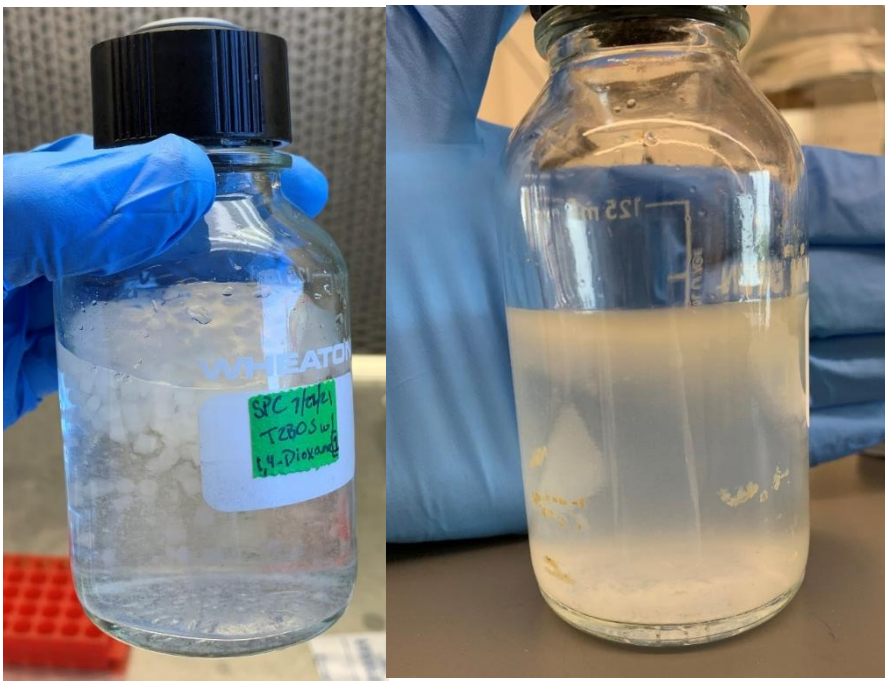

Figure 4.2. Images of the T2BOS 1 gellan gum bead batch reactor taken at the start of the study (left) and taken 47 days into the study (right).

There is also evidence that contaminant transformation had an impact on the beads' integrity. Figure 4.3 shows a comparison of two batch bottles 140 days into the study. The image on the left is from the T2BOS 1 batch bottle, which at that point had been exposed to and transformed *c*DCE and dioxane multiple times. The image on the right is from an acetylene control reactor. This bottle had also been exposed to *c*DCE and dioxane, but the acetylene within the bottle inhibited the monooxygenase enzyme from conducting transformation by cometabolism (Appendix A.1). The acetylene controls consumed oxygen, which supported that microbial growth was taking place. The lack of a decrease in dioxane and no *c*DCE epoxide being observed indicated that these reactors were successfully inhibited from conducting aerobic cometabolism, despite their significant oxygen consumption. It is also notable that their oxygen consumption differed from the non-control reactors. While they similarly showed higher rates of consumption early on (<50 days), their oxygen consumption remained significantly more

consistent throughout the incubation period (Appendix A.1). This further indicates that the acetylene control reactors had a healthier microbial population than the non-control T2BOS reactors by the end of the incubation period.

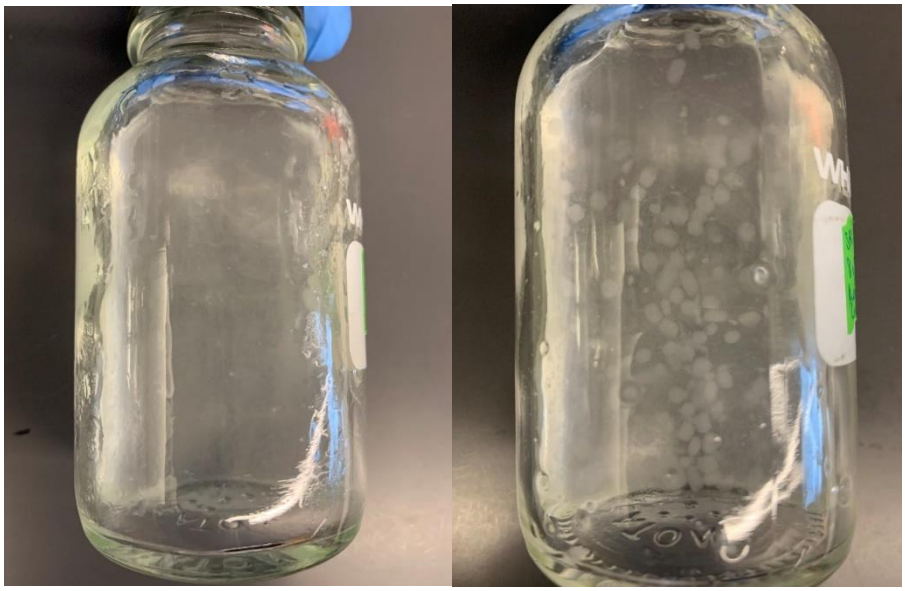

Figure 4.3. Images of the first T2BOS gellan gum bead non-control batch reactor (left) and the first T2BOS gellan gum bead acetylene control batch reactor (right) taken 140 days into the study.

The beads in this acetylene control batch reactor in the picture were much more intact than in the T2BOS 1 bottle. The T2BOS 1 bottle was devoid of recognizable beads by this point, with the bottle instead containing a cloudy media solution. The trend was the same for all three T2BOS non-control reactors when compared to both T2BOS acetylene control reactors. This suggests that the transformation of contaminants through aerobic cometabolism may have impacted the structure of the beads. The epoxide formed during *c*DCE transformation may have contributed to this. The acetylene control reactors were also exposed to significantly less contaminants on a total mass basis, which also could have contributed.

4.2 TBOS Batch Bottle Reactors

4.2.1 Dioxane and *c*DCE Rate Studies

Reactors were also created using gellan gum beads with TBOS as an SRS to measure the long-term effectiveness of these beads and to compare results to the T2BOS batch reactors. Batch bottle reactors were prepared as described in the methods section (3.4), using isobutane grown 21198 coencapsulated with TBOS in gellan gum beads. Due to a limited amount of beads being available, only duplicate reactors were created and only 3 grams of beads with 0.5 mg TSS / g bead were added to each reactor. As with the T2BOS bottles, dioxane was added upon creation of the bottles and *c*DCE was added on day 13. Oxygen consumption was monitored throughout, and oxygen was added to the bottles when oxygen reached the detection limit of ~5% (v/v) of the headspace. Results for the mass of oxygen, dioxane, and *c*DCE within the T2BOS batch reactors and the measured *c*DCE peak area within the reactors are displayed in Figure 4.4. Oxygen results illustrate when the reactors had sufficient oxygen to carry out the cometabolic transformation.

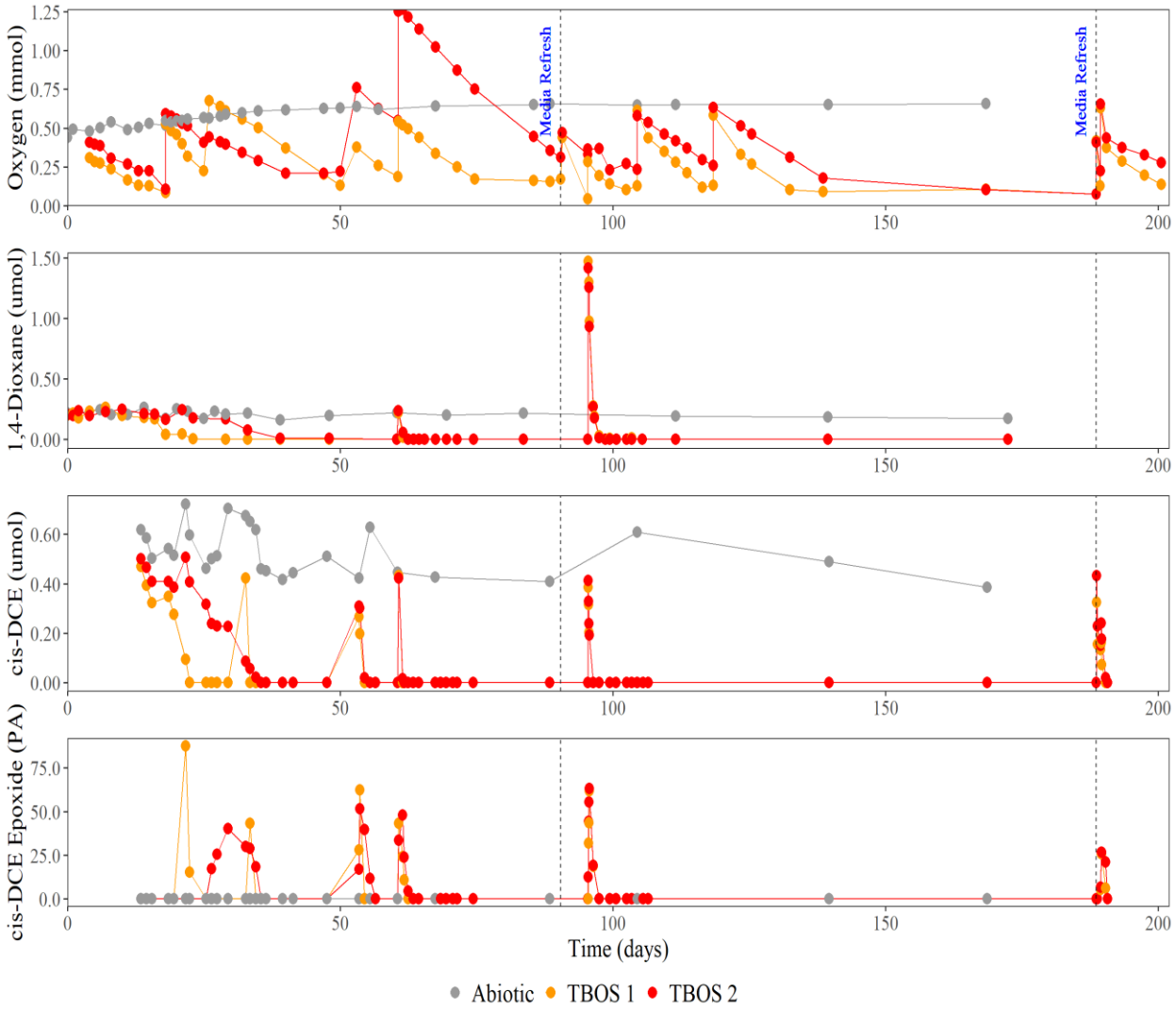

Figure 4.4. Mass of oxygen, dioxane, and *c*DCE, along with *c*DCE epoxide peak area, measured in the TBOS batch reactors over time. Results from the abiotic control are also displayed. Media was refreshed in the non-control reactors on days 90 and 188.

Depletion of the dioxane took a significant amount of time, despite the presence of oxygen being observed initially. After adding oxygen on day 18, dioxane transformation rapidly occurred in the TBOS 1 reactor. There was a longer lag period for the TBOS 2 bottle, but the dioxane was essentially completed removed by day 60. The bottles were exposed to dioxane two more times, on days 60 and 95, with the last addition being approximately 6 times the mass of the previous two additions. In these final two additions, dioxane was rapidly transformed without

a lag period, suggesting the bottles had sufficient oxygen and biomass. The additions of oxygen on day 18 also helped initiate the cometabolic transformation of *c*DCE within the reactors. Consistent with the dioxane results, the lag period for *c*DCE transformation was longer for TBOS 2 than TBOS 1. A second addition of *c*DCE was made to TBOS 1 on day 32 while TBOS 2 was still transforming the initial addition. *c*DCE was added to TBOS 1 and TBOS 2 six times and five times, respectively. All additions were of similar total mass. The final addition came after a two month long anaerobic period, but the reactors continued to show the ability to rapidly transform *c*DCE. However, the rate was significantly lower than the previous rate, likely indicating that the extended period without oxygen had a negative impact on biomass. The consistent appearance of *c*DCE epoxide following the additions of *c*DCE indicated that transformation was due to aerobic cometabolism. The results for the abiotic control show that the losses from the bottle for oxygen, dioxane, and *c*DCE were negligible.

The first-order rates of transformation for each dioxane addition are presented in Table 4.4, with rates omitted when there were insufficient data points. The rates are normalized to the mass of beads initially in each reactor. As there was a long delay, the rates for the first addition were obtained after the lag period. The rate of transformation increased significantly in both reactors from the first addition to the final addition, despite the final addition containing significantly more dioxane, which could have been harmful to the overall biomass. The final rate was 10-fold higher than the initial rate in TBOS 1, and the final rate was 17-fold higher than the initial rate in TBOS 2. These increases in transformation rates and the demonstrated consistent oxygen demand in both reactors (Figure 4.4) support that there was a significant increase in biomass within the reactors over time.

Table 4.4. First-order dioxane transformation rates for the TBOS gellan gum bead batch reactors by the day the contaminant was added. Rates are normalized to the initial mass of beads. Missing rate data is due to an insufficient number of data points being collected.

	TBOS 1	TBOS 2
Day	Rate (1/d-g bead)	Rate (1/d-g bead)
0	0.065	0.043
60	--	--
95	0.64	0.73

First-order rates of transformation for *c*DCE are summarized in Table 4.5. Rates were not calculated when the *c*DCE was transformed too rapidly to collect a sufficient number of data points. The rate of transformation of the initial addition was nearly twice as high for the first reactor compared to the second reactor. As the conditions they were exposed to were the same, this indicates some variance between the reactors. During this same period, the rate of oxygen consumption was also higher for TBOS 1 compared to TBOS 2. The rates of *c*DCE transformation indicate a greater microbial population was present in TBOS 1 in the early stages. However, final *c*DCE addition led to higher transformation rates in TBOS 2 than in TBOS 1. This suggests that the biomass of 21198 within the reactors changed significantly over time. This is evidence of that potential differences in the initial biomass was not hugely important for the long-term success of the hydrogel beads.

Table 4.5. First-order *c*DCE transformation rates for the TBOS gellan gum bead batch reactors by the day the contaminant was added. Rates are normalized to the initial mass of beads. Missing rate data is due to an insufficient number of data points being collected.

	TBOS 1	TBOS 2
Day	Rate (1/d-g bead)	Rate (1/d-g bead)
13	0.14	0.084
32	--	--
53	--	1.0
60	--	--
95	1.2	1.2
188	0.32	0.52

The rates of utilization for each oxygen addition and the mean rates are summarized in Table 4.6, with rates excluded when there were insufficient data points. The rates were zero-order for the TBOS reactors, which was a difference from the first-order rates demonstrated by the T2BOS reactors. From days 138 to 188, the bottles were depleted of oxygen. Despite this, the reactors immediately began consuming oxygen at a similar rate to previous spikes when oxygen was reintroduced (Figure 4.4). The rates of oxygen consumption were relatively consistent throughout the operating period of the reactors, indicating a steady microbial population being present.

Table 4.6. Zero-order oxygen utilization rates for the TBOS gellan gum bead batch reactors by the day oxygen was added. Rates are normalized to the initial mass of beads. Missing rate data is due to an insufficient number of data points being collected.

	TBOS 1	TBOS 2
Day	Rate (mmol/d-g bead)	Rate (mmol/d-g bead)
0	5.5E-03	6.8E-03
18	1.5E-02	8.8E-03
26	7.7E-03	5.7E-03
53	8.4E-03	9.3E-03
60	9.0E-03	1.1E-02
90	--	--
95	8.3E-03	5.2E-03
104	1.3E-02	7.8E-03
118	1.1E-02	7.5E-03
188	--	--
190	7.4E-03	7.1E-03
Mean	9.5E-03	7.7E-03

While the durability of the beads was an issue in the T2BOS bottles, it was not an issue to the same extent within the TBOS gellan gum batch bottles. Figure 4.5 shows an image of the TBOS 1 batch bottle at the end of the study. The beads shrunk considerably over the course of the study, but bead particles are still visible in this image, which was not true of the T2BOS beads. The orange tinge in this image is also evidence of significant 21198 growth, which is

consistent with the results from the dioxane and *c*DCE transformation.[11] These bottles were made with the same gellan gum formulation as the T2BOS bottles aside from the slow-release substrate used. However, the two sets of beads were made in separate batches. This suggests that unintended variations in the bead creation process may have led to the differences between the beads.

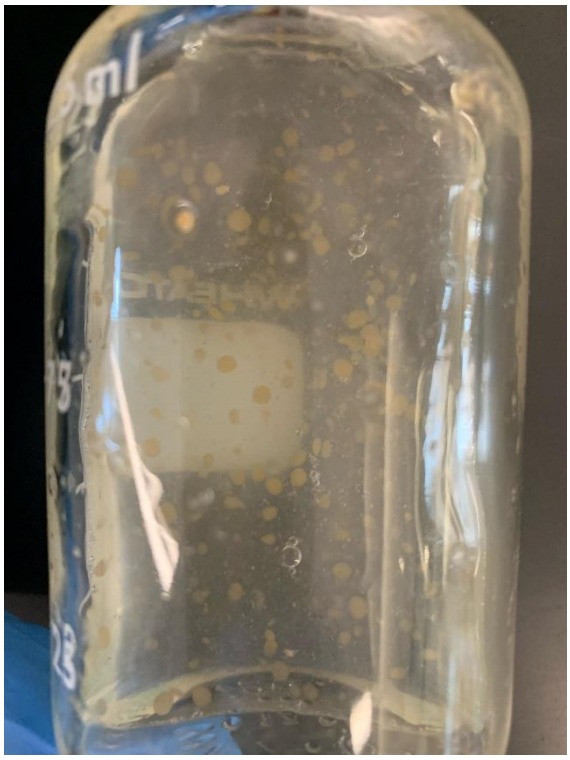

Figure 4.5. Image of the TBOS 1 gellan gum bead batch reactor taken at the end of the batch bottle study.

4.2.2 TBOS Batch Reactor Zebrafish Toxicity Study

One goal from the bead batch bottle experiments was to determine whether the cometabolic transformation of contaminants leads to the generation of toxic products. To do this, an embryonic zebrafish toxicity study was conducted. On day 188 of the batch bottle experiments, *c*DCE was added to the two TBOS batch reactors for a final time. Before this addition, a sample was collected from each reactor to use as an initial sampling point in the

toxicity study, labelled “Control.” After adding *c*DCE to the reactors, samples were immediately collected and labelled “Peak” samples. Samples were also collected when there was a moderate amount of *c*DCE and *c*DCE epoxide present, labelled “Mid,” and when there was a low level of *c*DCE present but a considerable amount of epoxide, termed “Epoxide.” The mass of *c*DCE and the peak area of epoxide in the reactors are displayed in Figure 4.6, along with the labels for each sampling point. The process for this is more thoroughly described in the Methods section (3.6). These collected samples were all sent for embryonic zebrafish toxicity testing.

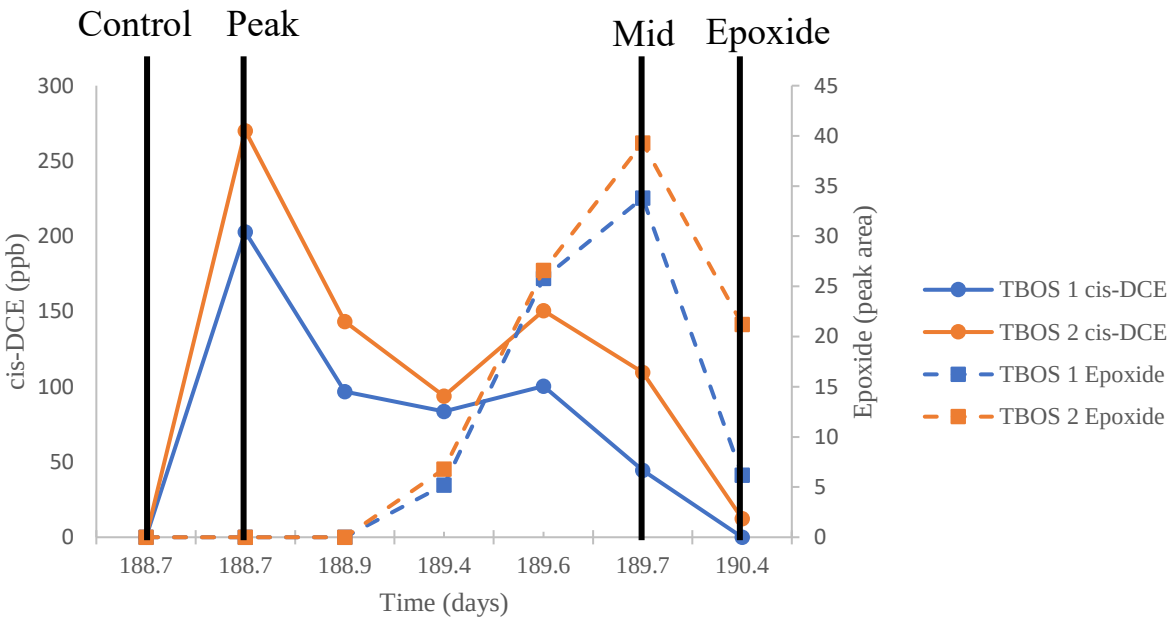

Figure 4.6. Results of the final *c*DCE spike in the TBOS gellan gum batch bottles for *c*DCE concentrations and *c*DCE epoxide peak areas. Labels are provided for the time points when samples were collected for embryonic zebrafish toxicity testing.

The results of the embryonic zebrafish toxicity study are shown in Figure 4.7. The methods for how these results were obtained and how significance was determined are described in the Methods section (3.7). The endpoints tested and their definitions are listed in Table 3.6. Studies were completed at 10x dilution and at 100x dilution. Parathion was used as a positive control.

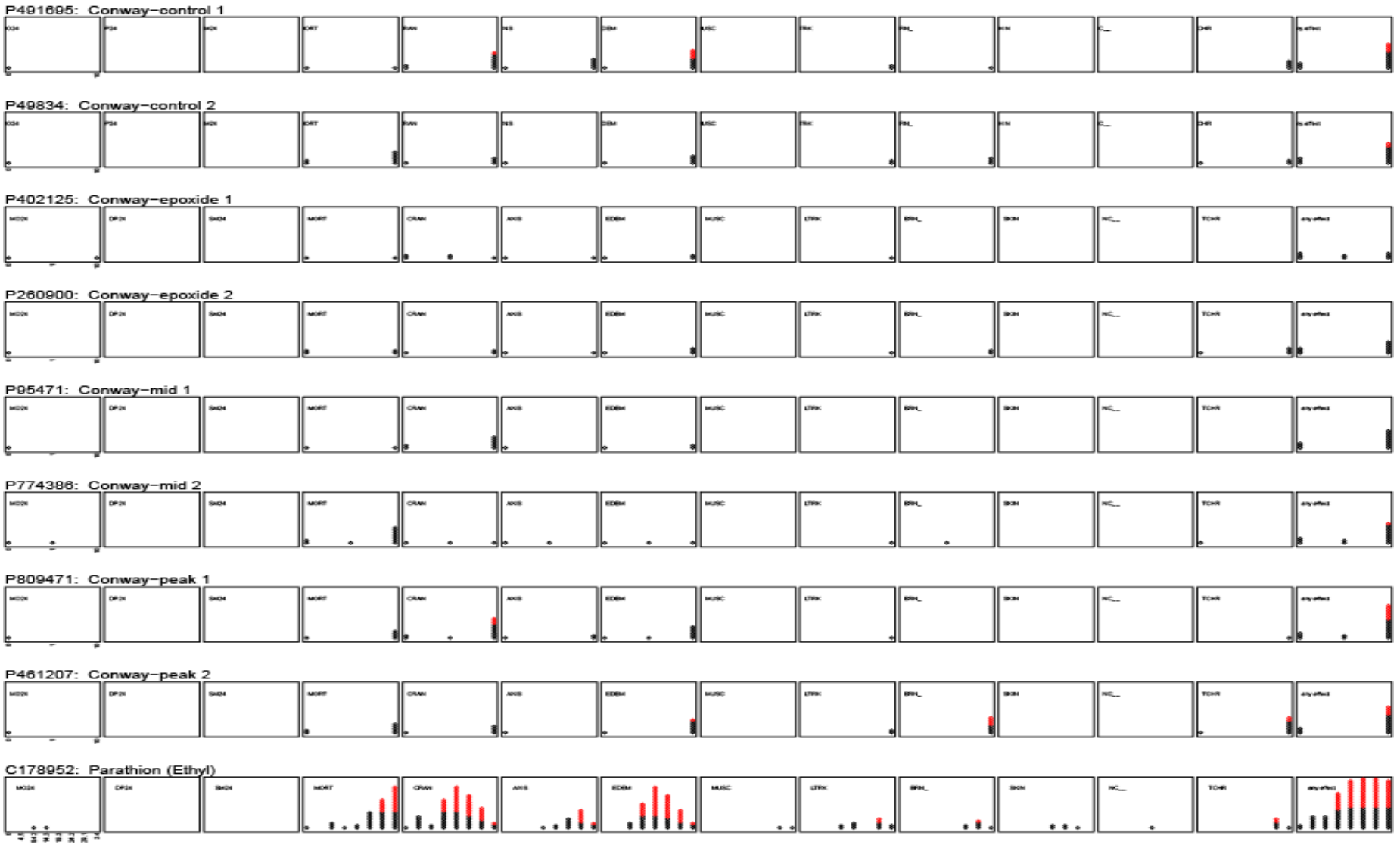

Figure 4.7. Results for the embryonic zebrafish toxicity tests conducted using the TBOS gellan gum batch reactors. Results are provided for, from the top row of plots down, the two samples taken prior to *c*DCE addition, the two samples taken immediately following *c*DCE addition, the two samples taken after significant *c*DCE transformation, the two samples taken when *c*DCE was negligible, and a positive control. The result is more significant when there are greater number of red dots. The statistical analysis for this test is provided in the Methods section (3.7) and the tested endpoints are presented in Table 3.6.

For the “Control” samples, significance was achieved for the malformed/missing/small eye, snout and/or jaw endpoint, the edema endpoint, and the any effect endpoint for “Control 1” at 10x dilution. “Control 2” showed significance for the any effect endpoint at 10x dilution. These controls were meant to be negative controls for toxicity, so these results make it difficult to draw conclusions from the rest of the samples. “Peak 1” showed significance for the malformed/missing/small eye, snout and/or jaw endpoint and the any effect endpoint for the 10x diluted sample. “Peak 2” showed significance for the edema endpoint, the brain malformation endpoint, the nonresponse to touch endpoint, and the any effect endpoint for the 10x diluted sample. “Mid 1” did not reach the significance threshold for any endpoints. “Mid 2” only showed significant results for the any effect endpoint at 10x dilution. Neither “Epoxide 1” or “Epoxide 2” reached any significance thresholds. Due to the samples taken prior to the *c*DCE spike showing significance for several endpoints, it is difficult to draw any conclusions about the toxicity of *c*DCE and its transformation products. The media itself was likely toxic to the zebrafish embryos. A proposed reasoning for this is that there was a build-up of 1-butanol within the bottles due to a lack of oxygen. These batch bottles had been anaerobic for two months, which would have allowed for a large build-up of 1-butanol within both bottles. Oxygen was added to the bottles right before the bottles were spiked, so there was likely still a substantial volume of 1-butanol remaining that had not yet been depleted by the 21198. A study on embryonic zebrafish toxicity showed evidence of moderate toxicity to zebrafish at levels as low as 50 mg/L 1-butanol.[171] As the microorganisms had time to degrade the *c*DCE, they also had time to consume the 1-butanol. This would explain why toxicity decreased over time in the samples. Despite this, it is encouraging that the samples with the lowest level of *c*DCE after the *c*DCE spike did not show toxicity. This suggests that there is no highly toxic compound that

remains after *c*DCE is transformed, as this would have meant significant toxicity in the “Mid” and “Epoxide” samples. Further testing with media free of 1-butanol would allow for better confirmation of this.

4.3 Batch Bottle Reactor Comparisons

The T2BOS gellan gum batch reactors and the TBOS gellan gum batch reactors exhibited significant differences over the course of their incubation periods. The primary difference can be seen by comparing their oxygen consumption data. Figure 4.8 displays the total oxygen consumption for the T2BOS and TBOS reactors. The T2BOS bottles rapidly utilized oxygen in the early stages of incubation before leveling off after about 50 days. In the later stages, oxygen consumption was so low that it was recorded as a slight negative because the vacuums within the reactor bottles were pulling in more oxygen during liquid sampling than was being consumed by the 21198 within the bottles. There was also potential leakage through the septa that had not been replaced. In contrast, the oxygen consumption for the TBOS bottles was fairly linear throughout the entire monitoring period, only flatlining when the bottles ran out of oxygen, which is especially evident from days 138 to 188. Initially, the T2BOS reactors consumed more total oxygen than the TBOS bottles. This trend lasted until ~50 days into the experiment, from which point the TBOS reactors consumed significantly more oxygen.

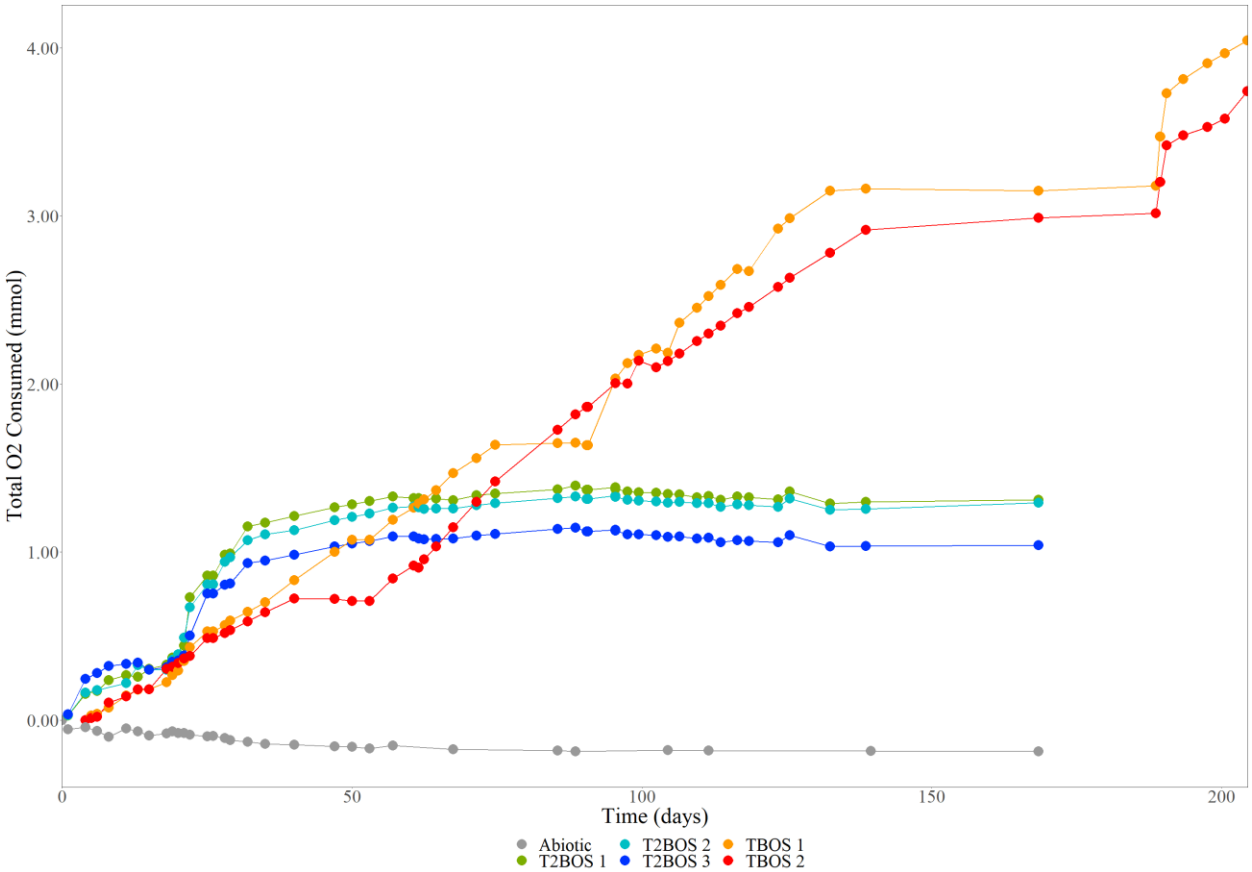

Figure 4.8. Total oxygen consumed (mmol) by each T2BOS and TBOS gellan gum batch reactor over the monitoring period. An abiotic control without added biomass is also displayed.

Figure 4.9 and Figure 4.10 showcase this by displaying the rates of oxygen utilization for each reactor based on the day the addition was made normalized to the initial bead mass. The rates cannot be directly compared due to the first-order trend of the T2BOS reactors and the zero-order trend of the TBOS reactors. The rates fell off sharply for the T2BOS reactors over time while they stayed relatively stable for the TBOS reactors, even after the TBOS reactors experienced 2 months of anaerobic conditions. One possibility is that the contaminant additions were more stressful for the T2BOS biomass due to the longer exposure due to their lower transformation rates when compared to the TBOS reactors. This also meant that there was also a longer period of exposure to *c*DCE epoxide, which could lead to additional toxicity.

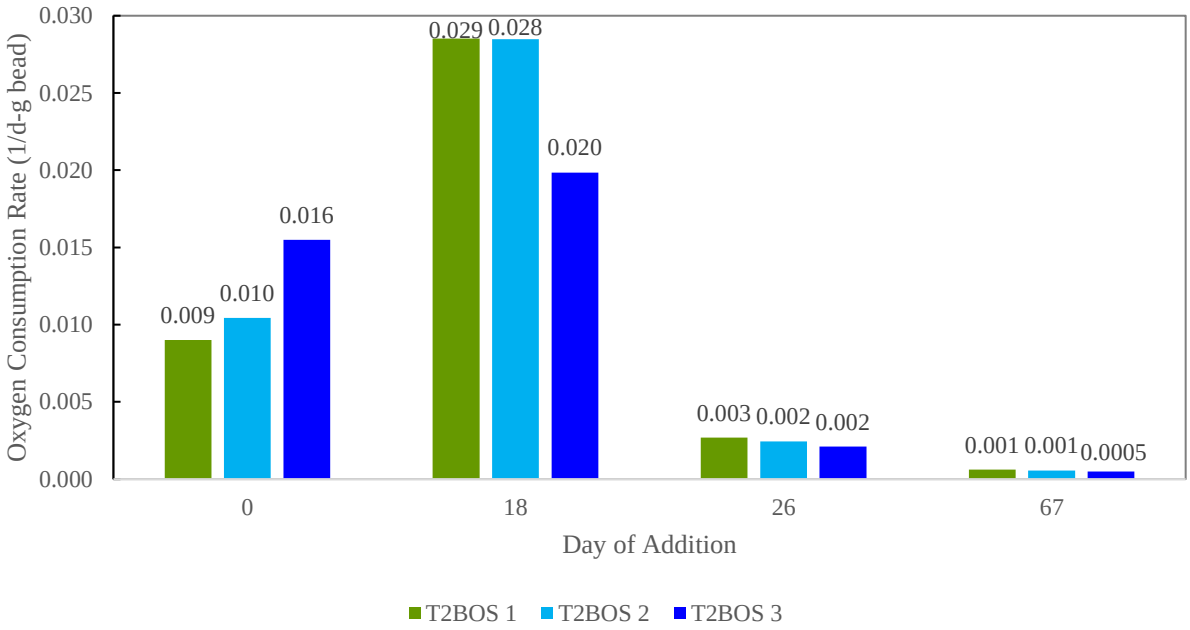

Figure 4.9. First-order oxygen consumption rates for the T2BOS gellan gum batch reactors normalized to the initial bead mass. Later spikes are excluded due to rates of utilization being lower than the rate oxygen entered the batch bottles through the vacuum created while conducting liquid sampling.

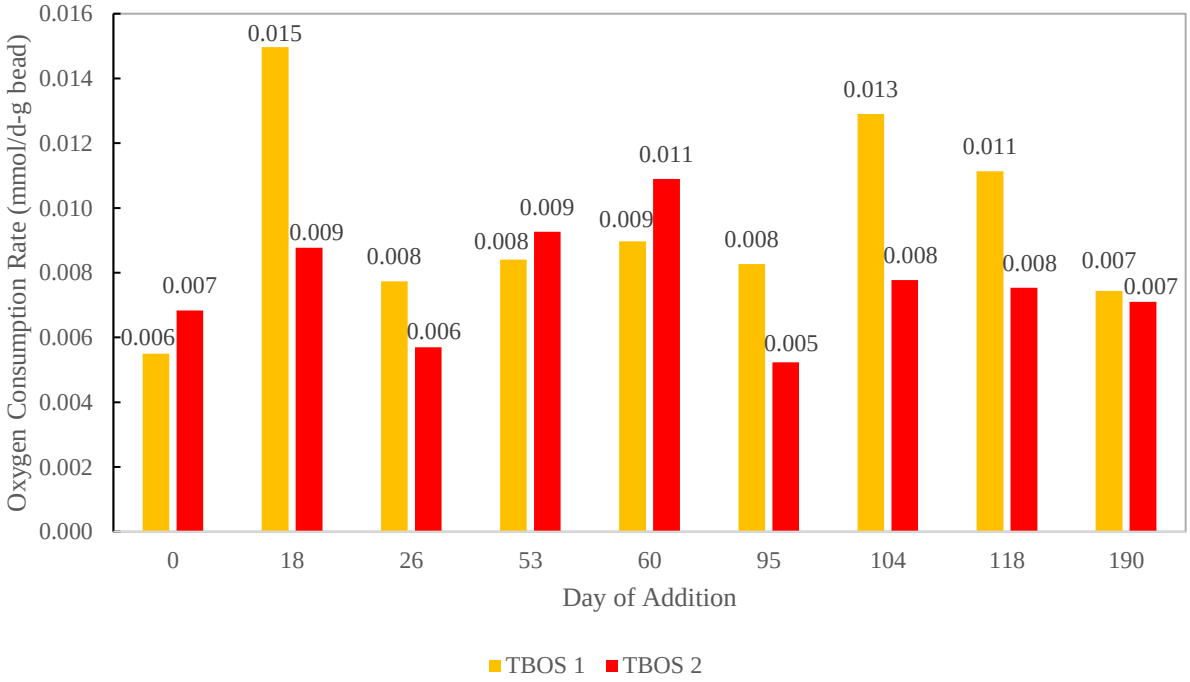

Figure 4.10. Zero-order oxygen consumption rates for the TBOS gellan gum batch reactors normalized to the initial bead mass.

The first-order transformation rates of dioxane are displayed for each of the batch reactors in Figure 4.11 by the day of the addition and normalized to the initial bead mass. For the first addition, the T2BOS and TBOS reactors had similar rates. However, the rates for the T2BOS reactors did not increase significantly for the second addition and decreased significantly for the final addition. The TBOS reactors instead showed a large increase in rate of transformation by the final addition. Rates were not determined for the TBOS reactors at 60 days due to an insufficient number of data points, but this does also indicate a faster rate than the T2BOS reactors, as they were sampled concurrently. This is consistent with the oxygen data as well. The constant oxygen demand exhibited in the TBOS reactors indicated a consistently increasing biomass within the bottles, and this rate data supports that. The dioxane introduced to all reactors at 95 days was ~6 times the mass of the previous two additions, and this may have negatively affected the biomass within the reactors.

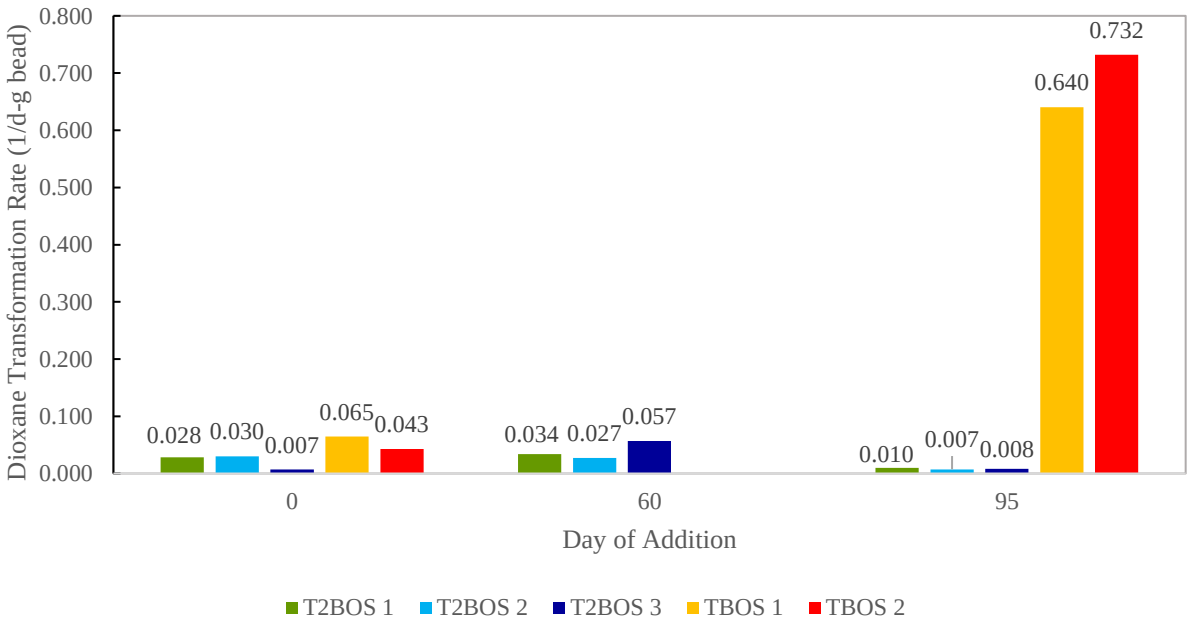

Figure 4.11. First-order dioxane transformation rates for the T2BOS and TBOS gellan gum bead batch reactors normalized to the initial bead mass.

The first-order *c*DCE transformation rates for each reactor are displayed in Figure 4.12 by the day of the addition and are normalized to the initial bead mass. Missing TBOS values are due to insufficient data points to calculate a rate. Because the T2BOS and TBOS reactors were sampled at the same time, this does suggest that the TBOS reactors had faster rates in these cases. There are no T2BOS values for the addition at 188 days because this addition was exclusive to the TBOS reactors.

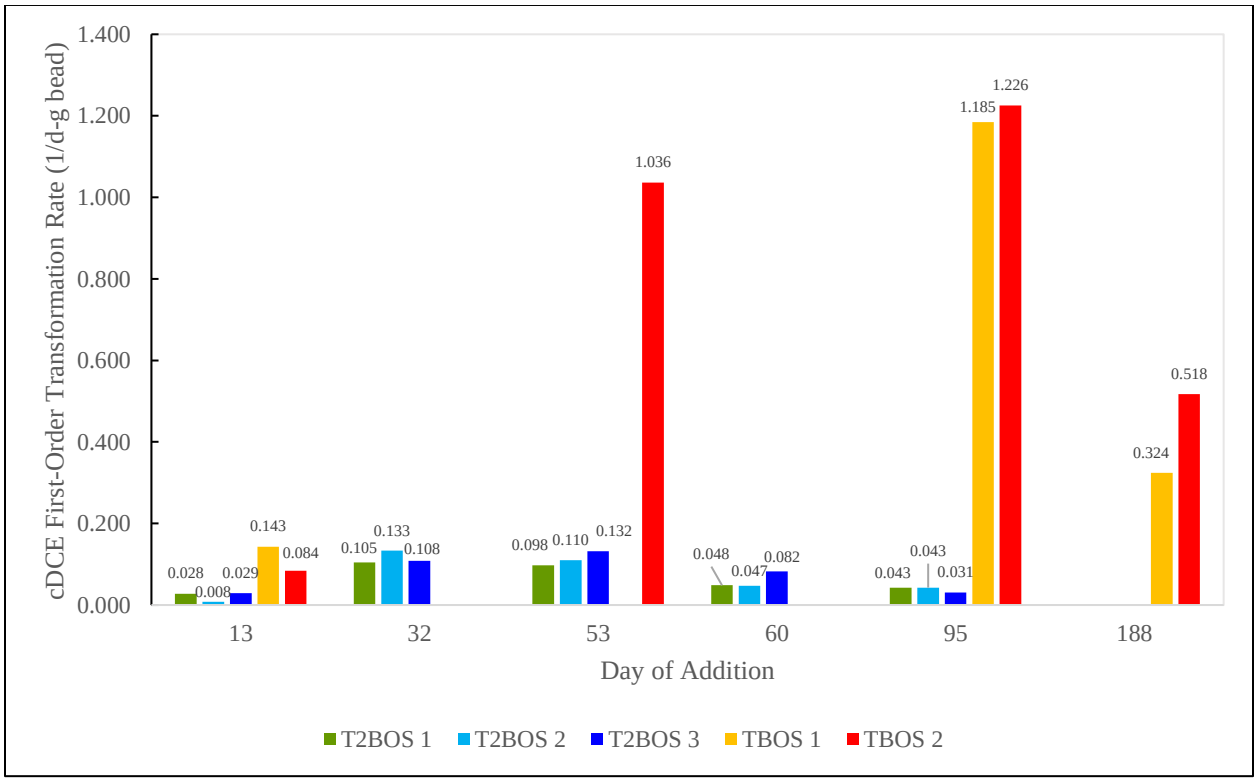

Figure 4.12. First-order *c*DCE transformation rates for the T2BOS and TBOS gellan gum bead batch reactors normalized to the initial bead mass. Missing TBOS data can be attributed to insufficient data points. There is no T2BOS data for the addition at 188 days as this was exclusive to the TBOS batch reactors.

As with the dioxane rates, the *c*DCE transformation rates were similar in the early stages between TBOS and T2BOS reactors. However, there was a more significant difference between the T2BOS and TBOS rates for the first addition of *c*DCE than for the first addition of dioxane. It took until the second addition for the T2BOS rates to match the transformation rates of the first

addition for the TBOS bottles. The T2BOS rates then did not increase for the third addition, at 53 days, and then decreased for the fourth and fifth additions at 60 and 95 days, respectively. In contrast, the TBOS rates increased significantly by the fifth additions at 95 days. The rates measured for this addition were approximately 30 times larger for the TBOS reactors than for the T2BOS reactors. This is consistent with the dioxane rate data, which indicated significantly higher rates of transformation in the TBOS reactors during the final dioxane addition. As previously mentioned, the TBOS reactors showed consistent oxygen demand throughout the study, suggesting steady 21198 growth. The T2BOS reactors did not demonstrate significant oxygen demand in the later stages of the study, after approximately 50 days of incubation. These *c*DCE transformation rates further support that the TBOS reactors were significantly more bioactive by the end of the study. The decrease in rates seen in the TBOS reactors for the addition at 188 days was likely due to the reactors spending 2 months without oxygen. While this may have negatively impacted biomass, the transformation rates at 188 days for the TBOS reactors were still higher than the T2BOS reactors demonstrated at any time point. In both the TBOS and the T2BOS reactors, *c*DCE was transformed at approximately twice the rate of dioxane when additions were made concurrently, suggesting *c*DCE is more readily transformed through aerobic cometabolism.

A previous study conducted by Rasmussen at al (2020) demonstrated significantly different results than the batch reactor studies presented here, although it should be noted that 1,1,1-TCA was present in these studies.[9] This study, completed using both T2BOS gellan gum beads and TBOS gellan gum beads co-encapsulated with 21198, did not have the bead durability issues observed in the T2BOS beads here. The beads did not fall apart like they did in this study. The bead formulation was the same, so this suggests that there was an issue with the fabrication.

The previous study did observe decreasing rates of transformation in the T2BOS reactors like this study. The rates of transformation for *c*DCE and dioxane were on the same order of magnitude between both studies for the T2BOS reactors. This was also true of the TBOS reactors for the first contaminant additions. However, the previous study observed decreasing rates of transformation for the TBOS reactors, while increasing transformation rates were observed here. Oxygen consumption was consistent between the two studies, with TBOS reactors necessitating significantly more oxygen additions over the course of the incubation periods. The results from these batch reactors presented here are consistent with the abiotic hydrolysis studies conducted by Rasmussen et al., indicating higher rates of substrate release and biomass growth when TBOS was present compared to T2BOS.

CHAPTER 5 – COLUMN STUDIES

Two separate column studies were conducted to determine the long-term contaminant transformation efficacy of 21198 coencapsulated beads. The first study was conducted using a T2BOS gellan gum bead pack, with the same batch of beads used for the reactor studies in Section 4.1. The objectives for this study were to measure the long-term ability to transform dioxane and *c*DCE through aerobic cometabolism, as well as to determine the effects this process had on bead durability. The second study was conducted using a TBOS PVA/SA gellan gum bead pack. The objectives for the second column study were to measure the long-term ability to transform *c*DCE through aerobic cometabolism and to determine, using embryonic zebrafish toxicity tests, whether this process released any toxic byproducts. Further objectives were to measure bead durability and changes to the permeability of the column over time. The full results for these two column studies are presented in the following sections.

5.1 Gellan Gum Bead Column

The gellan gum bead column was fabricated as described in the Methods section (3.5.1) using gellan gum beads co-encapsulated with isobutane grown 21198 and T2BOS. This was the same batch of beads used for the batch reactor studies in Section 4.1. An image of the column before startup is shown in Figure 5.1. Upon column startup, contaminants were not added to the column. The initial goal was to conduct a bromide tracer experiment to determine the retardation factor that the beads would have on contaminants. The pore volume (PV) of the column was measured as 26 mL, and at a flow rate of 1 mL/hr, an estimated 0.92 PV of influent feed solution was injected into the column each day. The influent feed solution was 10x diluted phosphate buffer MSM (Table 3.2).

Figure 5.1. Image of the T2BOS gellan gum bead column taken at the start of its operation.

For the bromide tracer test, 30 mg/L of bromide was added to the influent feed solution, which was then fed into the column using the influent syringe. The results of the bromide tracer test are displayed in Figure 5.2. The dashed line represents when bromide was removed from the influent feed solution. Approximately 10 days were required for the effluent bromide concentration to reach a steady state. The average HRT was obtained by determining the number of PVs for the effluent concentration to reach 50% of the influent concentration, which was 5.4

PVs. It took 5.4 times as long for the bromide to pass through the column than PV estimated based on the measured porosity. While bromide is not the same compound as dioxane and *c*DCE, the results indicate that the flow of contaminants through the column should be retarded. This is likely the result of diffusion into the gellan gum beads, which is consistent with observations from a previous similar column study conducted using gellan gum beads.[172] The elution curve of the bromide differed from the breakthrough curve. Once bromide was removed from the influent feed at 14 PV, bromide fell below detection level in the effluent after only 6.9 PV. It reached 50% of the steady state concentration 3.2 PV after bromide was eliminated from the influent feed solution. Bromide appeared to more readily diffuse out of the beads than diffuse into the beads.

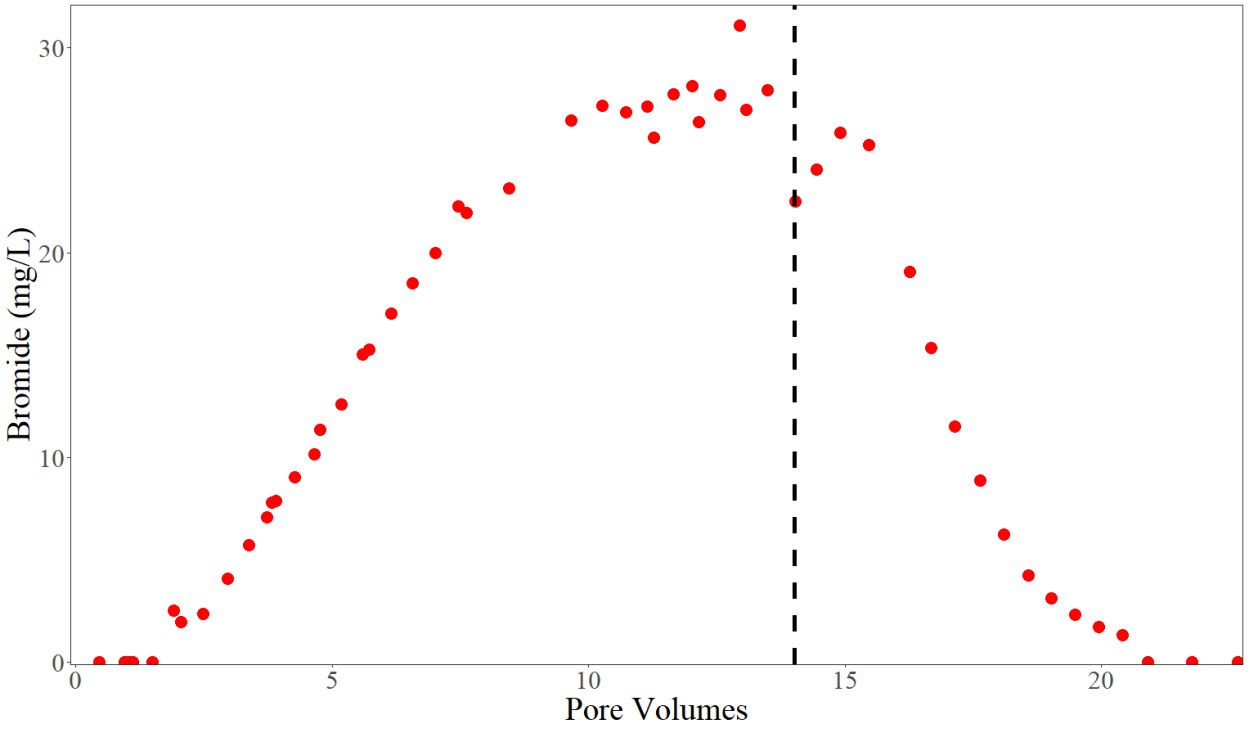

Figure 5.2. Bromide concentrations measured during the gellan gum bead column bromide tracer test versus the pore volumes of flow. The dashed line represents when bromide was removed from the influent feed solution.

The physical transport parameters of the gellan gum bead column are summarized in Table 5.1. The bromide retardation factor was 5.4, based on the results of the bromide tracer

study. This retardation factor may vary based on the contaminant. It does demonstrate that bromide diffused into the hydrogel bead pack which resulted in retarded transport. While the HRT was determined to be 26 hours based on the estimated porosity of the bead pack, the retarded transport time based on the bromide tracer study would be 5.4 times as long.

Table 5.1. Summary of the physical transport parameters determined for the gellan gum bead column.

Parameter	Value	Units
Column Length	20	cm
Cross Sectional Area	7.9	cm^2/hr
Mass of Beads	92	g
Volume	120	mL
Pore Volume	26	mL
Porosity	0.22	--
Flow Rate	1.0	mL/hr
Superficial Velocity	0.13	cm/hr
Average Linear Velocity	0.78	cm/hr
Retention Time	26	hr
Bromide Retardation Factor	5.4	--

During this bromide tracer study, the beads were not exposed to contaminants. In the first phase of the column, the main objective was to conduct the bromide tracer test and ensure that enough oxygen was present such that the microorganisms were able to deplete all the 2-butanol being created through the hydrolysis of T2BOS. A summarization of adjustments made to the column influent during this period is presented in Table 5.2. Figure 5.3 shows the results for 2-butanol and DO concentrations before contaminants were added at 52 PV.

Table 5.2. Summary of the adjustments made to the gellan gum bead column from 0 to 52 PV. The initial influent feed solution had no added oxygen or contaminants.

Pore Volumes	Flow Rate (mL/hr)	DO/H_2O_2 (mg/L)	*c*DCE (µg/L)	Dioxane (µg/L)
0 – 27	1.0	DO = 8.0	0	0
27 – 34	1.0	DO = 15	0	0
34 – 52	1.0	H_2O_2 = 50	0	0

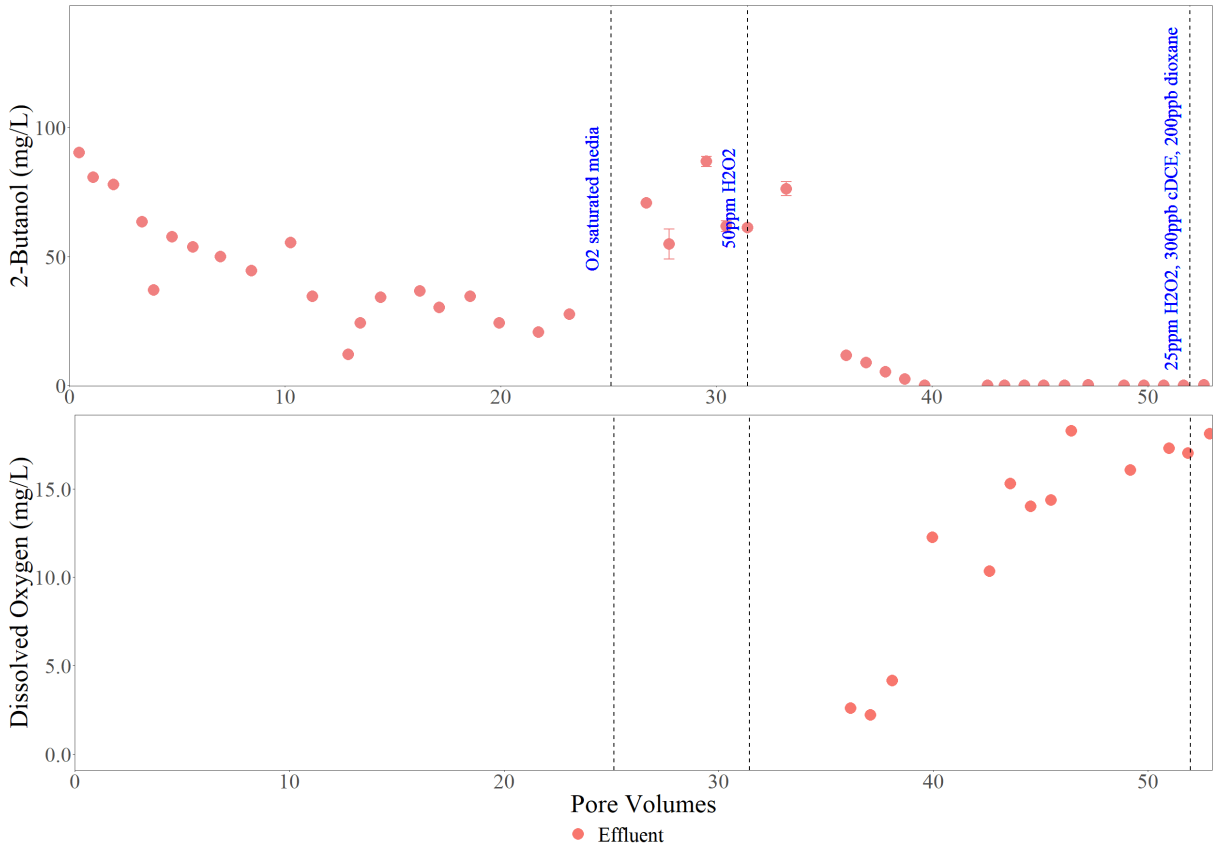

Figure 5.3. Effluent 2-butanol and DO concentration history for 0 to 53 PV. A summary of the adjustments made to the column during this period is contained in Table 5.2. No DO measurements were made from 0 to 31 PV. Error bars represent standard deviations of triplicate samples.

Initially, effluent 2-butanol was ~100 mg/L. The high level of 2-butanol likely resulted from the beads used to pack the column being fabricated months prior, so the T2BOS likely hydrolyzed over a long storage period. The beads were stored at 4°C, which likely slowed the rate of hydrolysis. The beads were rinsed multiple times before use, but it is likely that

significant 2-butanol remained trapped within the hydrogel beads along with T2BOS. 2-butanol levels steadily dropped over time until about 20 PV, where the concentration leveled off at ~25 mg/L. DO was not measured during this time period, but the odor coming from the column effluent suggested anoxic conditions existed in the column. When the influent DO was increased at 27 PV by using oxygen saturated media (~15 mg/L), 2-butanol levels rose in the effluent. This may have indicated that previously some anaerobic 2-butanol consumption was taking place. However, when 50 mg/L of hydrogen peroxide (H_2O_2) was added to the influent media at 34 PV, the effluent 2-butanol concentration quickly fell below detection (~5 µg/L). The DO in the effluent also rapidly increased from 2.5 mg/L to over 15 mg/L. The low level of 2-butanol and excess DO indicated successful biostimulation of 21198 in the hydrogel beads, suggesting that the column was prepared for aerobic cometabolism of contaminants.

*c*DCE and dioxane were added to the column influent feed solution at 52 PV. Approximately 300 µg/L of *c*DCE and 200 µg/L of dioxane were continuously added. At the same time, influent hydrogen peroxide was decreased from 50 mg/L to 25 mg/L because of the high effluent DO concentrations. A summary of the adjustments made to the column from 52 PV to 117 PV, the remainder of its operating period, is provided in Table 5.3. The results for the column from 51 PV to 89 PV are displayed in Figure 5.4.

Table 5.3. Summary of the adjustments made to the gellan gum bead column from 52 to 117 PV. Flow was paused for 27 days at 88 PV.

Pore Volumes	Flow Rate (mL/hr)	H_2O_2 (mg/L)	*c*DCE (µg/L)	Dioxane (µg/L)
52 – 58	1.0	H_2O_2 = 25	300	200
58 – 75	1.0	H_2O_2 = 50	300	200
75 – 78	90	H_2O_2 = 50	300	200
78 – 88	1.0	H_2O_2 = 50	0	200
88	0	N/A	N/A	N/A
88 – 117	1.0	H_2O_2 = 100	0	0

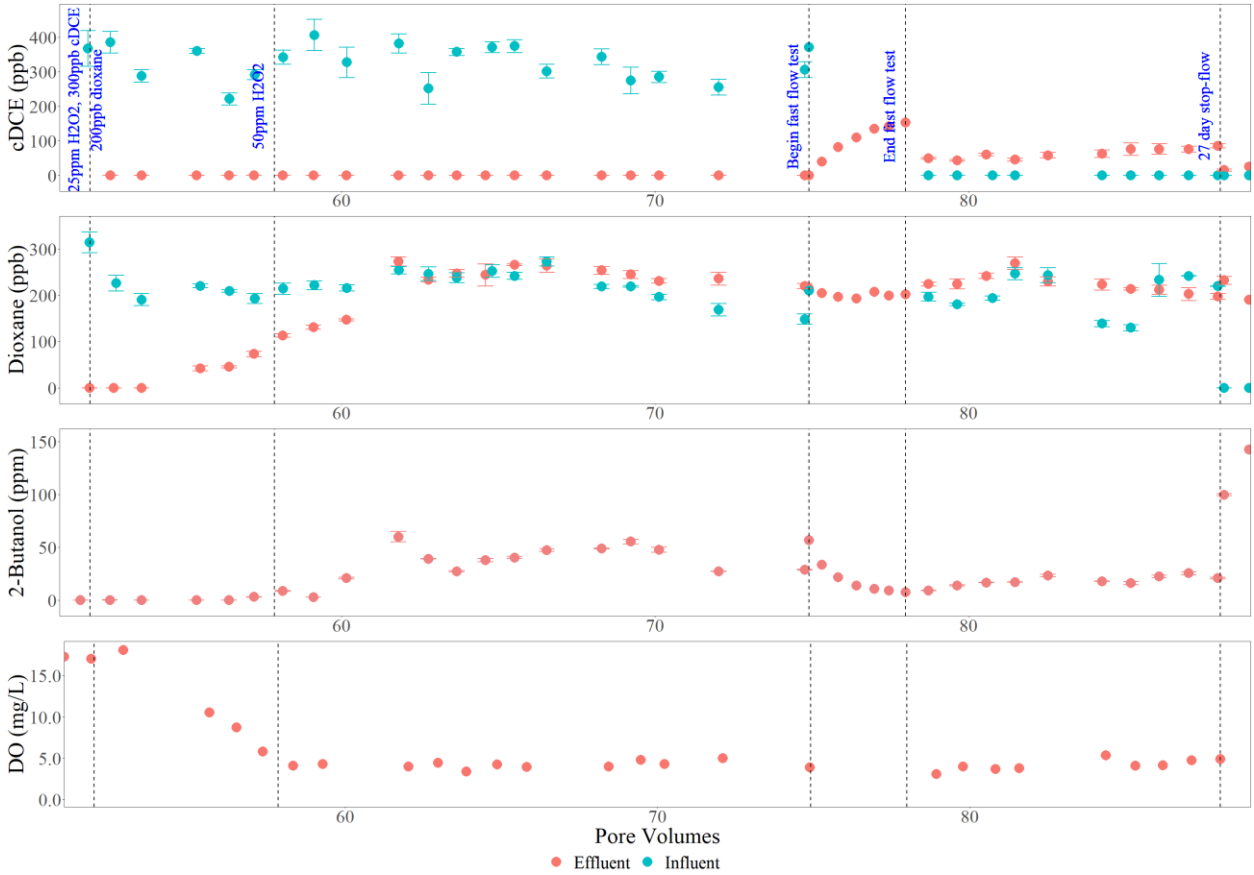

Figure 5.4. Concentration histories for influent and effluent *c*DCE and dioxane, as well as effluent 2-butanol and dissolved oxygen for the gellan gum column study from 51 PV to 89 PV. Adjustments to the column during this period are summarized in Table 5.3. Error bars represent standard deviations for triplicate samples.

Immediately upon adding the contaminants to the influent feed solution, the DO began to drop in the effluent. As a result, H_2O_2 was returned to 50 mg/L in the influent at 58 PV. Despite

this increase, DO did not rise in the effluent, and 2-butanol began to increase in the effluent. 2-butanol eventually reached an effluent concentration of ~50 mg/L at ~65 PV before it stopped increasing. Breakthrough of dioxane was also observed in the effluent. By 62 PV, the column influent and effluent had similar concentrations of dioxane. The column was packed using the same batch of beads used in the batch reactors (Section 4.1) which had demonstrated the ability to transform dioxane, however there was no evidence of dioxane transformation taking place in the gellan gum bead column. However, *c*DCE breakthrough did not occur in the effluent, providing evidence of transformation for *c*DCE. Due to this, essentially all (>99%) influent *c*DCE from 52 to 75 PV was estimated to have been transformed by the 21198 within the hydrogel bead pack. The presence of 2-butanol or *c*DCE may have had an inhibitory effect on dioxane transformation. While no detectable *c*DCE broke through the column by 75 PV, there was also no measured *c*DCE epoxide up to this point. The presence of *c*DCE epoxide would provide a better indication that aerobic cometabolism was occurring, rather than purely adsorption of *c*DCE to the hydrogel beads. A high-flow study was designed which would rapidly increase the flow rate of media into the column in an effort to ensure the breakthrough of *c*DCE and *c*DCE epoxide.

For this high-flow study, the flow rate was increased from 1 mL/hr to 90 mL/hr. 3 PV were pumped into the column over the course of 53 minutes. The results of this study are displayed within Figure 5.4 from 75 to 78 PV. A zoomed in version of this high-flow period displaying exclusively *c*DCE and *c*DCE epoxide results is shown in Figure 5.5.

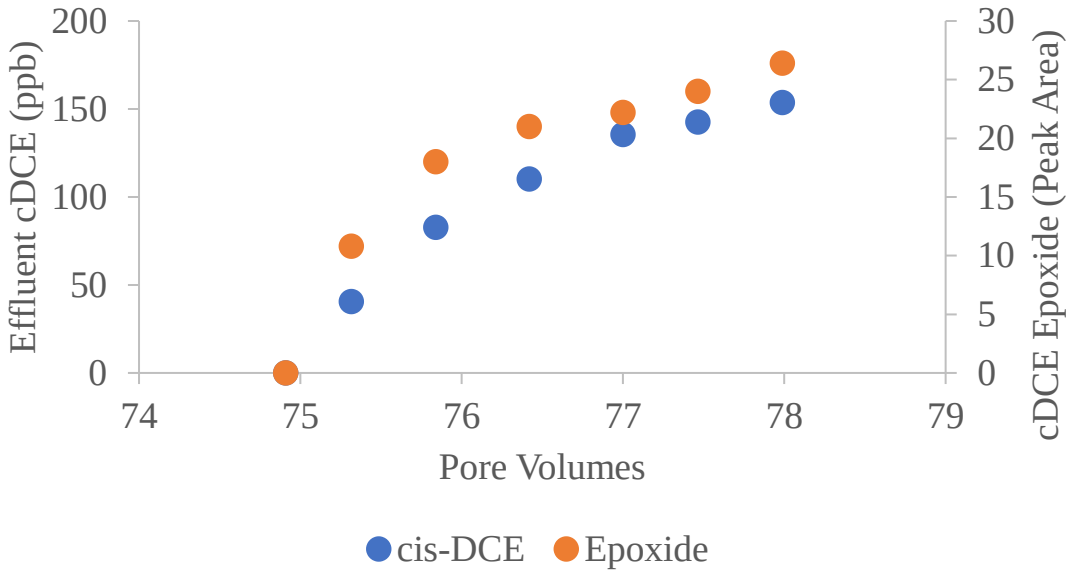

Figure 5.5. Effluent concentrations of *c*DCE and effluent peak areas of *c*DCE epoxide during the course of the high flow study for the gellan gum bead column.

During this period, *c*DCE broke through the column as intended. In addition, peak areas of *c*DCE epoxide were detectable for the first time, with the peak areas on the GC-ECD increasing from 0 to 25 over the course of the fast flow study. The presence of the epoxide supported that *c*DCE was being transformed through aerobic cometabolism by 21198 rather than solely sorbed to the beads.

Effluent dioxane stayed relatively steady during the high-flow study. 2-butanol decreased while the flow rate was increased. This was likely due to the lower HRT, which allowed for less time for 2-butanol to be released via the abiotic hydrolysis within the beads. At 78 PV, the flow was reduced to back 1 mL/hr and *c*DCE was removed from the influent to evaluate if dioxane was transformed in the absence of *c*DCE and if 2-butanol utilization was inhibited by *c*DCE. The effluent *c*DCE level remained steady at ~50 µg/L from 78 PV to 88 PV. Over this time period, cDCE epoxide levels in the effluent were in the range of 10-15 peak area. This suggests that either transformation of *c*DCE was continuing to occur at a low rate, or some sorbed *c*DCE

epoxide was being released. With no *c*DCE entering the column, *c*DCE was eluting from the column that had been trapped by the hydrogel beads during the high-flow event. Introducing so much *c*DCE to the entire length of the column so rapidly and exposing cells to *c*DCE epoxide may have damaged the microbial population. There was no evidence of dioxane transformation at this time. DO remained near the detection limit, and the sulfur odor was still present in the effluent. Oxygen demand thus remained high despite the possible damage done to 21198 during the high-flow study.

At 88 PV, a stop-flow study was conducted to investigate the effect of a long period of anoxic conditions. This stop-flow period lasted for 27 days. During this time, the column received no influent media, and no effluent samples were taken. Figure 5.6 shows an image of the column prior to stopping the flow as compared to immediately before flow resumption. With no flow and no DO, hydrolyzed 2-butanol was allowed to build up within the column. The yellow color of the column, which is especially visible at the bottom, after the stop flow study may be attributable to the high levels of 2-butanol.

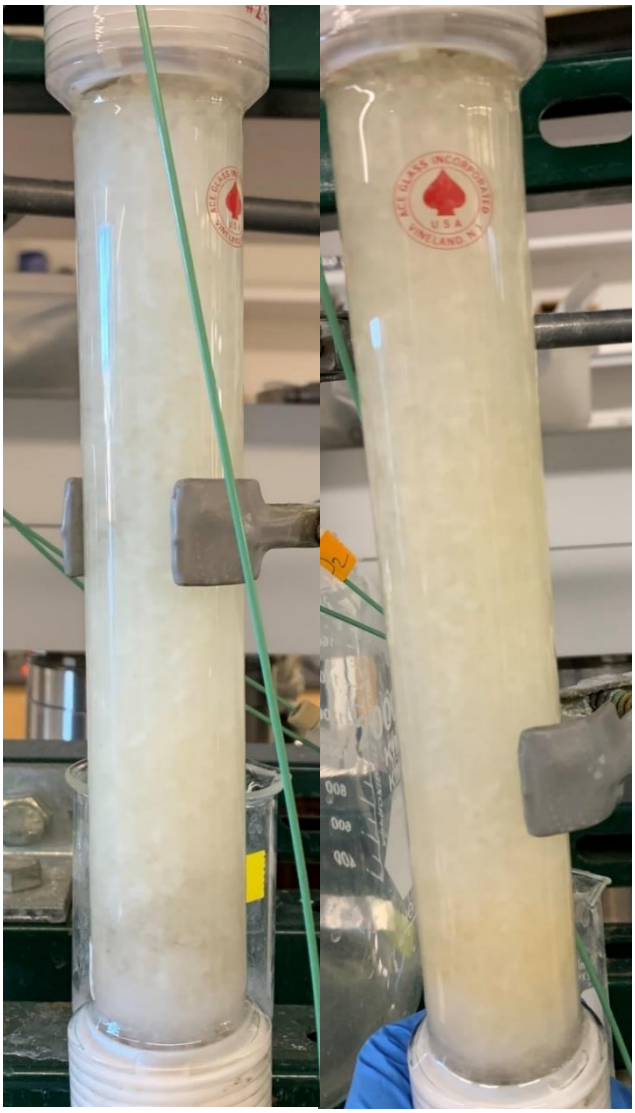

Figure 5.6. Images of the T2BOS gellan gum bead column prior to stopping flow (left: taken 12/10/2021) and immediately before resuming flow (right: taken 1/6/2022).

The column flow was resumed at 1 mL/hr with H_2O_2 increased to 100 mg/L. The results of this final phase of the column study are displayed in Figure 5.7. No *c*DCE or dioxane was added to the influent feed during this phase. The high 2-butanol concentrations measured initially when flow was resumed are consistent with the prolonged stop-flow period for the abiotic hydrolysis to occur.

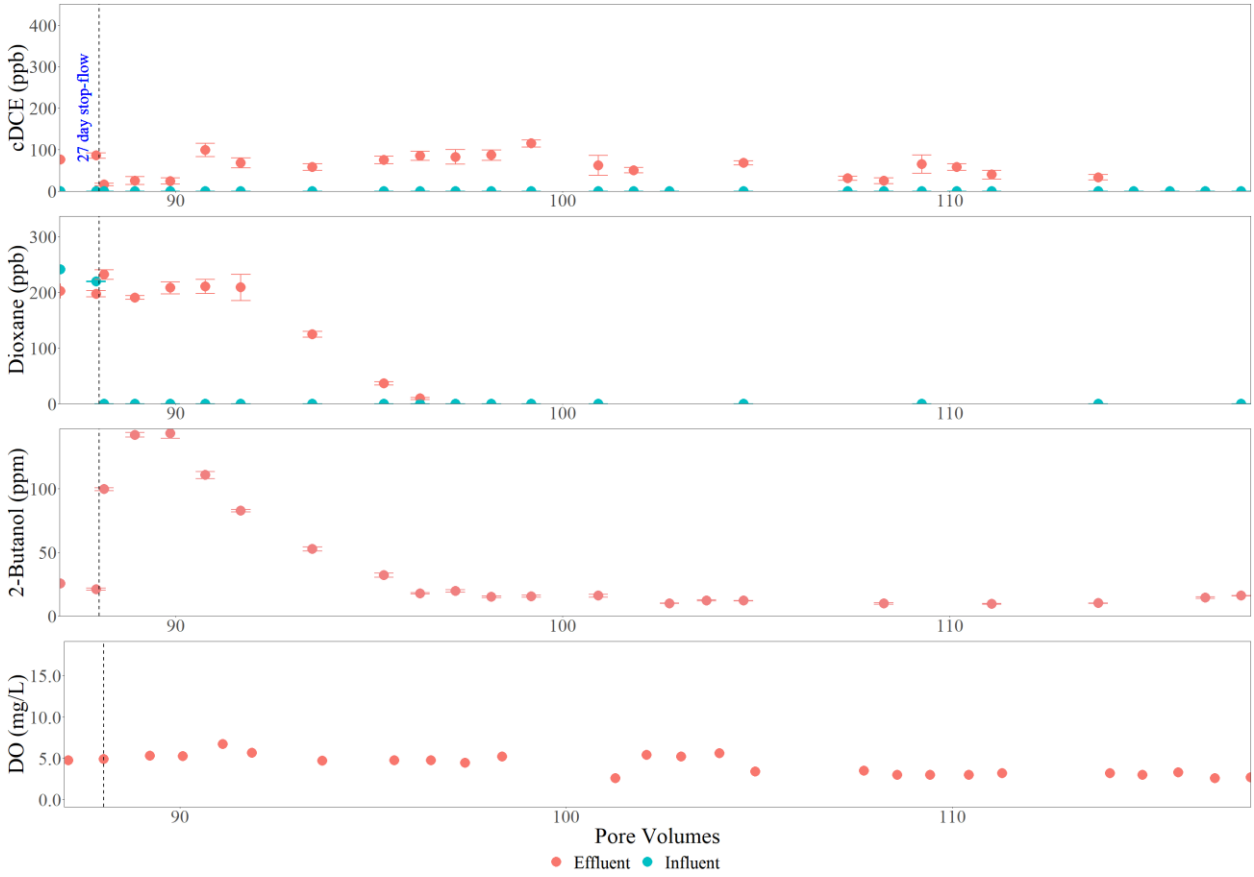

Figure 5.7. Concentration histories for influent and effluent *c*DCE and dioxane, as well as effluent 2-butanol and DO for the final phase of the gellan gum bead column study (87 to 117 PV). A 27 day stop-flow study was conducted at 88 PV and dioxane was removed from the influent media at this time. Error bars represent standard deviations of triplicate samples.

Upon flow resumption, the 2-butanol concentration decreased over time from ~150 mg/L to ~25 mg/L. Effluent *c*DCE remained in the range of ~50 to ~100 µg/L despite there being no *c*DCE added to the influent feed solution since 78 PV. While low levels of *c*DCE epoxide were detected prior to the stop flow period, no epoxide was measured once flow was resumed. The biomass may have been significantly impacted, or transformation may have been occurring in the bottom section of the column. The effluent *c*DCE concentration fell below detection level by 114 PV. Dioxane was quickly eluted from the column once it was removed from the influent, decreasing from ~200 µg/L at 88 PV to below detection by 97 PV. Dioxane being completely eluted from the column much more rapidly than *c*DCE is evidence that *c*DCE more readily sorbs

to the bead matrix. This suggests that a bromide tracer test may not be an accurate representation of the sorption tendencies of contaminants within the column, since there is a significant difference between how *c*DCE and dioxane were eluted from the column.

A mass balance was completed for the contaminants by estimating the total masses added to the influent feed solution and the total masses eluted from the column. None of the influent dioxane was successfully transformed by the 21198 within column. However, 71.5% of the influent *c*DCE was removed. This provides evidence that aerobic cometabolism was occurring and preventing *c*DCE breakthrough up until the high-flow study disrupted column operation.

Figure 5.8 shows images of the column taken on the first day of its operation and at the end of its operation. A dark spot is evident near the bottom of the column at the end of the study. Oxygen demand remained high within the column after the stop flow period even though there was no evidence of transformation taking place. Effluent DO remained near the detection limit (~4 mg/L). It is possible that contamination was responsible for this oxygen demand and the dark spot on the column. While steps were taken to avoid contamination, the column was not operated under aseptic conditions. The dark spot may also have been due to a large number of dead cells, as this portion of the column would have been exposed to the highest concentrations of *c*DCE, *c*DCE epoxide, and dioxane throughout the column's period of operation. Streak plating liquid samples from the column onto TSGA plates yielded inconclusive results as far as the presence of contamination (Appendix A.2).

Figure 5.8. Images of the T2BOS gellan gum bead column from the start of operation (left: 0 PV) and the end of operation (right: 117 PV). The red arrow indicates the darkened area that became more prevalent over time.

The durability of the gellan gum beads used within this column was measured by conducting compression tests on the beads used to pack the column and on bead samples taken from the influent and effluent sections of the column after shutdown. The results of these

compression tests are displayed in Figure 5.9. Assuming compressibility is a marker for bead strength, the beads were used to pack the column were much stronger than after their use in the column. The beads from the effluent section may have had slightly more strength on average than those from the influent section, but with the error bars indicate no significant difference. One possible reason for this slight strength difference could have been that the beads near the influent were exposed to more DO, resulting in more microbial growth. More contaminant transformation likely occurred in this section as well. The results in Section 4.1 showed evidence that the process of transformation may be partially responsible for bead degradation. All the beads from the column showed decreased strength. This may mean that the growth of microorganisms can also negatively impact the solid matrix. Long term exposure to contaminants, nutrients, and oxygen had a major effect on how strong the beads were, but it is unclear how large a role each of these had.

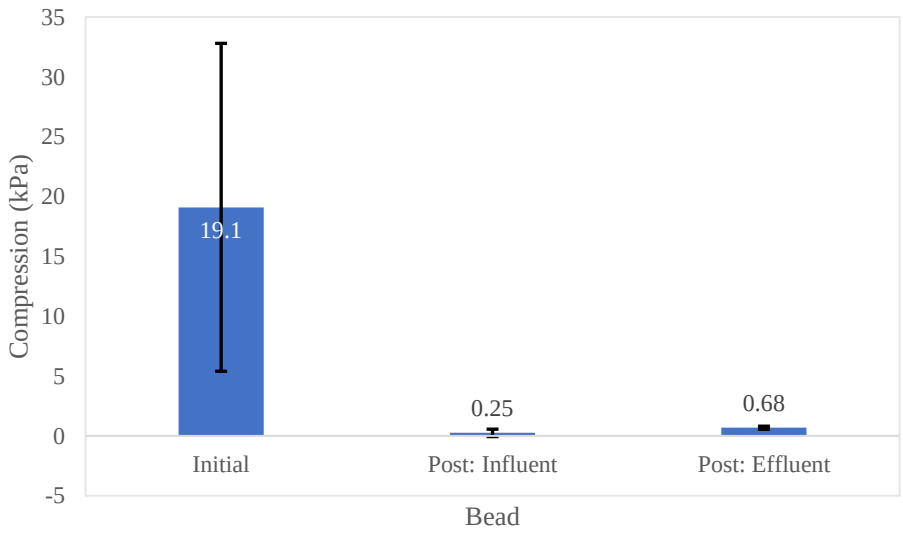

Figure 5.9. Bead compression test results for the gellan gum bead column. From left to right, results are for beads taken prior to column start-up, after column shutdown from the influent portion of the column, and after column shutdown from the effluent section of the column. Error bars represent standard deviations of triplicate tests.

5.2 Polyvinyl Alcohol/Sodium Alginate Bead Column

5.2.1 Column Operation

While the research for this thesis was being conducted, parallel work was being conducted in an attempt to optimize beads, mainly to improve durability. One iteration of beads developed during that work was then used for this column experiment. The PVA/SA bead column was packed as described in the Methods section (3.5.2) using polyvinyl alcohol/sodium alginate beads coencapsulated with isobutane grown 21198 (0.5 mg TSS/g bead) and TBOS (10% v/v). Aside from the beads and SRS used, this column differed from the column used for the gellan gum bead study in that it had three sampling ports on the side that allowed for sampling within the column. An image of the column prior to beginning operation is provided in Figure 5.10.

Figure 5.10. Image of the PVA/SA bead column taken prior to column operation.

Before beginning flow through the column, a constant head test was conducted. The goal of this test was to measure changes in flow rate through the column at different heads. Doing the same test after the column operation was concluded would allow for an estimate in the changes of permeability between column startup and column shutdown. A constant head was maintained while 20 mL of media was allowed to flow through the bottom of the column and out of the top of the column. The results from this test are shown in Figure 5.11. As expected, the flow rate through the column was slower when the difference in head was smaller, consistent with Darcy's Law. Slower flow rates in this repeated test could mean a loss of conductivity resulting from bead degradation and clogging. Faster flower rates, higher conductivity, could mean that preferential flow pathways have formed.

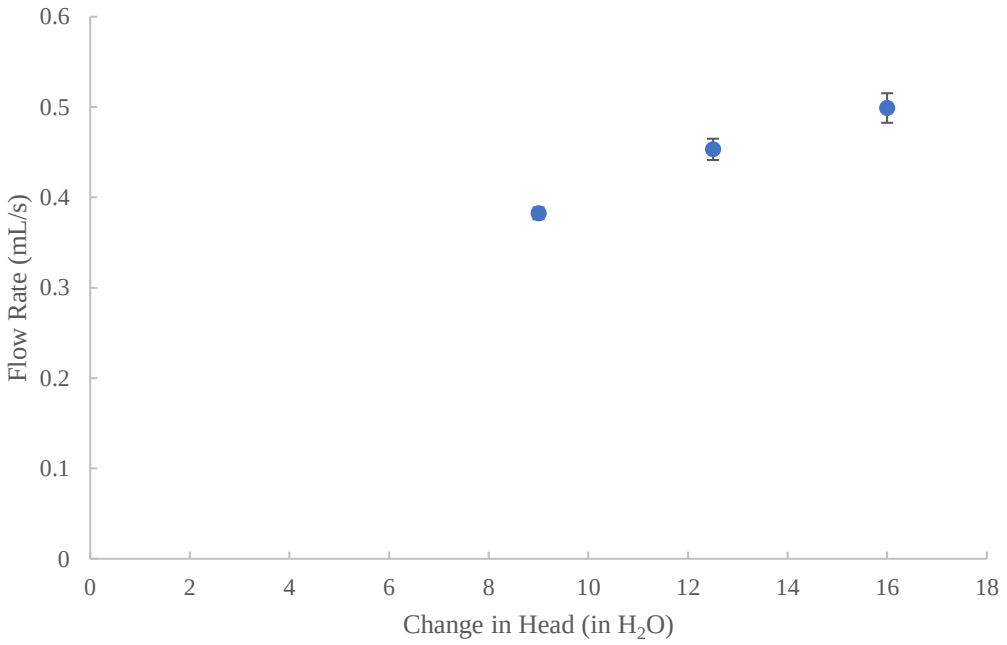

Figure 5.11. Flow rate through the PVA/SA bead column versus the change in head measured prior to column operation. Error bars represent standard deviations of triplicate tests.

As with the gellan gum bead column, a bromide tracer test was conducted. The pore volume based on weight measurements was determined to be 28 mL. The column was initially

operated at 1.0 mL/hr. This equates to a flow rate of 0.86 PV per day. Unlike with the previous column, the beads in this column were fabricated the day before packing the column. Due to this, *c*DCE was added to the influent syringe at 0 PV because the beads should have had active biomass. At the same time, the bromide tracer test was conducted. The results from the bromide tracer study are presented in Figure 5.12. The vertical dashed line represents when bromide was removed from the column's influent media. The horizontal solid line represents the average influent bromide concentration, which was 47 mg/L.

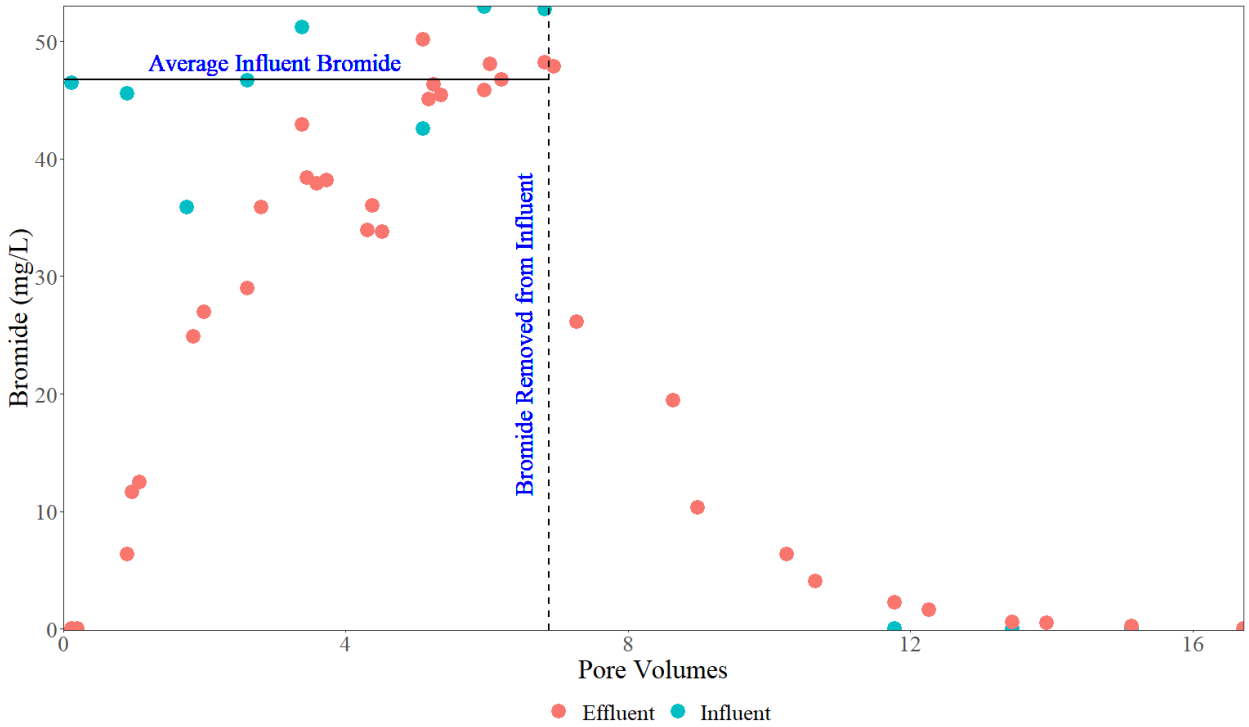

Figure 5.12. Bromide concentration history for the PVA/SA bead column. The solid horizontal line represents the average influent bromide. The dashed horizontal line demarcates when bromide was removed from the influent. The flow rate was also increased from 1.0 mL/hr to 1.9 mL/hr at this point.

The effluent bromide concentration reached 50% of the influent bromide concentration at about 1.8 PV, resulting in an estimated bromide retardation factor of 1.8. It took about 5.2 PV for the effluent concentration to level off at the average influent concentration. The bromide was

removed from the influent media at 6.9 PV. At the same time, the flow rate was nearly doubled to 1.9 mL/hr, or 1.7 pore volumes per day. This was done as part of an effort to decrease effluent 1-butanol levels, which is discussed later. As with the previous column, bromide was rapidly eluted from the column. By approximately 8.5 PV, the effluent concentration had returned to 50% of the earlier influent bromide concentration. The elution tail was more drawn out for these beads than with the gellan gum beads. Bromide did not return to below detection in the effluent until 17 PV. It took nearly 10 PV for the bromide to completely leave the system, compared to 6.9 PV for the gellan gum column. Both the bromide tracer tests conducted using the gellan gum bead column and using the PVA/SA bead column support that transport through the column is retarded due to bromide diffusion into the beads.

The physical transport parameters of the PVA/SA bead column are summarized in Table 5.4. The bromide retardation factor was determined to be 1.8, which was significantly lower than the value of 5.4 calculated for the gellan gum bead column. This suggests that bromide transport may have been less retarded by the PVA/SA bead column. This is mainly a measurement of a combination of the porosity of fluid flow and retardation due to diffusion into the hydrogel bed and the hydrogel internal porosity.

Table 5.4. Summary of the physical transport parameters determined for the PVA/SA bead column. Values are displayed for the initial phase when flow was 1.0 mL/hr and for the next phase when flow was 1.9 mL/hr.

Parameter	Phase 1	Phase 2	Units
Pore Volumes	0 - 6.9	6.9 - 97	--
Column Length	10	10	cm
Cross Sectional Area	7.9	7.9	cm^2/hr
Mass of Beads	48	48	g
Volume	67	67	mL
Pore Volume	28	28	mL
Porosity	0.37	0.37	--
Flow Rate	1.0	1.9	mL/hr
Superficial Velocity	0.13	0.24	cm/hr
Average Linear Velocity	0.36	0.70	cm/hr
Retention Time	28	14	hr
Bromide Retardation Factor	1.8	1.8	--

The PVA/SA bead column was exposed to *c*DCE immediately. *c*DCE, *c*DCE epoxide, 1-butanol, and DO concentrations were measured in samples from the column effluent, top port, middle port, and bottom port, as well as the influent solution. Table 5.5 has a summary of the changes made to the column up until 44 PV. The results for the measurements from 0 PV to 44 PV are presented in Figure 5.13.

Table 5.5. Summary of the adjustments made to the PVA/SA bead column from 0 to 44 PV. Samples were collected for embryonic zebrafish toxicity testing at 30 PV.

Pore Volumes	Flow Rate (mL/hr)	pH	H_2O_2 (mg/L)	*c*DCE (µg/L)
0 – 6.9	1.0	7.0	50	200
6.9 – 26	1.9	7.0	100	200
26 – 44	1.9	7.0	200	200

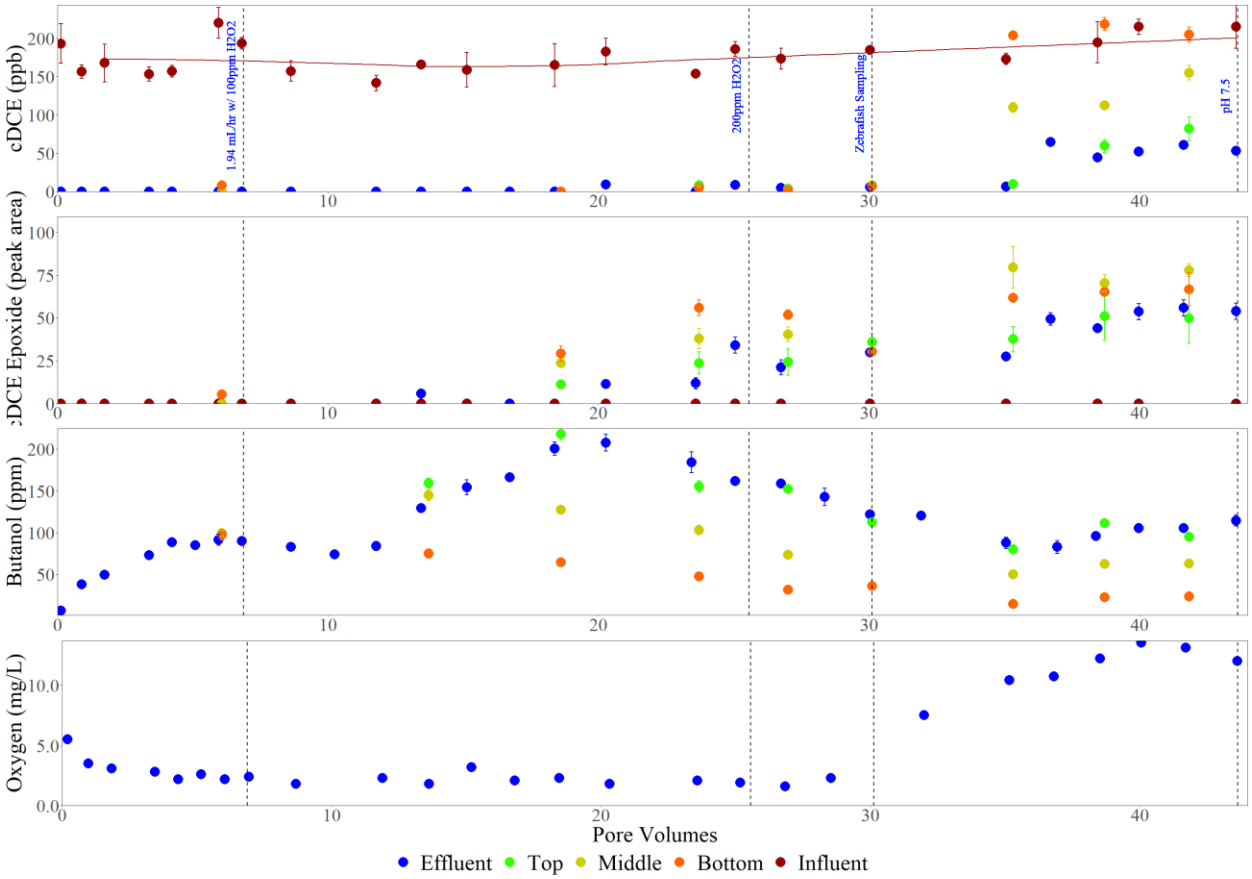

Figure 5.13. Concentration histories of *c*DCE, *c*DCE epoxide, 1-butanol, and DO for the PVA/SA bead column from 0 PV to 44 PV. Results are displayed for the column effluent, top port, middle port, bottom port, and influent. Column adjustments are summarized in Table 5.5. The red line represents a 5-sample rolling mean for influent *c*DCE. Error bars represent standard deviations for triplicate samples.

Initially, there was no breakthrough of *c*DCE, but there was a gradual increase in effluent *c*DCE epoxide beginning at approximately 18 PV. This provided support that aerobic cometabolism of *c*DCE was taking place. The DO concentration remained near the detection limit (~2 mg/L) during this early period. This was reflected by high levels of 1-butanol in the effluent (~200 mg/L). In order to supply more DO, H_2O_2 was doubled at 26 PV. This resulted in a slow decline in effluent 1-butanol from ~200 mg/L to ~100 mg/L. It also resulted in an increase of DO from the near detection limit in the effluent to a steady state concentration of ~14 mg/L. Despite the excess DO, the 1-butanol concentration remained at ~100 mg/L.

In an effort to measure possible toxicity generated by the process of aerobic cometabolism, 5 mL of sample were taken from the column side ports at 30 PV to use in embryonic zebrafish toxicity testing. This much liquid sampling may have had an impact on the column, which contained 28 mL of pore volume. Starting at ~35 PV, *c*DCE was detected in the side port samples taken closest to the influent at a concentration approximately equal to the influent concentration (~175 µg/L). *c*DCE was also detected in the middle port samples at this point, at approximately half the concentration of the influent feed. This further indicated that some combination of transformation and retardation was occurring. *c*DCE was detected at ~50 µg/L in the effluent by ~37 PV. *c*DCE remained at approximately this level in the effluent until 44 PV, again indicating that transformation was occurring.

*c*DCE epoxide initially was detected in the column effluent at ~18 PV. The epoxide continued to increase in the column effluent until 44 PV. The epoxide was generally measured highest in the bottom and middle port samples. This indicated that 21198 stimulation had occurred at the bottom of the column, as the epoxide is a product of aerobic cometabolism. The epoxide generally decreased slightly in the top port and effluent samples, which may have been due to transformation of the epoxide or abiotic degradation. The epoxide also increased in the effluent throughout this period.

Due to the significant presence of *c*DCE, *c*DCE epoxide, and 1-butanol throughout the column by 44 PV, there was concern about the microbial health of the bead pack. The pH of the effluent was ~6.0, so the column influent pH was increased from 7.0 to 7.5 at 44 PV by decreasing the volume of hydrochloric acid in the media in an effort to slow TBOS hydrolysis and increase microbial growth. Table 5.6 describes the changes made to the column over this period. Figure 5.14 displays the next phase of the PVA/SA column from 43 to 100 PV and

Table 5.6. Summary of the adjustments made to the PVA/SA bead column from 44 to 97 PV. Samples were collected for embryonic zebrafish toxicity testing at 97 PV.

Pore Volumes	Flow Rate (mL/hr)	pH	H_2O_2 (mg/L)	*c*DCE (µg/L)
44 – 64	1.9	7.5	200	200
64 – 88	1.9	7.5	250	200
88 – 97	1.9	7.9	250	200

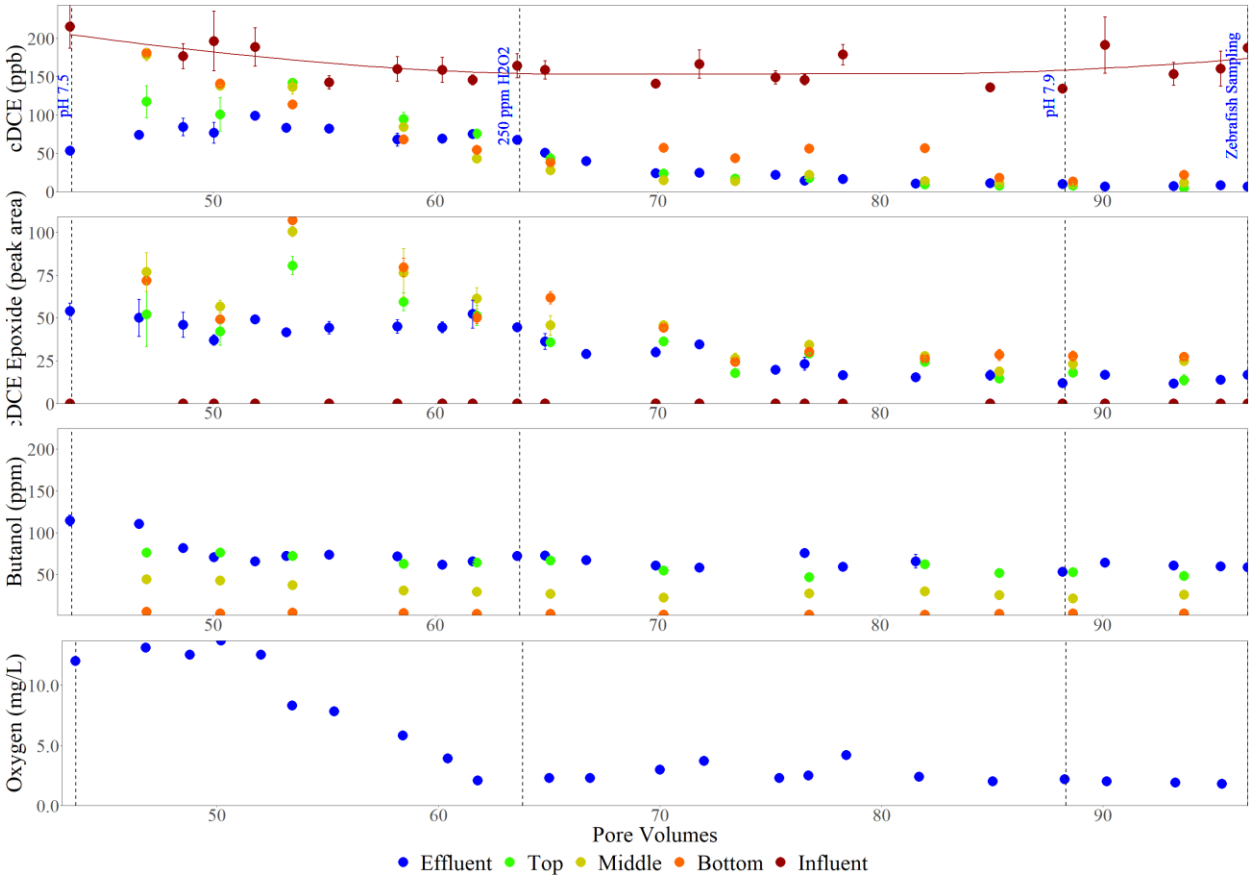

Figure 5.14. Concentration histories of *c*DCE, *c*DCE epoxide, 1-butanol, and DO for the PVA/SA bead column from 43 PV to 97 PV. Results are displayed for the column effluent, top port, middle port, bottom port, and influent. Column adjustments are summarized in Table 5.6. The red line represents a 5-sample rolling mean for influent *c*DCE. Error bars represent standard deviations for triplicate samples.

The column immediately responded to this increase in pH. The effluent butanol decreased from ~115 mg/L to ~75 mg/L by ~50 PV. The effluent DO also decreased, going from

~12 mg/L to the detection limit by ~62 PV. This is evidence of an increase in microbial biomass, as the column went from a surplus of dissolved oxygen to being oxygen limited. It is also possible that the pH affected the hydrolysis rate of the TBOS within the beads. A previous study found that neutral pH led to the lowest hydrolysis rate of TBOS, while hydrolysis increased under both more acidic and more basic conditions.[173]

*c*DCE was not immediately influenced by this increase in pH, as the effluent *c*DCE continued to rise until ~50 PV. It remained steady until the influent H_2O_2 was increased to 250 mg/L at 64 PV. However, the *c*DCE concentration measured at the bottom sampling port decreased from ~175 µg/L to ~50 µg/L from 44 PV to 64 PV. This suggests that the pH change did impact cometabolism within the column, despite effluent *c*DCE remaining relatively unchanged. This supports the increase in microbial biomass indicated by the decrease in DO. A long-term decrease in effluent *c*DCE was observed in the column effluent from 64 PV to 80 PV following an increase in H_2O_2 to 250 mg/L. This further indicated that biomass within the column was increasing through this period, represented by an increase in aerobic cometabolism of *c*DCE. This is also supported by the *c*DCE epoxide results. The effluent epoxide level did not immediately respond to the pH increase at 44 PV, but the increase in H_2O_2 at 64 PV led to a steady decrease in *c*DCE epoxide measurements in all port samples and in the column effluent. As the biomass of 21198 increased within the hydrogel bed, the rate of aerobic cometabolism increased. The process of cometabolism was capable of transforming both *c*DCE and its epoxide.[20] At 53 PV, *c*DCE epoxide was measured at ~100 peak area in the sampling port closest to the influent of the column. By 75 PV, this had decreased to a steady level of ~25 peak area. This suggested that the biomass was transforming the *c*DCE epoxide as well, as the HRT was unchanged. The decreases in *c*DCE, *c*DCE epoxide, and DO all coinciding with one another is

evidence that an increased microbial population resulted in the increase in transformation of both *c*DCE and *c*DCE epoxide.

Increasing the H_2O_2 at 64 PV did not cause notable changes to effluent 1-butanol or DO. From 43 PV to 97 PV, 1-butanol was consistently near zero in the bottom port before increasing in successive port samples, consistent with continued hydrolysis of TBOS into 1-butanol. The bottom portion of the column was most microbially active, as indicated by the development of the orange color in Figure 5.16. The limited decrease in *c*DCE and *c*DCE epoxide when going from the bottom port sample to the effluent is further evidence that the column was not well stimulated throughout, but rather only near the region up until the bottom sampling port. Despite this, greater than 95% removal of *c*DCE was achieved by the end of the operating period.

Figure 5.15 displays the 1-butanol concentrations averaged over the period from 64 PV to 88 PV, when the results were relatively consistent spatially and following the increase to 250 mg/L of H_2O_2. The results for the bottom port were near zero, and 1-butanol increased at each sampling point successively along the column. This indicates that 1-butanol was hydrolyzed throughout the column. Only the bottom port had sufficient oxygen and microbial growth to utilize the majority of it. The near-linear increase in 1-butanol between the bottom to top ports is consistent with a zero-order rate of release of 1-butanol. The results are consistent with the zero-order rate of hydrolysis observed in batch reactor tests presented later in Figure 5.20.

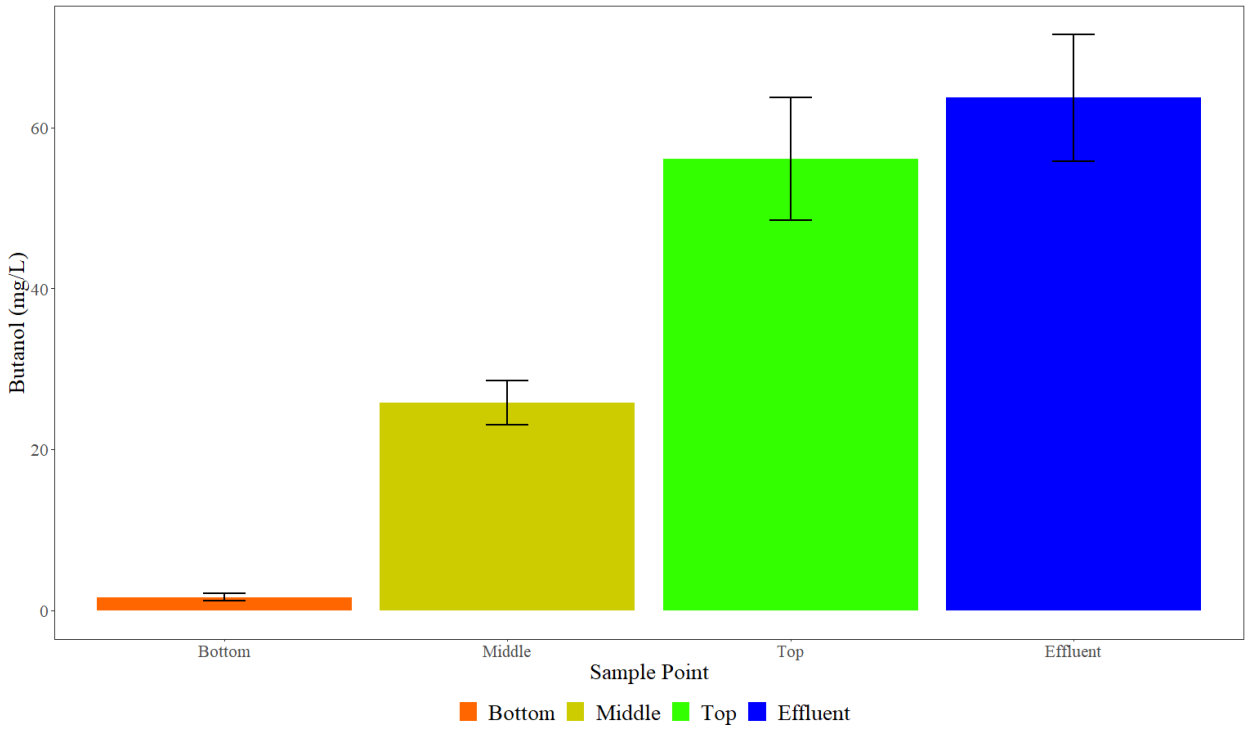

Figure 5.15. Average 1-butanol concentrations for port and effluent sampling in the PVA/SA bead column from 64 PV to 88 PV. Error bars represent standard deviations.

Figure 5.16 shows a comparison of pictures taken of the column at 0 PV, 63 PV, and 96 PV. The orange near the bottom of the column is evidence of growth of 21198[9]. This orange section growing more distinct by the final image shows that this portion continued to grow more active over time. However, significant growth was not evident throughout the rest of the column. This is supported by the data in Figures 5.14 and 5.15, as most transformation and substrate usage occurred by the bottom sampling port, especially after 85 PV.

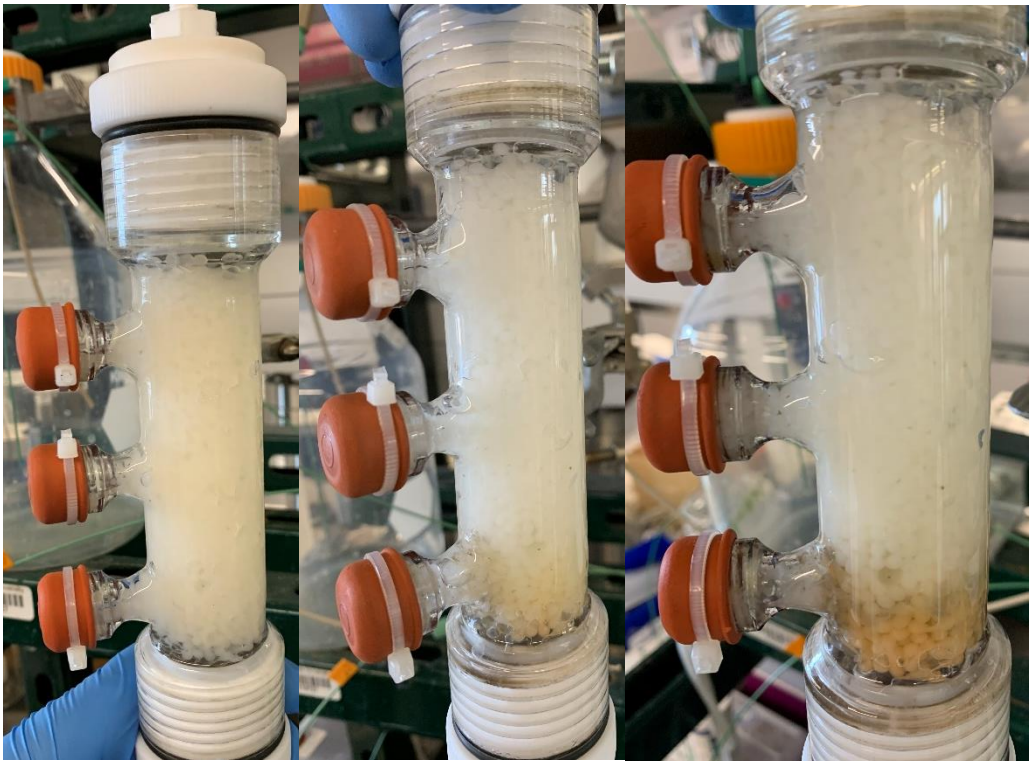

Figure 5.16. Images of the PVA/SA bead column taken, from left to right, at 0, 63, and 96 PV.

5.2.2 Column Sample Embryonic Zebrafish Toxicity Tests

One objective from the PVA/SA column study was to determine whether there were toxic byproducts generated through cometabolism of *c*DCE by 21198. To study this, embryonic zebrafish assays were conducted to measure for significant toxicity produced by column samples. Samples were collected for embryonic zebrafish toxicity studies at 30 PV and at 97 PV. At 30 PV, samples were collected from the influent, effluent, bottom port, and side port. The influent sample was collected prior to H_2O_2 addition, as it was theorized this alone would lead to significant toxicity. However, *c*DCE and all other compounds in the influent solution were present. At the time of sampling, *c*DCE was measured near the detection limit in all sampling points and *c*DCE epoxide was measured at ~35 peak area in the side port samples and in the column effluent. The results from this toxicity test for both undiluted and 10x diluted samples are displayed in Figure 5.17.

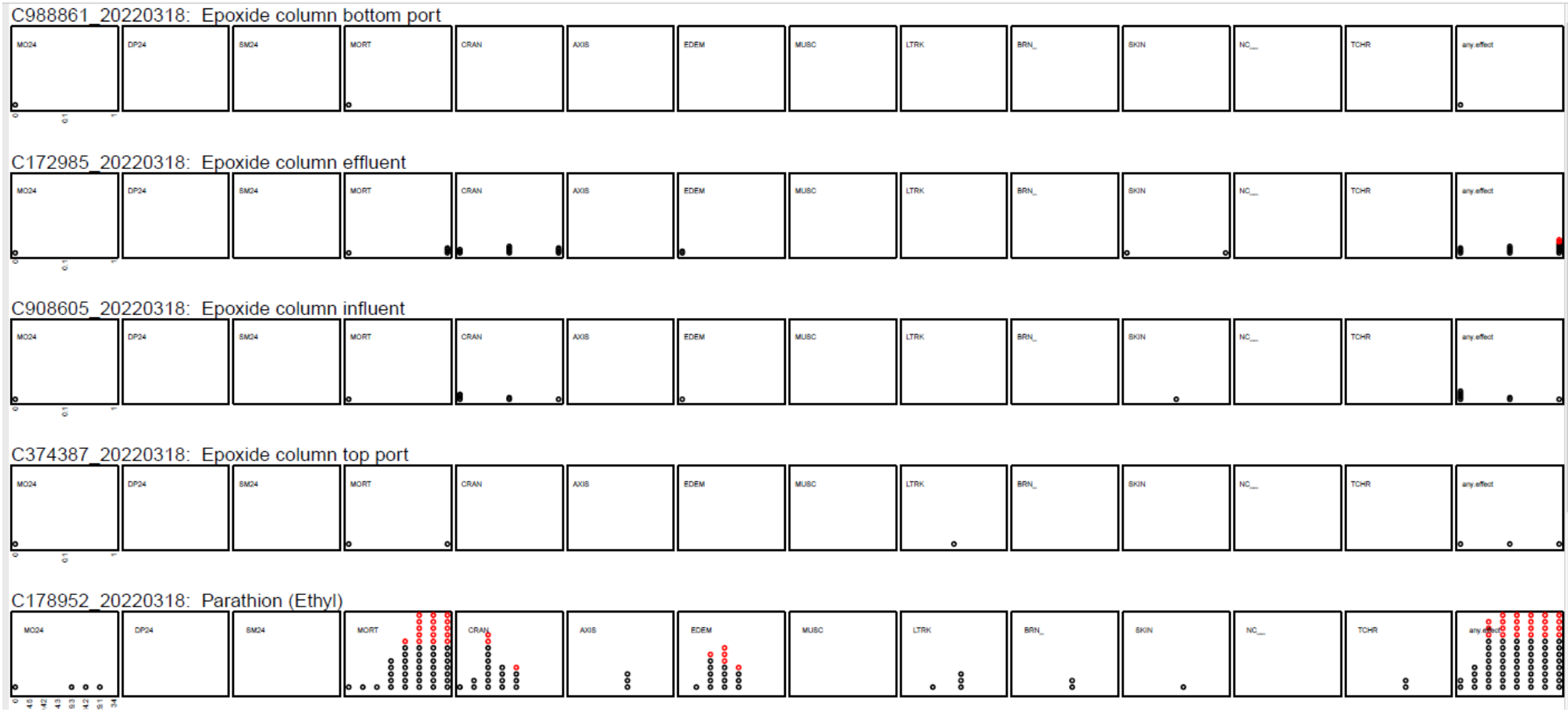

Figure 5.17. Results for the embryonic zebrafish toxicity tests conducted using samples from the PVA/SA bead column at 30 PV. Results are provided for, from the top row of plots down, the bottom port, effluent, influent, the top port, and a positive poisoned control. Each row shows the plotted results for each tested endpoint. The qualitative descriptions for each endpoint are provided in Table 3.6. For the column samples, each individual plot shows results for, from left to right, a negative control, 10x diluted sample, and undiluted sample. Red dots symbolize points over the significance threshold for that endpoint in particular. The result is more significant when there are greater number of red dots. The statistical analysis for this test is provided in the Methods section (3.7).

Out of the four sampling points, the sole point that demonstrated toxicity above the significance threshold was the column effluent for the any effect endpoint. Since *c*DCE was much lower in the effluent sample than in the influent, and the influent sample showed no significant toxicity, *c*DCE was likely not the cause of the toxicity. The other main difference between the influent and effluent was that the effluent had ~120 mg/L of 1-butanol at this point in the column's operation. A previous study showed that 1-butanol was toxic to zebrafish at 50 mg/L.[171] Due to this, 1-butanol was considered a possible cause of the effluent toxicity. However, this is not supported by the results for the top sampling port. The 1-butanol concentration was essentially equal in the top sampling port to the effluent sample, but the top sampling port did not demonstrate significant toxicity. One reason for this could be that fewer zebrafish were tested using the side port samples because of a limited sample volume. As the effluent sample only reached the significance threshold by one zebrafish, the smaller sample size for the top sampling port may have been significant.

To provide further support for 1-butanol being the cause of the toxicity, influent and effluent column samples were taken for embryonic zebrafish toxicity testing at 97 PV. At this point, the concentration of 1-butanol in the column effluent was ~60 mg/L, significantly lower than in the previous zebrafish test. Effluent *c*DCE was measured to be ~5 µg/L and effluent *c*DCE epoxide was measured to be ~20 peak area, slightly lower than during the previous toxicity test. For this test, the influent sample was collected after the addition of H_2O_2 to confirm its toxicity. The results from this toxicity test are given in Figure 5.18.

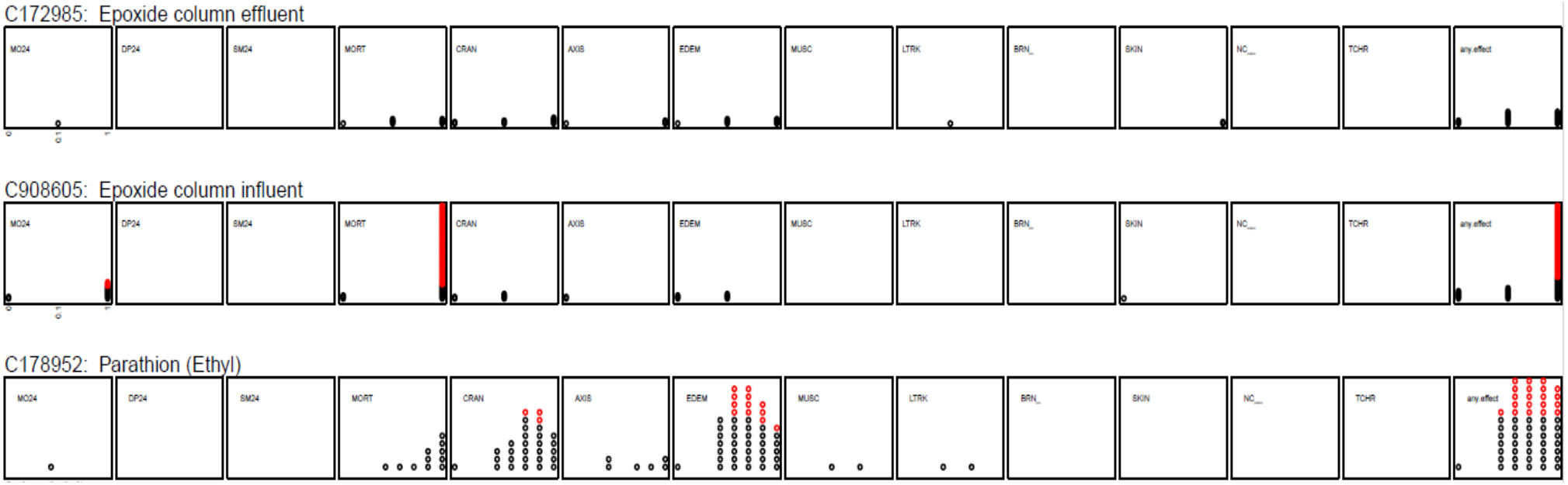

Figure 5.18. The results for the embryonic zebrafish toxicity tests conducted using samples from the PVA/SA bead column at 97 PV. Results are provided for, from the top row of plots down, the effluent, influent, and a positive poisoned control. Each row shows the plotted results for each tested endpoint. The qualitative descriptions for each endpoint are provided in Table 6. For the column samples, each individual plot shows results for, from left to right, a negative control, 10x diluted sample, and undiluted sample. Red dots symbolize points over the significance threshold for that endpoint in particular. The result is more significant when there are a greater number of red dots. The statistical analysis for this test is provided in the Methods section (3.7).

In this case, the undiluted influent sample reached the significance threshold for the 24-hour mortality endpoint, the mortality endpoint, and the any effect endpoint. It far exceeded the threshold in the mortality endpoint, clearly demonstrating the toxicity of this sample. The primary difference between this influent sample and the previous influent sample at 30 PV, which showed no significant toxicity, was that this influent sample had added 250 mg/L of added H_2O_2. The significant H_2O_2 concentration of the influent was likely the cause of the toxicity in the influent sample.

The effluent sample did not show significant toxicity for any of the tested endpoints. There was ~50% less 1-butanol and ~57% less *c*DCE epoxide measured in this effluent sample than in the previous column effluent sample that did show slight toxicity. In the previous sample, only the effluent sample met the significance threshold despite 1-butanol being approximately equal in the previous top port sample and *c*DCE epoxide being approximately equal in all previous samples. Due to this, it is difficult to draw any conclusions as to the cause of the toxicity demonstrated by the effluent sample at 30 PV. The toxicity tests conducted using the TBOS batch reactors (Section 4.2.2) showed decreasing toxicity when going from the early samples to the later samples, which aligned with going from significant 1-butanol, allowed to generated over 2 months of anoxic conditions, to lower 1-butanol. 1-butanol may be causing toxicity, but conclusions cannot be made based on these three toxicity studies. Overall, there is not strong evidence that the process of aerobic cometabolism by 21198 within hydrogel beads generates significantly toxic byproducts. However, 1-butanol overproduction may be drawback of TBOS as an SRS. In addition to significant oxygen demand, there is also the possible toxicity caused from high 1-butanol concentrations.

5.3 Column Studies Discussion

A previously published study on gellan gum bead columns demonstrated several differences from the column studies conducted for this thesis.[172] One of the columns from this previous study used a very similar setup to the gellan gum bead column in this thesis, using gellan gum bead co-encapsulated with T2BOS and 21198 and the same influent feed solution. In the previous column study, H_2O_2 was not required to meet the 2-butanol demands. The 2-butanol concentration decreased ~0.3 mg/L after a period of ~40 PV of biostimulation. The influent solution was aerated with 15 mg/L of DO, which was sufficient for biostimulation throughout the column and transformation of essentially all (>99%) influent *c*DCE and dioxane.

In contrast, 50 mg/L H_2O_2 was needed to drive the 2-butanol level to the detection limit in the T2BOS gellan gum bead column study conducted for this thesis (Section 5.1). The 2-butanol concentration also increased in the effluent once contaminants were added to the column, ranging from ~20 to ~50 mg/L. This was approximately 10-fold higher than the previous study observed at any point. In the results presented here, transformation of *c*DCE was observed without transformation of dioxane. In the previous study, dioxane, *c*DCE, and 1,1,1-TCA were all effectively transformed with over 99% removal achieved. This further supports that there was something fundamentally different about the gellan gum beads used for the studies presented here, despite the formulation and method of creation being identical. There needs to be an investigation into why the previous study observed both *c*DCE and dioxane transformation, while the column presented here only demonstrated *c*DCE transformation. This is especially necessary as batch reactor studies using the same beads (Section 4.1) indicated transformation of both compounds. 2-butanol may have an inhibitory effect on dioxane transformation. In the previous study, 2-butanol was utilized to very low concentrations.

The previous study also investigated two columns composed of gellan gum beads coencapsulated with TBOS and 21198. These previous columns were able to achieve growth of 21198 throughout the whole column, indicated by an orange tint, compared to the column in Section 5.2.1 only having significant growth of 21198 in the bottom portion of the column (Figure 5.16). These previous columns also only necessitated the addition of 100 mg/L of H_2O_2 to bring 1-butanol levels below detection in the effluent. Comparatively, the PVA/SA TBOS column operated for this thesis demonstrated a minimum effluent 1-butanol concentration of ~50 mg/L, even after the addition of up to 300 mg/L of H_2O_2. One reason for this may be that the PVA/SA beads hydrolyze TBOS significantly faster than the gellan gum beads. However, this is not supported by the results from abiotic hydrolysis tests (Section 5.4), which showed that the PVA/SA beads released 1-butanol 4 times more slowly than the bead formulations used in the columns from this previous study.

Another possibility is that the difference in influent solution led to a significant difference in the rate of TBOS hydrolysis. The previous column studies used 10x diluted phosphate buffer MSM, while the PVA/SA column study conducted here used an influent solution formulated to more closely align with groundwater. The influent feed solution in the previous studies was buffered at a pH of 7.0, which was also measured in the effluent. The influent solution used in the PVA/SA column study here entered at 7.0, 7.5, and 7.9 pH, depending on the time period, and the column effluent was slightly acidic (~6.0 to 6.4 pH). The beads in the PVA/SA bead column experienced a range of pH values, and pH is known to affect the rate of TBOS hydrolysis.[173] Neutral pH has the lowest rate of hydrolysis, which could explain why the previous column studies were able to demonstrate effluent 1-butanol levels below detection.

Future studies should further investigate the effects that changes to the solution composition and pH buffering capacity have on the co-encapsulated bead systems.

The previous column studies using gellan gum beads coencapsulated with TBOS and 21198 demonstrated an ability to transform >99% of influent *c*DCE after 10 PV.[172] Full biostimulation of the column, represented by a strong orange coloration throughout, was evident by 100 PV. However, the TBOS PVA/SA column study presented here necessitated 80 PV to achieve >95% transformation of *c*DCE. The orange color demonstrating 21198 growth was only observed in the bottom section of the column (Figure 5.16), indicating that full biostimulation was not achieved. Another possibility for the lower transformation efficiency demonstrated by the PVA/SA bead column may be a lower retardation factor compared to the gellan gum hydrogel beads (Section 5.2.1), which would lead to contaminants transporting through the bead pack more rapidly.

5.4 Abiotic Hydrolysis Studies

Abiotic hydrolysis studies were conducted for the T2BOS gellan gum beads and the PVA/SA TBOS beads in an effort to determine the rate that 2-butanol and 1-butanol were being released within the two columns packed for this thesis. These tests were done by poisoning 2 g beads in 100 mL of carbonate buffer MSM and then measuring the 2-butanol and 1-butanol generated over time as described in Rasmussen (2018).[11] The results for the T2BOS gellan gum batch bottles are displayed in Figure 5.19. Both batch bottles were created identically, and the replicate results were near-identical. These batch bottles averaged a 2-butanol generation rate of 0.027 µmol/d-g bead. This rate of production was nearly twice as high as the previous study conducted using the same bead formulation and buffered solution, which had an estimated rate of 0.015 µmol/d-g bead.[11] This provides further evidence that this batch of gellan gum beads was

structurally different from the batches used in previous studies, despite the formulation and method for creation being identical. It should be noted that different students fabricated the beads between the studies, and the study completed here used beads that had been stored at 4°C for about 2 months.

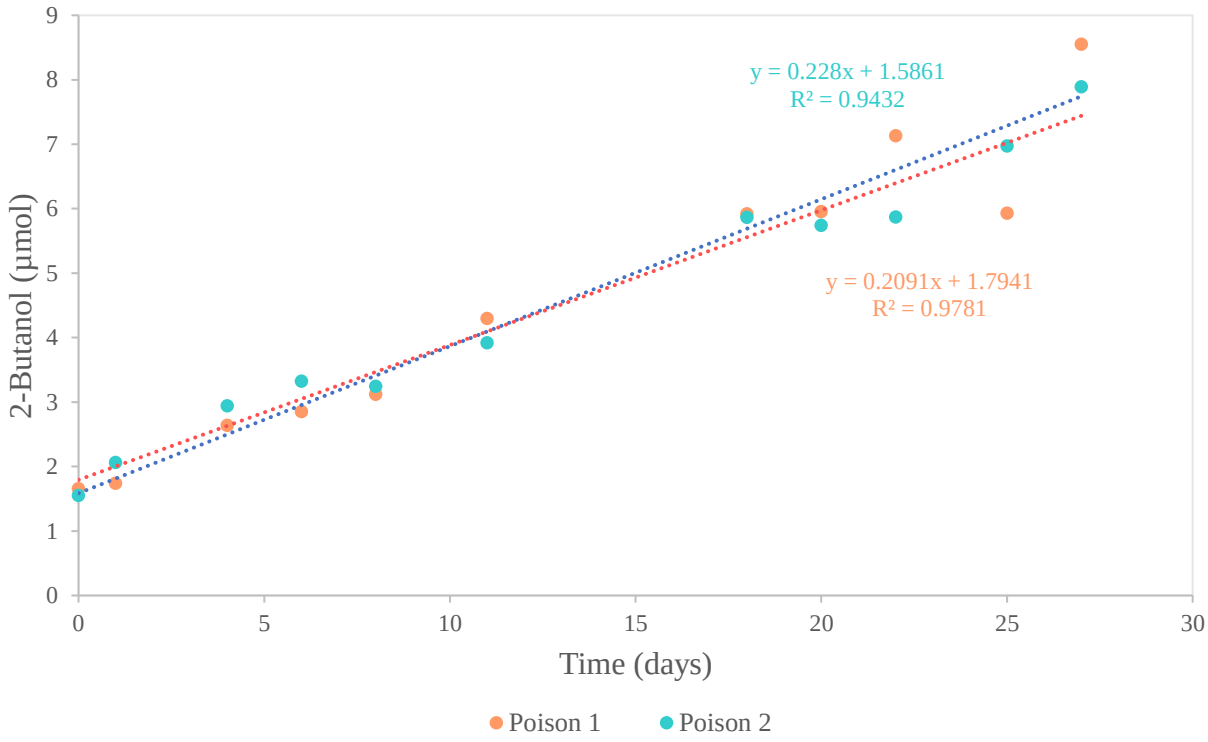

Figure 5.19. 2-butanol concentrations measured over time during the abiotic hydrolysis study conducted on the T2BOS gellan gum beads. Both batch reactors were set up identically.

For the PVA/SA beads used in the column study (Section 5.2), the abiotic hydrolysis test was the same. The carbonate buffer MSM was used to be able to compare results to previous abiotic hydrolysis studies done with gellan gum beads coencapsulated with TBOS. The results from this study are presented in Figure 5.20. The results from both reactors were similar, with an average zero-order 1-butanol generation rate of 0.16 µmol/d-g bead. This rate was approximately 4 times slower than the rate of 0.65 µmol/d-g bead demonstrated by the TBOS gellan gum beads in a previous study.[11] This may be evidence of the increased durability of the PVA/SA beads, as

the slower rate could show that these beads are stronger and more densely cross-linked. The difference could result from the gellan gum beads having more TBOS exposed to water, leading to higher rates of hydrolysis.[73]

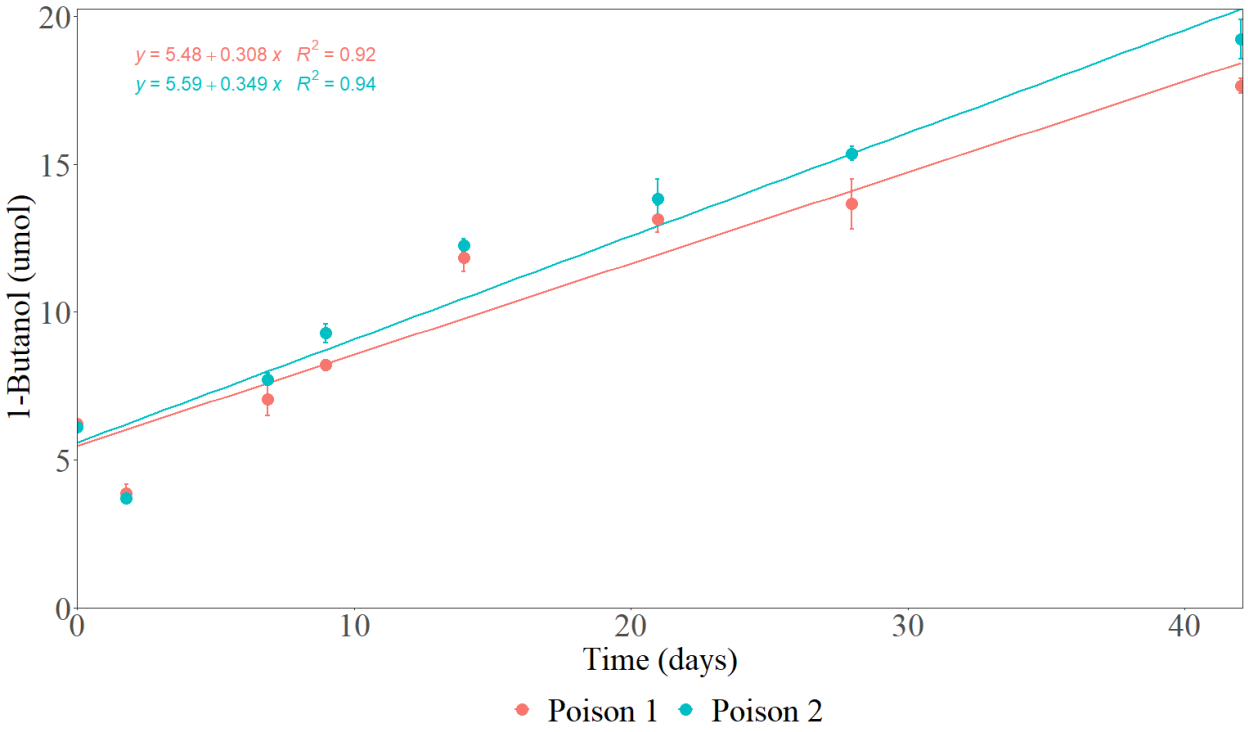

Figure 5.20. 1-butanol concentrations measured over time during the abiotic hydrolysis study conducted on the TBOS PVA/SA gum beads. Both batch reactors were set up identically. Error bars represent standard deviations of triplicate samples.

These results are inconsistent with the column studies completed previously (Azizian et al., 2022) and here (Sections 5.1 and 5.2), as these previous studies using gellan gum beads had significantly lower effluent 1-butanol and 2-butanol concentrations throughout the studies.[172] This contrasts with both abiotic hydrolysis tests, which found lower rates of T2BOS and TBOS hydrolysis in the batch reactors here than in previous studies. It would be expected that if the column studies presented here are hydrolyzing the SRSs at a faster rate, that would be reflected in the batch reactors.

The hydrolysis rates were used to estimate the maximum butanol concentrations in the effluent samples of the column by multiplying the rates by the mass of beads per volume of liquid within the column, as determined by weight measurements prior to column start-up. This result was then multiplied by the HRT and the ratio of the column porosity to the batch reactor porosity to estimate a maximum butanol concentration, assuming that none of the butanol was utilized by 21198. These porosities were determined by column weight measurements and the bead volume compared to the media volume in the batch reactors. The maximum 1-butanol that would have been generated by the TBOS PVA/SA bead column, if it was hydrolyzing TBOS at the same rate as the batch reactors, would have been ~390 mg/L. The actual maximum concentrations found in the column study here were ~200 mg/L, about half of that. This would make sense, as much of the 1-butanol was likely being utilized by the 21198.

Using the same estimations, the maximum 2-butanol concentrations for the T2BOS gellan gum bead column should have been ~17 mg/L, assuming none of it was utilized by 21198. The actual maximum concentrations observed during steady flow were ~50 mg/L, ~3 times the estimate. This indicates that the beads within the columns were likely hydrolyzing their respective SRSs at a much higher rate than observed in the batch reactors. This may be partially due to the higher rate of bead degradation observed in beads that were actively transforming contaminants (Section 4.1), like they would have been in the column. Further abiotic hydrolysis tests using varying solution compositions at a range of pH values would be beneficial for determining more conclusive reasoning for differences in hydrolysis between beads.

CHAPTER 6 – CONCLUSIONS

In assessing the long-term efficacy of gellan gum encapsulated *Rhodococcus rhodochrous* strain ATCC 21198, the results were mixed. The batch bottle reactors containing either T2BOS or TBOS gellan gum beads were able to transform essentially all added *c*DCE and dioxane. This verifies the results of previous research into this method of cell immobilization.[8,11,73] The rates of contaminant transformation were similar between T2BOS and TBOS bead reactors during the first addition. However, T2BOS batch reactors had significantly slower transformation rates than the TBOS batch bottles by the end of the study. This contrasts with previous research, which showed that 2-butanol as a substrate promotes faster transformation rates of dioxane than 1-butanol in the case of 21198.[73] However, this work was conducted in suspension as opposed to with hydrogel beads. A faster rate of TBOS hydrolysis compared to T2BOS likely resulted in a higher biomass within the batch reactors, which also led to less exposure time to possibly toxic *c*DCE epoxide. This faster hydrolysis rate is supported by previous research.[9]

The T2BOS gellan gum beads demonstrated slowing oxygen consumption rates over time, while the TBOS gellan gum beads remained relatively consistent in their oxygen use. Successive spikes of *c*DCE and dioxane may have impacted the long-term health of 21198 in the T2BOS beads. The TBOS reactors also showed the ability to withstand a two month long anaerobic period. Transformation and oxygen consumption rates decreased after this period, but this provides evidence of significant biomass that developed within the beads.

Issues with long-term gellan gum bead efficacy were largely found with the durability of the beads. By day 47 of the T2BOS gellan gum batch reactor study, the beads had fallen apart, as discussed in Section 4.1. This diverges from previous research using this same bead formulation

which did not have bead durability problems.[9,11] Similarly, the TBOS gellan gum bead batch reactor study (Section 4.2) did not have this issue. This suggests that the bead fabrication method is not completely reproducible, and slight issues with the heating step may have caused issues for the beads long term. It should be noted that the beads used in this study were scaled-up in the amounts fabricated compared to the original study of Rasmussen et al, (2020)[9]. Developing a more easily replicable bead creation process was part of the work conducted in parallel with this thesis, which is where the PVA/SA beads were developed.

The column packed with gellan gum beads showed long-term success at transforming *c*DCE at ~300 µg/L. Essentially complete transformation was achieved until the high-flow test was conducted at 75 PV. Rapid exposure to *c*DCE and *c*DCE epoxide throughout the entire column during this test may have influenced bead efficacy. By the end of the study, a total of 71.5% of the *c*DCE that entered the column was transformed. However, a mass balance found that essentially no dioxane entering the column was transformed. This diverges from the results from the batch reactor studies, which showed the ability to transform both contaminants. This suggests that dioxane transformation in the column may have been inhibited by the presence of 2-butanol. Similarly to the batch reactors, the gellan gum bead column demonstrated issues with bead durability. Compression tests conducted on beads pre- and post-use in the column showed that the beads were approximately 40x stronger prior to their use within the column.

The gellan gum bead column with T2BOS did not demonstrate an ability to recover from exposure to high levels of *c*DCE epoxide throughout the column during and after the high-flow rate test. Despite continuously adding media with high levels of hydrogen peroxide and nutrients, there was no evidence of *c*DCE or dioxane transformation after the stop-flow period. This corresponded with the T2BOS gellan gum batch bottle studies which showed evidence that

successive contaminant additions gradually harmed the microbial population as indicated by lower contaminant transformation and oxygen consumption rates.

The column packed with PVA/SA beads with TBOS was successful in achieving over 95% transformation of ~200 µg/L *c*DCE after a period of biostimulation and adjustments to influent H_2O_2 and pH. The majority of this transformation took place prior to flow reaching the first sampling port. Pictures of the column supported that this portion of the column had higher biomass than the rest of the column based on orange coloration. Increasing the pH from 7.0 to 7.5 in the influent solution stimulated microbial growth, evidenced by a decrease in effluent 1-butanol and dissolved oxygen. High levels (>200 mg/L) of H_2O_2 were required for significant transformation to occur. However, this was still not sufficient in reducing 1-butanol to negligible levels. 1-butanol was released more rapidly than the microorganisms could utilize it with the given DO and nutrient conditions. TBOS may be an issue as an SRS for this reason, but it does show evidence of promoting effective microbial growth. This column showed a resilience to high levels (>100 peak area) of *c*DCE epoxide, demonstrating an ability to decrease these levels and to continue transforming *c*DCE after exposure.

There were advantages to both TBOS and T2BOS as SRSs. For TBOS, the beads displayed evidence of higher microbial biomass in the form of higher transformation rates and oxygen consumption. For the T2BOS beads, their lower oxygen consumption was beneficial in requiring fewer oxygen addtions. This would be useful in real-world applications where adding oxygen would be challenging. The goal of PRBs is to have them passively perform treatment. However, the T2BOS beads did not show the resilience that the TBOS beads did when exposed to high levels of contaminants or prolonged periods without oxygen.

Embryonic zebrafish toxicity tests were inconclusive in regards to possible toxicity generated through use of the beads. Toxicity decreased from the start of the batch reactor toxicity tests to the end, even when no *c*DCE was initially present. It is possible that the assumed high levels of 1-butanol that were present at the beginning of the study, which decreased throughout the course of the study, were responsible for the toxicity. For the PVA/SA bead column, the only sample that reached the significance threshold for toxicity was from the column effluent, where the 1-butanol concentration was ~125 mg/L. 1-butanol has been shown to toxic to zebrafish embryos at levels as low as 50 mg/L, which was exceeded by ~75 mg/L in the column effluent.[171] However, the top port sample with a similar 1-butanol concentration did not show significant toxicity. There is not enough data to declare that the beads and the process of aerobic cometabolism do not generate toxicity, but there is also nothing that points to the generation of an unknown hazardous byproduct.

CHAPTER 7 – FUTURE WORK

This thesis discovered a number of issues related to the co-encapsulated hydrogel beads, both fabricated from gellan gum and PVA/SA, that should be investigated further. A better understanding of how the beads react to certain environmental conditions should be obtained. To do this, abiotic hydrolysis tests should be conducted in various media solutions at various pH levels. It is likely that the rates of 1-butanol and 2-butanol release are affected by these conditions, but this needs to be quantified. This thesis showed a marked difference in hydrolysis rates from previous studies. Hydrolysis tests should also be performed using groundwater from different contaminated sites.

In addition, further tests should be conducted in regard to bead durability. This thesis demonstrated that beads are not structurally sound in the long-term in every situation. The mechanism for this breakdown should be investigated. Possibilities include microbial growth overwhelming the solid matrix, the contaminants or their degradation products affecting the matrix, or the beads themselves being used in transformation or respiration. Determining the method for this structural failure will allow for an understanding of suitable environments for the beads.

A method to better quantify the mass of microorganisms within the beads would be useful as well. Currently, it is assumed that microbial growth is high when the beads become orange tinted. A microbial method that allows for one to easily measure that biomass would allow for stronger evidence that microbial growth occurs long-term.

The gellan gum T2BOS beads within the column study did not demonstrate any ability to transform dioxane. This was in direct contradiction to previous gellan gum bead studies and the batch bottle work conducted for this thesis. One possibility for this inhibited transformation

could be that 2-butanol levels were never negligible when dioxane was being added to the column. Future work should investigate whether 2-butanol inhibits dioxane transformation, as this would be a significant issue with using T2BOS as an SRS. This would mean that there would always need to be an extensive amount of oxygen present to ensure that 2-butanol was depleted so that dioxane transformation could occur. The reasoning for why earlier column tests with gellan gum beads with T2BOS were successful in transforming dioxane, while the column study presented here was not, needs to be investigated.

The PVA/SA TBOS bead column is still in operation. It would also be useful to add dioxane to this column. 1-butanol levels are still an issue with this column, but it has shown the ability to transform more than 95% of influent *c*DCE. If it does not show the ability to transform any dioxane, this would suggest that 1-butanol could inhibit dioxane transformation as well. Changing the influent solution formulation could also be beneficial, as using a more buffered solution may decrease the rate of TBOS hydrolysis.

Once these potential problems are addressed, future bead work may benefit from focusing on T2BOS as the primary SRS as opposed to TBOS, as the oxygen demand of TBOS beads may not be feasible in a real-world scenario. However, results from studies conducted for this thesis found that T2BOS beads tend to lead to microbial populations that are less resilient to long-term contaminant exposure and long periods with limited oxygen. Testing beads that use a combination of TBOS and T2BOS could be beneficial, as this may lead to a bead that fosters a high level of microbial growth due to the TBOS and that has a significantly lower oxygen demand due to the T2BOS. It would be necessary to conduct several studies to determine the ideal ratio between the two.

Finally, future work should settle the bead formulation. This thesis and past work have investigated gellan gum and PVA/SA beads of varying formulations. Using bead durability information, a best formulation should be decided upon that will allow for future work to consistently use one bead formulation that is easy to replicate. Once this formulation has been determined, it should be used in column studies similar to the ones presented here to verify long-term efficacy and for a comparison of results. From there, a larger scale test should be conducted that more closely models the soil and groundwater media in real environmental settings. Concurrently to the work presented here, a study is being conducted using a larger aquifer model and TBOS gellan gum beads in an attempt to have a more representative environment. These results may provide the evidence necessary to then move toward *in situ* testing.

CHAPTER 8 – REFERENCES

(1) Riser-Roberts, E. Bioremediation of Petroleum Contaminated Sites. Boca Raton (FL). CRC Press, Inc 1992.

(2) Doherty, R. E. A History of the Production and Use of Carbon Tetrachloride, Tetrachloroethylene, Trichloroethylene and 1,1,1-Trichloroethane in the United States: Part 1 - Historical Background; Carbon Tetrachloride and Tetrachloroethylene. *Environmental Forensics* **2000**, *1* (2), 69–81. https://doi.org/10.1006/enfo.2000.0010 WE - Science Citation Index Expanded (Sci-Expanded).

(3) Zenker, M. J.; Borden, R. C.; Barlaz, M. A.; Zenker, M. J.; Borden, R. C.; Barlaz, M. A. Occurrence and Treatment of 1,4-Dioxane in Aqueous Environments. *Environmental Engineering Science*. [Larchmont, NY] : 2003, pp 423–432. https://doi.org/10.1089/109287503768335913.

(4) Abe, Y.; Aravena, R.; Zopfi, J.; Parker, B.; Hunkeler, D. Evaluating the Fate of Chlorinated Ethenes in Streambed Sediments by Combining Stable Isotope, Geochemical and Microbial Methods. *Journal of Contaminant Hydrology* **2009**, *107* (1–2), 10–21. https://doi.org/10.1016/J.JCONHYD.2009.03.002.

(5) Derosa, C. T.; Wilbur, S.; Holler, J.; Richter, P.; Stevens, Y.-W. Health Evaluation of 1,4-Dioxane. *Toxicology and Industrial Health* **1996**, *12* (1), 1–43. https://doi.org/10.1177/074823379601200101.

(6) US EPA (United States Environmental Protection Agency). *Remediation Technology Descriptions for Cleaning Up Contaminated Sites*. https://www.epa.gov/remedytech/remediation-technology-descriptions-cleaning-contaminated-sites (accessed 2022-02-16).

(7) Mueller, J. G.; Cerniglia, C. E.; Pritchard, P. H. Bioremediation of Environments Contaminated by Polycyclic Aromatic Hydrocarbons. In *Bioremediation: Principles and Applications*; Crawford, D. L., Crawford, R. L., Eds.; Biotechnology Research; Cambridge University Press: Cambridge, 1996; pp 125–194. https://doi.org/DOI: 10.1017/CBO9780511608414.007.

(8) Rolston, H. M.; Hyman, M. R.; Semprini, L. Aerobic Cometabolism of 1,4-Dioxane by Isobutane-Utilizing Microorganisms Including *Rhodococcus Rhodochrous* Strain 21198 in Aquifer Microcosms: Experimental and Modeling Study. *Science of The Total Environment* **2019**, *694*, 133688. https://doi.org/10.1016/j.scitotenv.2019.133688.

(9) Rasmussen, M. T.; Saito, A. M.; Hyman, M. R.; Semprini, L. Co-Encapsulation of Slow Release Compounds and *Rhodococcus Rhodochrous* ATCC 21198 in Gellan Gum Beads to Promote the Long-Term Aerobic Cometabolic Transformation of 1,1,1-Trichloroethane, Cis -1,2-Dichloroethene and 1,4-Dioxane. *Environmental Science: Processes & Impacts* **2020**, *22* (3), 771–791.

(10) US EPA (United States Environmental Protection Agency). *Risk Assessment Guidance for Superfund, Volume I: Human Health Evaluation Manual (Part A)*; EPA/540/1-89/002, http://www. epa. gov/superfund/programs/risk/ragsa/index. htm: Washington, DC, 1989.

(11) Rasmussen, M. T. Co-Encapsulation of Slow Release Substrates and Microbial Cultures in Alginate and Gellan Gum Beads to Promote the Co-Metabolic Transformation of 1,4-Dioxane and Chlorinate Aliphatic Hydrocarbons, Oregon State University, 2018.

(12) Geissen, V.; Mol, H.; Klumpp, E.; Umlauf, G.; Nadal, M.; van der Ploeg, M.; van de Zee, S. E. A. T. M.; Ritsema, C. J. Emerging Pollutants in the Environment: A Challenge for Water Resource Management. *International Soil and Water Conservation Research* **2015**, *3* (1), 57–65. https://doi.org/10.1016/j.iswcr.2015.03.002.

(13) Aminot, Y.; Sayfritz, S. J.; Thomas, K. v.; Godinho, L.; Botteon, E.; Ferrari, F.; Boti, V.; Albanis, T.; Köck-Schulmeyer, M.; Diaz-Cruz, M. S.; Farré, M.; Barceló, D.; Marques, A.; Readman, J. W. Environmental Risks Associated with Contaminants of Legacy and Emerging Concern at European Aquaculture Areas. *Environmental Pollution* **2019**, *252*, 1301–1310. https://doi.org/10.1016/J.ENVPOL.2019.05.133.

(14) Kroon, F. J.; Berry, K. L. E.; Brinkman, D. L.; Kookana, R.; Leusch, F. D. L.; Melvin, S. D.; Neale, P. A.; Negri, A. P.; Puotinen, M.; Tsang, J. J.; van de Merwe, J. P.; Williams, M. Sources, Presence and Potential Effects of Contaminants of Emerging Concern in the Marine Environments of the Great Barrier Reef and Torres Strait, Australia. *Science of The Total Environment* **2020**, *719*, 135140. https://doi.org/10.1016/j.scitotenv.2019.135140.

(15) Shaw, P. M.; Johns, R. B. Organic Geochemical Studies of a Recent Inner Great Barrier Reef Sediment—I. Assessment of Input Sources. *Organic Geochemistry* **1985**, *8* (2), 147–156. https://doi.org/10.1016/0146-6380(85)90032-4.

(16) Vogel, T. M.; Criddle, C. S.; McCarty, P. L. ES&T Critical Reviews: Transformations of Halogenated Aliphatic Compounds. *Environmental Science & Technology* **1987**, *21* (8), 722–736. https://doi.org/10.1021/es00162a001.

(17) Popek, E. Environmental Chemical Pollutants. In *Sampling and Analysis of Environmental Chemical Pollutants*; Popek, E., Ed.; Elsevier, 2018; pp 13–69. https://doi.org/10.1016/B978-0-12-803202-2.00002-1.

(18) Horvath, R. S. Microbial Co-Metabolism and the Degradation of Organic Compounds in Nature. *Bacteriological Reviews* **1972**, *36* (2), 146–155. https://doi.org/10.1128/br.36.2.146-155.1972.

(19) Doble, M.; Kumar, A. Chlorinated Hydrocarbons and Aromatics, and Dioxins. In *Biotreatment of Industrial Effluents*; Doble, M., Kumar, A., Eds.; Elsevier: Burlington, 2005; pp 65–82. https://doi.org/10.1016/B978-075067838-4/50007-5.

(20) Kim, Y.; Semprini, L. Cometabolic Transformation of Cis-1 2-Dichloroethylene and Cis-1,2-Dichloroethylene Epoxide by a Butane-Grown Mixed Culture. *Water Science And Technology* **2005**, *52* (4th World Water Congress of the International-Water-Association), 125–131. https://doi.org/10.2166/wst.2005.0242 WE - Conference Proceedings Citation Index - Science (CPCI-S) WE - Science Citation Index Expanded (Sci-Expanded).

(21) van Hylckama Vlieg, J. E. T.; de Koning, W.; Janssen, D. B. Transformation Kinetics of Chlorinated Ethenes by *Methylosinus Trichosporium* OB3b and Detection of Unstable Epoxides by On-Line Gas Chromatography. *Applied and Environmental Microbiology* **1996**, *62* (9), 3304–3312. https://doi.org/10.1128/aem.62.9.3304-3312.1996.

(22) Oldenhuis, R.; Oedzes, J. Y.; van der Waarde, J. J.; Janssen, D. B. Kinetics of Chlorinated Hydrocarbon Degradation by Methylosinus Trichosporium OB3b and Toxicity of Trichloroethylene. *Applied and Environmental Microbiology* **1991**, *57* (1), 7–14. https://doi.org/10.1128/aem.57.1.7-14.1991.

(23) Janssen, D. B.; Grobben, G.; Hoekstra, R.; Oldenhuis, R.; Witholt, B. Degradation of Trans-1,2-Dichloroethene by Mixed and Pure Cultures of Methanotrophic Bacteria. *Applied Microbiology and Biotechnology* **1988**, *29* (4), 392–399. https://doi.org/10.1007/BF00265825.

(24) Alvarez-Cohen, L.; McCarty, P. L. Product Toxicity and Cometabolic Competitive Inhibition Modeling of Chloroform and Trichloroethylene Transformation by Methanotrophic Resting Cells. *Applied and Environmental Microbiology* **1991**, *57* (4), 1031–1037. https://doi.org/10.1128/aem.57.4.1031-1037.1991.

(25) Abe, A. Distribution of 1,4-Dioxane in Relation to Possible Sources in the Water Environment. *Science of the Total Environment* **1999**, *227* (1), 41–47. https://doi.org/10.1016/S0048-9697(99)00003-0.

(26) Adamson, D. T.; Piña, E. A.; Cartwright, A. E.; Rauch, S. R.; Hunter Anderson, R.; Mohr, T.; Connor, J. A. 1,4-Dioxane Drinking Water Occurrence Data from the Third Unregulated Contaminant Monitoring Rule. *Science of the Total Environment* **2017**, *596–597*, 236–245. https://doi.org/10.1016/j.scitotenv.2017.04.085.

(27) Jackson, R. E.; Dwarakanath, V. Chlorinated Decreasing Solvents: Physical-Chemical Properties Affecting Aquifer Contamination and Remediation. *Groundwater Monitoring & Remediation* **1999**, *19* (4), 102–110. https://doi.org/10.1111/j.1745-6592.1999.tb00246.x.

(28) Eckhardt, A. Positive Trends Emerge in Reducing Exposure to 1,4-Dioxane. *Journal AWWA* **2018**, *110* (7), 54–59. https://doi.org/https://doi.org/10.1002/awwa.1116.

(29) US EPA (United States Environmental Protection Agency). *Technical Fact Sheet: 1.4-Dioxane*; 2017.

(30) Mohr, T. K. G.; DiGuiseppi, W. H.; Hatton, J. W.; Anderson, J. K. *Environmental Investigation and Remediation: 1,4-Dioxane and Other Solvent Stabilizers*; CRC Press, 2020.

(31) Adams, C. D.; Scanlan, P. A.; Secrlst, N. D. Oxidation and Biodegradability Enhancement of 1,4-Dioxane Using Hydrogen Peroxide and Ozone. **1994**, *28* (11), 1812–1818.

(32) Beckett, M. A.; Hua, I. Enhanced Sonochemical Decomposition of 1,4-Dioxane by Ferrous Iron. *Water Research* **2003**, *37* (10), 2372–2376. https://doi.org/10.1016/S0043-1354(03)00005-8.

(33) Kim, C. G.; Seo, H. J.; Lee, B. R. Decomposition of 1,4-Dioxane by Advanced Oxidation and Biochemical Process. *Journal of Environmental Science and Health - Part A Toxic/Hazardous Substances and Environmental Engineering* **2006**, *41* (4), 599–611. https://doi.org/10.1080/10934520600574807.

(34) Son, H. S.; Choi, S. B.; Khan, E.; Zoh, K. D. Removal of 1,4-Dioxane from Water Using Sonication: Effect of Adding Oxidants on the Degradation Kinetics. *Water Research* **2006**, *40* (4), 692–698. https://doi.org/10.1016/j.watres.2005.11.046.

(35) Stefan, M. I.; Bolton, J. R. Mechanism of the Degradation of 1,4-Dioxane in Dilute Aqueous Solution Using the UV Hydrogen Peroxide Process. *Environmental Science & Technology* **1998**, *32* (11), 1588–1595. https://doi.org/10.1021/es970633m WE - Science Citation Index Expanded (Sci-Expanded).

(36) Hill, R. R.; Jeffs, G. E.; Roberts, D. R. Photocatalytic Degradation of 1,4-Dioxane in Aqueous Solution. *Journal of Photochemistry and Photobiology A: Chemistry* **1997**, *108* (1), 55–58. https://doi.org/10.1016/S1010-6030(96)04463-2.

(37) Adamson, D. T.; de Blanc, P. C.; Farhat, S. K.; Newell, C. J. Implications of Matrix Diffusion on 1,4-Dioxane Persistence at Contaminated Groundwater Sites. *Science of The Total Environment* **2016**, *562*, 98–107. https://doi.org/10.1016/j.scitotenv.2016.03.211.
(38) Sale, T.; Parker, B. L.; Newell, C. J.; Devlin, J. F. *Management of Contaminants Stored in Low Permeability Zones - A State-of-the-Science Review*; Strategic Environmental Research and Development Program: Arlington, VA, 2013.
(39) Parker, B. L.; Chapman, S. W.; Guilbeault, M. A. Plume Persistence Caused by Back Diffusion from Thin Clay Layers in a Sand Aquifer Following TCE Source-Zone Hydraulic Isolation. *Journal of Contaminant Hydrology* **2008**, *102* (1–2), 86–104. https://doi.org/10.1016/j.jconhyd.2008.07.003.
(40) Mahendra, S.; Alvarez-Cohen, L. Kinetics of 1,4-Dioxane Biodegradation by Monooxygenase-Expressing Bacteria. *Environmental Science and Technology* **2006**, *40* (17), 5435–5442. https://doi.org/10.1021/es060714v.
(41) Mahendra, S.; Petzold, C. J.; Baidoo, E. E.; Keasling, J. D.; Alvarez-Cohen, L. Identification of the Intermediates of in Vivo Oxidation of 1,4-Dioxane by Monooxygenase-Containing Bacteria. *Environmental Science and Technology* **2007**, *41* (21), 7330–7336. https://doi.org/10.1021/es0705745.
(42) Kennen, K.; Kirkwood, N. Phyto: Principles and Resources for Site Remediation and Landscape Design. *Phyto: Principles and Resources for Site Remediation and Landscape Design* **2015**, 1–346. https://doi.org/10.4324/9781315746661/Phyto-Kate-Kennen-Niall-Kirkwood.
(43) Thiruvenkatachari, R.; Vigneswaran, S.; Naidu, R. Permeable Reactive Barrier for Groundwater Remediation. *Journal of Industrial and Engineering Chemistry* **2008**, *14* (2), 145–156. https://doi.org/10.1016/j.jiec.2007.10.001.
(44) Vidali, M. Bioremediation. An Overview. *Pure and Applied Chemistry* **2001**, *73* (7), 1163–1172. https://doi.org/10.1351/pac200173071163.
(45) Stanier, R. Y.; Ingraham, J. L.; Wheelis, M. L.; Painter, P. R. *The Microbial World*, 5th ed.; Prentice Hall: NJ, 1986.
(46) Adriaens, P.; Hickey, W. J. *Biotechnology for the Treatment of Hazardous Waste.*; Lewis Publications: Ann Arbor, MI, 1993.
(47) Boopathy, R. Factors Limiting Bioremediation Technologies. *Bioresource Technology* **2000**, *74* (1), 63–67. https://doi.org/10.1016/S0960-8524(99)00144-3.
(48) Azubuike, C. C.; Chikere, C. B.; Okpokwasili, G. C. Bioremediation Techniques–Classification Based on Site of Application: Principles, Advantages, Limitations and Prospects. *World Journal of Microbiology and Biotechnology* **2016**, *32* (11), 180. https://doi.org/10.1007/s11274-016-2137-x.
(49) Semprini, L. Strategies for the Aerobic Co-Metabolism of Chlorinated Solvents. *Current Opinion in Biotechnology* **1997**, *8* (3), 296–308. https://doi.org/10.1016/S0958-1669(97)80007-9.
(50) Gavaskar, A. R.; Gupta, N.; Sass, B.; Janosy, R.; O`Sullivan, D. Permeable Barriers for Groundwater Remediation. Battelle Press, Columbus, OH (United States) December 31, 1998.
(51) Yang, X.; Fan, L. T.; Erickson, L. E. A Conceptual Study on the Bio-Wall Technology: Feasibility and Process Design. *Remediation Journal* **1995**, *6* (1), 55–67. https://doi.org/10.1002/rem.3440060105.

(52) Obiri-Nyarko, F.; Grajales-Mesa, S. J.; Malina, G. An Overview of Permeable Reactive Barriers for In Situ Sustainable Groundwater Remediation. *Chemosphere* **2014**, *111*, 243–259. https://doi.org/10.1016/j.chemosphere.2014.03.112.
(53) Vesela, L.; Nemecek, J.; Siglova, M.; Kubal, M. The Biofiltration Permeable Reactive Barrier: Practical Experience from Synthesia. *International Biodeterioration & Biodegradation* **2006**, *58* (3–4), 224–230. https://doi.org/10.1016/J.IBIOD.2006.06.013.
(54) Yerushalmi, L.; Manuel, M. F.; Guiot, S. R. Biodegradation of Gasoline and BTEX in a Microaerophilic Biobarrier. *Biodegradation* **1999**, *10* (5), 341–352. https://doi.org/10.1023/A:1008327815105.
(55) Johnson, S. J.; Woolhouse, K. J.; Prommer, H.; Barry, D. A.; Christofi, N. Contribution of Anaerobic Microbial Activity to Natural Attenuation of Benzene in Groundwater. *Engineering Geology* **2003**, *70* (3–4), 343–349. https://doi.org/10.1016/S0013-7952(03)00102-9.
(56) Yeh, C. H.; Lin, C. W.; Wu, C. H. A Permeable Reactive Barrier for the Bioremediation of BTEX-Contaminated Groundwater: Microbial Community Distribution and Removal Efficiencies. *Journal of Hazardous Materials* **2010**, *178* (1–3), 74–80. https://doi.org/10.1016/J.JHAZMAT.2010.01.045.
(57) Bianchi-Mosquera, G. C.; Allen-King, R. M.; Mackay, D. M. Enhanced Degradation of Dissolved Benzene and Toluene Using a Solid Oxygen-Releasing Compound. *Groundwater Monitoring & Remediation* **1994**, *14* (1), 120–128. https://doi.org/10.1111/J.1745-6592.1994.TB00097.X.
(58) Borden, R. C.; Goin, R. T.; Kao, C. M. Control of BTEX Migration Using a Biologically Enhanced Permeable Barrier. *Groundwater Monitoring & Remediation* **1997**, *17* (1), 70–80. https://doi.org/10.1111/J.1745-6592.1997.TB01186.X.
(59) Schipper, L. A.; Robertson, W. D.; Gold, A. J.; Jaynes, D. B.; Cameron, S. C. Denitrifying Bioreactors—An Approach for Reducing Nitrate Loads to Receiving Waters. *Ecological Engineering* **2010**, *36* (11), 1532–1543. https://doi.org/10.1016/j.ecoleng.2010.04.008.
(60) Vogan, J. L. *The Use of Emplaced Denitrifying Layers to Promote Nitrate Removal from Septic Effluent.*; University of Waterloo, 1993.
(61) Robertson, W. D.; Vogan, J. L.; Lombardo, P. S. Nitrate Removal Rates in a 15-Year-Old Permeable Reactive Barrier Treating Septic System Nitrate. *Ground Water Monitoring & Remediation* **2008**, *28* (3), 65–72. https://doi.org/10.1111/j.1745-6592.2008.00205.x.
(62) Robertson, W. D.; Cherry, J. A. In Situ Denitrification of Septic-System Nitrate Using Reactive Porous Media Barriers: Field Trials. *Ground Water* **1995**, *33* (1), 99–111. https://doi.org/10.1111/j.1745-6584.1995.tb00266.x.
(63) Waybrant, K. R.; Ptacek, C. J.; Blowes, D. W. Treatment of Mine Drainage Using Permeable Reactive Barriers: Column Experiments. *Environmental Science and Technology* **2002**, *36* (6), 1349–1356. https://doi.org/10.1021/ES010751G.
(64) Wilson, J. T.; He, Y.; Henry, B.; Evans, P. Abiotic and Biotic Transformation of TCE under Sulfate Reducing Conditions: The Role of Spatial Heterogeneity. In *7th International Battelle Conference*; Monterey, CA, 2010.
(65) Henry, B. M.; Hartfelder, T.; Goodspeed, M.; Gonzales, J. R.; Haas, P. E.; Oakley, D. Permeable Mulch Biowall for Enhanced Bioremediation of Chlorinated Ethenes. In *In Situ and On-Site Bioremediation Symposium*; Magar, V. S., Kelley, M. E., Eds.; Battelle Press: Orlando, FL, 2003; p K03.

(66) Öztürk, Z.; Tansel, B.; Katsenovich, Y.; Sukop, M.; Laha, S. Highly Organic Natural Media as Permeable Reactive Barriers: TCE Partitioning and Anaerobic Degradation Profile in Eucalyptus Mulch and Compost. *Chemosphere* **2012**, *89* (6), 665–671. https://doi.org/10.1016/j.chemosphere.2012.06.006.

(67) Larkin, M. J.; Kulakov, L. A.; Allen, C. C. Biodegradation and *Rhodococcus* – Masters of Catabolic Versatility. *Current Opinion in Biotechnology* **2005**, *16* (3), 282–290. https://doi.org/10.1016/j.copbio.2005.04.007.

(68) Shields-Menard, S. A.; Brown, S. D.; Klingeman, D. M.; Indest, K.; Hancock, D.; Wewalwela, J. J.; French, W. T.; Donaldson, J. R. Draft Genome Sequence of *Rhodococcus Rhodochrous* Strain ATCC 21198. *Genome Announcements* **2014**, *2* (1), 0–1. https://doi.org/10.1128/genomeA.e00054-14.

(69) Babu, J. P.; Brown, L. R. New Type of Oxygenase Involved in the Metabolism of Propane and Isobutane. *Applied and Environmental Microbiology* **1984**, *48* (2), 260–264. https://doi.org/10.1128/aem.48.2.260-264.1984.

(70) Bennett, P.; Hyman, M.; Smith, C.; el Mugammar, H.; Chu, M.-Y.; Nickelsen, M.; Aravena, R. Enrichment with Carbon-13 and Deuterium during Monooxygenase-Mediated Biodegradation of 1,4-Dioxane. *Environmental Science & Technology Letters* **2018**, *5* (3), 148–153. https://doi.org/10.1021/acs.estlett.7b00565.

(71) Krippaehne, K. J. Cometabolism of 1,4-Dioxane and Chlorinated Aliphatic Hydrocarbons by Pure Cultures of *Rhodococcus Rhodochrous* 21198 and *Mycobacterium* ELW1 and in Groundwater Microcosms Fed Isobutane and Isobutene as Growth Substrates, Oregon State University, 2018.

(72) Hyman, M. R.; Wood, P. M. Suicidal Inactivation and Labelling of Ammonia Mono-Oxygenase by Acetylene. *Biochemical Journal* **1985**, *227* (3), 719–725. https://doi.org/10.1042/bj2270719.

(73) Murnane, R. A.; Chen, W.; Hyman, M.; Semprini, L. Long-Term Cometabolic Transformation of 1,1,1-Trichloroethane and 1,4-Dioxane by *Rhodococcus Rhodochrous* ATCC 21198 Grown on Alcohols Slowly Produced by Orthosilicates. *Journal of Contaminant Hydrology* **2021**, *240*, 103796. https://doi.org/10.1016/j.jconhyd.2021.103796.

(74) Bettmann, H.; Rehm, H. J. Degradation of Phenol by Polymer Entrapped Microorganisms. *Applied Microbiology and Biotechnology* **1984**, *20* (5), 285–290. https://doi.org/10.1007/BF00270587.

(75) Manohar, S.; Karegoudar, T. B. Degradation of Naphthalene by Cells of *Pseudomonas* Sp. Strain NGK 1 Immobilized in Alginate, Agar and Polyacrylamide. *Applied Microbiology and Biotechnology* **1998**, *49* (6), 785–792. https://doi.org/10.1007/s002530051247.

(76) Paje, M. L.; Marks, P.; Couperwhite, I. Degradation of Benzene by a *Rhodococcus* Sp. Using Immobilized Cell Systems. *World Journal of Microbiology and Biotechnology 1998 14:5* **1998**, *14* (5), 675–680. https://doi.org/10.1023/A:1008898922908.

(77) Somerville, H. J.; Mason, J. R.; Ruffell, R. N. Benzene Degradation by Bacterial Cells Immobilized in Polyacrylamide Gel. *European Journal of Applied Microbiology* **1977**, *4* (2), 75–85. https://doi.org/10.1007/BF00929158.

(78) Hall, B. M.; McLoughlin, A. J.; Leung, K. T.; Trevors, J. T.; Lee, H. Transport and Survival of Alginate-Encapsulated and Free Lux-Lac Marked *Pseudomonas Aeruginosa* UG2Lr Cells in Soil. *FEMS Microbiology Ecology* **1998**, *26* (1), 51–61. https://doi.org/10.1111/j.1574-6941.1998.tb01561.x.

(79) Suzuki, T.; Yamaguchi, T.; Ishida, M. Immobilization of *Prototheca Zopfü* in Calcium-Alginate Beads for the Degradation of Hydrocarbons. *Process Biochemistry* **1998**, *33* (5), 541–546. https://doi.org/10.1016/S0032-9592(98)00022-3.

(80) Trevors, J. T. Use of Alginate and Other Carries for Encapsulation of Microbial Cells for Use in Soil. *Microvial. Rel.* **1992**, *1*, 61–69.

(81) Weir, S. C.; Providenti, M. A.; Lee, H.; Trevors, J. T. Effect of Alginate Encapsulation and Selected Disinfectants on Survival of and Phenanthrene Mineralization by *Pseudomonas* Sp UG14Lr in Creosote-Contaminated Soil. *Journal of Industrial Microbiology* **1996**, *16* (1), 62–67. https://doi.org/10.1007/BF01569923.

(82) Lapponi, M. J.; Méndez, M. B.; Trelles, J. A.; Rivero, C. W. Cell Immobilization Strategies for Biotransformations. *Current Opinion in Green and Sustainable Chemistry* **2022**, *33*, 100565. https://doi.org/10.1016/j.cogsc.2021.100565.

(83) Górecka, E.; Jastrzębska, M. Review Article: Immobilization Techniques and Biopolymer Carriers. *Biotechnology and Food Science* **2011**, *75* (1), 65–86.

(84) Costerton, J. W.; Lewandowski, Z.; Caldwell, D. E.; Korber, D. R.; Lappin-Scott, H. M. Microbial Biofilms. *Annual Review of Microbiology* **1995**, *49* (1), 711–745. https://doi.org/10.1146/annurev.mi.49.100195.003431.

(85) Abee, T.; Kovács, Á. T.; Kuipers, O. P.; van der Veen, S. Biofilm Formation and Dispersal in Gram-Positive Bacteria. *Current Opinion in Biotechnology* **2011**, *22* (2), 172–179. https://doi.org/10.1016/j.copbio.2010.10.016.

(86) Davey, M. E.; O'toole, G. A. Microbial Biofilms: From Ecology to Molecular Genetics. *Microbiol Mol Biol Rev* **2000**, *64* (4), 847–867. https://doi.org/10.1128/MMBR.64.4.847-867.2000.

(87) Costerton, J. W.; Marrie, T. J.; Cheng, K.-J. Phenomena of Bacterial Adhesion. In *Bacterial Adhesion*; Savage, D. C., Fletcher, M., Eds.; Springer US: Boston, MA, 1985; pp 3–43. https://doi.org/10.1007/978-1-4615-6514-7_1.

(88) Mitra, A.; Mukhopadhyay, S. Biofilm Mediated Decontamination of Pollutants from the Environment. *AIMS Bioengineering* **2016**, *3* (1), 44–59. https://doi.org/10.3934/bioeng.2016.1.44.

(89) Toyofuku, M.; Inaba, T.; Kiyokawa, T.; Obana, N.; Yawata, Y.; Nomura, N. Environmental Factors That Shape Biofilm Formation. *Bioscience, Biotechnology, and Biochemistry* **2016**, *80* (1), 7–12. https://doi.org/10.1080/09168451.2015.1058701.

(90) Singh, R.; Paul, D.; Jain, R. K. Biofilms: Implications in Bioremediation. *Trends in Microbiology* **2006**, *14* (9), 389–397. https://doi.org/10.1016/j.tim.2006.07.001.

(91) Ramakrishna, S. v; Prakasham, R. S. Microbial Fermentations with Immobilized Cells. *Current Science* **1999**, *77* (1), 87-100 WE-Science Citation Index Expanded (Sci-Expanded).

(92) Morikawa, M. Beneficial Biofilm Formation by Industrial Bacteria *Bacillus Subtilis* and Related Species. *Journal of Bioscience and Bioengineering* **2006**, *101* (1), 1–8. https://doi.org/10.1263/jbb.101.1.

(93) Bayat, Z.; Hassanshahian, M.; Cappello, S. Immobilization of Microbes for Bioremediation of Crude Oil Polluted Environments: A Mini Review. *Open Microbiol J* **2015**, *9*, 48–54. https://doi.org/10.2174/1874285801509010048.
(94) Smet, C.; van Derlinden, E.; Mertens, L.; Noriega, E.; van Impe, J. F. Effect of Cell Immobilization on the Growth Dynamics of *Salmonella Typhimurium* and *Escherichia Coli* at Suboptimal Temperatures. *International Journal of Food Microbiology* **2015**, *208*, 75–83. https://doi.org/10.1016/j.ijfoodmicro.2015.05.011.
(95) Cassidy, M. B.; Lee, H.; Trevors, J. T. Environmental Applications of Immobilized Microbial Cells: A Review. *Journal of Industrial Microbiology* **1996**, *16* (2), 79–101. https://doi.org/10.1007/BF01570068.
(96) Cláudia, S.; Martins, S.; Martins, C. M.; Cidrão, L. M.; Fiúza, G.; Santaella, S. T. Immobilization of Microbial Cells: A Promising Tool for Treatment of Toxic Pollutants in Industrial Wastewater. *African Journal of Biotechnology* **2016**, *12* (28), 4473. https://doi.org/10.4314/ajb.v12i28.
(97) Zucca, P.; Sanjust, E. Inorganic Materials as Supports for Covalent Enzyme Immobilization: Methods and Mechanisms. *Molecules* **2014**, *19* (9), 14139–14194. https://doi.org/10.3390/molecules190914139.
(98) Zhao, W.; Zhang, Y.; Liu, Y.; Tan, M.; Yu, W.; Xie, H.; Ma, Y.; Sun, G.; Lv, G.; Zhao, S.; Ma, X. Oxygen Diffusivity in Alginate/Chitosan Microcapsules. *Journal of Chemical Technology & Biotechnology* **2013**, *88* (3), 449–455. https://doi.org/10.1002/jctb.3845.
(99) Antwi, M.; Geeraerd, A. H.; Vereecken, K. M.; Jenné, R.; Bernaerts, K.; van Impe, J. F. Influence of a Gel Microstructure as Modified by Gelatin Concentration on *Listeria Innocua* Growth. *Innovative Food Science & Emerging Technologies* **2006**, *7* (1–2), 124–131. https://doi.org/10.1016/j.ifset.2005.08.001.
(100) Junter, G.-A.; Coquet, L.; Vilain, S.; Jouenne, T. Immobilized-Cell Physiology: Current Data and the Potentialities of Proteomics. *Enzyme and Microbial Technology* **2002**, *31* (3), 201–212. https://doi.org/10.1016/S0141-0229(02)00073-X.
(101) Dulieu, C.; Poncelet, D.; Neufeld, R. J. Encapsulation and Immobilization Techniques. In *Cell Encapsulation Technology and Therapeutics*; Birkhäuser Boston: Boston, MA, 1999; pp 3–17. https://doi.org/10.1007/978-1-4612-1586-8_1.
(102) Robitaille, R.; Pariseau, J.-F.; Leblond, F. A.; Lamoureux, M.; Lepage, Y.; Halle, J.-P. Studies on Small (<350 µm) Alginate-Poly-L-Lysine Microcapsules. III. Biocompatibility of Smaller versus Standard Microcapsules. *Journal of Biomedical Materials Research* **1999**, *44* (1), 116–120. https://doi.org/10.1002/(SICI)1097-4636(199901)44:1<116::AID-JBM13>3.0.CO;2-9.
(103) Strand, B. L.; Gåserød, O.; Kulseng, B.; Espevik, T.; Skjåk-Bræk, G. Alginate-Polylysine-Alginate Microcapsules: Effect of Size Reduction on Capsule Properties. *http://dx.doi.org.ezproxy.proxy.library.oregonstate.edu/10.1080/02652040210144243* **2008**, *19* (5), 615–630. https://doi.org/10.1080/02652040210144243.
(104) Żur, J.; Wojcieszyńska, D.; Guzik, U. Metabolic Responses of Bacterial Cells to Immobilization. *Molecules* **2016**, *21* (7), 958. https://doi.org/10.3390/molecules21070958.
(105) Osmałek, T.; Froelich, A.; Tasarek, S. Application of Gellan Gum in Pharmacy and Medicine. *International Journal of Pharmaceutics* **2014**, *466* (1–2), 328–340. https://doi.org/10.1016/j.ijpharm.2014.03.038.

(106) Morris, E. R.; Nishinari, K.; Rinaudo, M. Gelation of Gellan - A Review. *Food Hydrocolloids* **2012**, *28* (2), 373–411. https://doi.org/10.1016/j.foodhyd.2012.01.004.
(107) Pollock, T. J. Gellan-Related Polysaccharides and the *Genus Sphingomonas*. *Journal of General Microbiology* **1993**, *139* (8), 1939–1945. https://doi.org/10.1099/00221287-139-8-1939.
(108) Kang, K. S.; Veeder, G. T.; Mirrasoul, P. J.; Kaneko, T.; Cottrell, I. W. Agar-Like Polysaccharide Produced by a *Pseudomonas* Species: Production and Basic Properties. *Applied and Environmental Microbiology* **1982**, *43* (5), 1086–1091. https://doi.org/10.1128/aem.43.5.1086-1091.1982.
(109) Jansson, P.-E.; Lindberg, B.; Sandford, P. A. Structural Studies of Gellan Gum, an Extracellular Polysaccharide Elaborated by *Pseudomonas Elodea*. *Carbohydrate Research* **1983**, *124* (1), 135–139. https://doi.org/10.1016/0008-6215(83)88361-X.
(110) *Thickening and Gelling Agents for Food*; Imeson, A. P., Ed.; Springer US: Boston, MA, 1997. https://doi.org/10.1007/978-1-4615-2197-6.
(111) Moslemy, P.; Neufeld, R. J.; Guiot, S. R. Biodegradation of Gasoline by Gellan Gum-Encapsulated Bacterial Cells. *Biotechnology and Bioengineering* **2002**, *80* (2), 175–184. https://doi.org/10.1002/bit.10358.
(112) Karamba, K. I.; Ahmad, S. A.; Zulkharnain, A.; Yasid, N. A.; Khalid, A.; Shukor, M. Y. Biodegradation of Cyanide and Evaluation of Kinetic Models by Immobilized Cells of *Serratia Marcescens* Strain AQ07. *International Journal of Environmental Science and Technology* **2017**, *14* (9), 1945–1958. https://doi.org/10.1007/S13762-017-1287-1/TABLES/2.
(113) Wang, X.; Gai, Z.; Yu, B.; Feng, J.; Xu, C.; Yuan, Y.; Lin, Z.; Xu, P. Degradation of Carbazole by Microbial Cells Immobilized in Magnetic Gellan Gum Gel Beads. *Applied and Environmental Microbiology* **2007**, *73* (20), 6421–6428. https://doi.org/10.1128/AEM.01051-07/ASSET/BA8673F2-069C-49B2-870E-BE546A6FB500/ASSETS/GRAPHIC/ZAM0200782580005.JPEG.
(114) Ahmad, S. A.; Shamaan, N. A.; Arif, N. M.; Koon, G. B.; Shukor, M. Y. A.; Syed, M. A. Enhanced Phenol Degradation by Immobilized *Acinetobacter* Sp. Strain AQ5NOL 1. *World Journal of Microbiology and Biotechnology* **2012**, *28* (1), 347–352. https://doi.org/10.1007/s11274-011-0826-z.
(115) Klöck, G.; Pfeffermann, A.; Ryser, C.; Gröhn, P.; Kuttler, B.; Hahn, H.-J.; Zimmermann, U. Biocompatibility of Mannuronic Acid-Rich Alginates. *Biomaterials* **1997**, *18* (10), 707–713. https://doi.org/10.1016/S0142-9612(96)00204-9.
(116) Mi, F.-L.; Sung, H.-W.; Shyu, S.-S. Drug Release from Chitosan–Alginate Complex Beads Reinforced by a Naturally Occurring Cross-Linking Agent. *Carbohydrate Polymers* **2002**, *48* (1), 61–72. https://doi.org/10.1016/S0144-8617(01)00212-0.
(117) *Kelco Algin : Hydrophilic Derivatives of Alginic Acid for Scientific Water Control.*, 2nd ed.; Clark N.J. (75 Terminal Avenue Clark N.J. 07066), 1976.
(118) Matsumoto, T.; Kawai, M.; Masuda, T. Influence of Concentration and Mannuronate/Gluronate Ratio on Steady Flow Properties of Alginate Aqueous Systems. *Biorheology* **1992**, *29* (4), 411–417. https://doi.org/10.3233/BIR-1992-29404.

(119) Wang, B.; Wan, Y.; Zheng, Y.; Lee, X.; Liu, T.; Yu, Z.; Huang, J.; Ok, Y. S.; Chen, J.; Gao, B. Alginate-Based Composites for Environmental Applications: A Critical Review. *Critical Reviews in Environmental Science and Technology* **2019**, *49* (4), 318–356. https://doi.org/10.1080/10643389.2018.1547621.

(120) Klein, J.; Stock, J.; Vorlop, K.-D. Pore Size and Properties of Spherical Ca-Alginate Biocatalysts. *European Journal of Applied Microbiology and Biotechnology* **1983**, *18* (2), 86–91. https://doi.org/10.1007/BF00500829.

(121) Stewart, W. W.; Swaisgood, H. E. Characterization of Calcium Alginate Pore Diameter by Size-Exclusion Chromatography Using Protein Standards. *Enzyme and Microbial Technology* **1993**, *15* (11), 922–927. https://doi.org/10.1016/0141-0229(93)90167-Z.

(122) Sarma, S. J.; Pakshirajan, K. An Immobilized Cell System for Biodegradation of Pyrene by *Mycobacterium Frederiksbergense*. *Polycyclic Aromatic Compounds* **2010**, *30* (3), 129–140. https://doi.org/10.1080/10406631003800662.

(123) Abarian, M.; Hassanshahian, M.; Esbah, A. Degradation of Phenol at High Concentrations Using Immobilization of *Pseudomonas Putida* P53 into Sawdust Entrapped in Sodium-Alginate Beads. *Water Science and Technology* **2019**, *79* (7), 1387–1396. https://doi.org/10.2166/wst.2019.134.

(124) Zhang, K.; Liu, Y.; Luo, H.; Chen, Q.; Zhu, Z.; Chen, W.; Chen, J.; Ji, L.; Mo, Y. Bacterial Community Dynamics and Enhanced Degradation of Di-n-Octyl Phthalate (DOP) by Corncob-Sodium Alginate Immobilized Bacteria. *Geoderma* **2017**, *305*, 264–274. https://doi.org/10.1016/j.geoderma.2017.06.009.

(125) Yi-cheng, W.; Ai-li, Y.; Wei, G.; Hai-yan, F.; Ze-jie, W. Al2O3 Nanoparticles Promote the Removal of Carbamazepine in Water by *Chlorella Vulgaris* Immobilized in Sodium Alginate Gel Beads. *Journal of Chemistry* **2020**, *2020*, 1–6. https://doi.org/10.1155/2020/8758432.

(126) Ying, Z.; Qingyuan, Z.; Chao, N.; Shijie, G.; Zhao, J.; Miao, H.; Bo, C. Biodegradation Of Atrazine By Free And Immobilized Cells Of *Arthrobacter* Sp. Strain DNS10. *Environmental Engineering and Management Journal* **2015**, *14* (4), 819–826. https://doi.org/10.30638/eemj.2015.091.

(127) Zhou, X.; Liu, L.; Chen, Y.; Xu, S.; Chen, J. Efficient Biodegradation of Cyanide and Ferrocyanide by Na-Alginate Beads Immobilized with Fungal Cells of *Trichoderma Koningii*. *Canadian Journal of Microbiology* **2007**, *53* (9), 1033–1037. https://doi.org/10.1139/W07-070/ASSET/IMAGES/LARGE/W07-070F3.JPEG.

(128) Doble, M.; Kumar, A. Degradation of Polymers. In *Biotreatment of Industrial Effluents*; Doble, M., Kumar, A. B. T.-B. of I. E., Eds.; Elsevier: Burlington, 2005; pp 101–110. https://doi.org/10.1016/B978-075067838-4/50010-5.

(129) ben Halima, N. Poly(Vinyl Alcohol): Review of Its Promising Applications and Insights into Biodegradation. *RSC Advances* **2016**, *6* (46), 39823–39832. https://doi.org/10.1039/C6RA05742J.

(130) Stauffer, S. R.; Peppast, N. A. Poly(Vinyl Alcohol) Hydrogels Prepared by Freezing-Thawing Cyclic Processing. *Polymer (Guildf)* **1992**, *33* (18), 3932–3936. https://doi.org/10.1016/0032-3861(92)90385-A.

(131) Hassan, C. M.; Peppas, N. A. Cellular PVA Hydrogels Produced by Freeze/Thawing. *Journal of Applied Polymer Science* **2000**, *76* (14), 2075–2079. https://doi.org/10.1002/(SICI)1097-4628(20000628)76:14.

(132) Muscat, A.; Prüße, U.; Vorlop, K.-D. Stable Support Materials for the Immobilization of Viable Cells. In *Immobilized Cells*; Wijffels, R. H., Buitelaar, R. M., Bucke, C., Tramper, J. B. T.-P. in B., Eds.; Elsevier, 1996; Vol. 11, pp 55–61. https://doi.org/10.1016/S0921-0423(96)80008-6.

(133) Rostron, W. M.; Stuckey, D. C.; Young, A. A. Treatment of High Strength Ammonia Wastewaters Using Immobilized Biomass. In *Immobilized Cells*; Wijffels, R. H., Buitelaar, R. M., Bucke, C., Tramper, J. B. T.-P. in B., Eds.; Elsevier, 1996; Vol. 11, pp 703–709. https://doi.org/10.1016/S0921-0423(96)80095-5.

(134) Partovinia, A.; Naeimpoor, F. Phenanthrene Biodegradation by Immobilized Microbial Consortium in Polyvinyl Alcohol Cryogel Beads. *International Biodeterioration & Biodegradation* **2013**, *85*, 337–344. https://doi.org/10.1016/j.ibiod.2013.08.017.

(135) El-Naas, M. H.; Al-Muhtaseb, S. A.; Makhlouf, S. Biodegradation of Phenol by *Pseudomonas Putida* Immobilized in Polyvinyl Alcohol (PVA) Gel. *Journal of Hazardous Materials* **2009**, *164* (2–3), 720–725. https://doi.org/10.1016/j.jhazmat.2008.08.059.

(136) Bai, X.; Shi, H.; Ye, Z.; Sun, Q.; Wang, Q.; Wang, Z. Degradation of Bisphenol A by Microorganisms Immobilized on Polyvinyl Alcohol Microspheres. *Frontiers of Environmental Science & Engineering* **2013**, *7* (6), 844–850. https://doi.org/10.1007/s11783-013-0487-2.

(137) Liu, N.; Li, H.; Shi, Y.; Zhu, B.; Gao, S. Biodegradation of High Concentration of Nitrobenzene by *Pseudomonas Corrugata* Embedded in Peat-Phosphate Esterified Polyvinyl Alcohol. *World Journal of Microbiology and Biotechnology* **2013**, *29* (10), 1859–1867. https://doi.org/10.1007/s11274-013-1348-7.

(138) He, S.-Y.; Lin, Y.-H.; Hou, K.-Y.; Hwang, S.-C. J. Degradation of Dimethyl-Sulfoxide-Containing Wastewater Using Airlift Bioreactor by Polyvinyl-Alcohol-Immobilized Cell Beads. *Bioresource Technology* **2011**, *102* (10), 5609–5616. https://doi.org/10.1016/j.biortech.2011.02.030.

(139) Cunningham, C. J.; Ivshina, I. B.; Lozinsky, V. I.; Kuyukina, M. S.; Philp, J. C. Bioremediation of Diesel-Contaminated Soil by Microorganisms Immobilised in Polyvinyl Alcohol. *International Biodeterioration & Biodegradation* **2004**, *54* (2–3), 167–174. https://doi.org/10.1016/j.ibiod.2004.03.005.

(140) Siripattanakul, S.; Wirojanagud, W.; McEvoy, J. M.; Casey, F. X. M.; Khan, E. Atrazine Removal in Agricultural Infiltrate by Bioaugmented Polyvinyl Alcohol Immobilized and Free *Agrobacterium Radiobacter* J14a: A Sand Column Study. *Chemosphere* **2009**, *74* (2), 308–313. https://doi.org/10.1016/j.chemosphere.2008.09.005.

(141) Bhatnagar, Y.; Singh, G. B.; Mathur, A.; Srivastava, S.; Gupta, S.; Gupta, N. Biodegradation of Carbazole by *Pseudomonas* Sp. GBS.5 Immobilized in Polyvinyl Alcohol Beads. *Journal of Biochemical Technology* **2016**, *6* (3), 1003–1007.

(142) Han, X.; Huo, P.; Ding, Z.; Kumar, P.; Liu, B. Preparation of Lutein-Loaded PVA/Sodium Alginate Nanofibers and Investigation of Its Release Behavior. *Pharmaceutics* **2019**, *11* (9), 449. https://doi.org/10.3390/pharmaceutics11090449.

(143) Mirzaie, Z.; Reisi-Vanani, A.; Barati, M. Polyvinyl Alcohol-Sodium Alginate Blend, Composited with 3D-Graphene Oxide as a Controlled Release System for Curcumin. *Journal of Drug Delivery Science and Technology* **2019**, *50*, 380–387. https://doi.org/10.1016/j.jddst.2019.02.005.

(144) Yi, X.; Sun, F.; Han, Z.; Han, F.; He, J.; Ou, M.; Gu, J.; Xu, X. Graphene Oxide Encapsulated Polyvinyl Alcohol/Sodium Alginate Hydrogel Microspheres for Cu (II) and U (VI) Removal. *Ecotoxicology and Environmental Safety* **2018**, *158*, 309–318. https://doi.org/10.1016/j.ecoenv.2018.04.039.

(145) Kim, J. O.; Park, J. K.; Kim, J. H.; Jin, S. G.; Yong, C. S.; Li, D. X.; Choi, J. Y.; Woo, J. S.; Yoo, B. K.; Lyoo, W. S.; Kim, J.-A.; Choi, H.-G. Development of Polyvinyl Alcohol–Sodium Alginate Gel-Matrix-Based Wound Dressing System Containing Nitrofurazone. *International Journal of Pharmaceutics* **2008**, *359* (1–2), 79–86. https://doi.org/10.1016/j.ijpharm.2008.03.021.

(146) Kim, J. O.; Choi, J. Y.; Park, J. K.; Kim, J. H.; Jin, S. G.; Chang, S. W.; Li, D. X.; Hwang, M.-R.; Woo, J. S.; Kim, J.-A.; Lyoo, W. S.; Yong, C. S.; Choi, H.-G. Development of Clindamycin-Loaded Wound Dressing with Polyvinyl Alcohol and Sodium Alginate. *Biological and Pharmaceutical Bulletin* **2008**, *31* (12), 2277–2282. https://doi.org/10.1248/bpb.31.2277.

(147) Wang, Q.; Liu, J.; Zhang, L.; Ci, M.; Zhang, X.; Jiang, Z.; Zhu, P. Preparation and Characterization of Polyvinyl Alcohol/Sodium Alginate/Pyrovatex CP Composite Fibers. *Ferroelectrics* **2020**, *562* (1), 125–125. https://doi.org/10.1080/00150193.2020.1760600.

(148) Wang, H. L.; Zuo, Y.; Zhang, L.; Yang, W. H.; Zou, Q.; Zhou, S.; Li, Y. B. Preparation and Characterisation of Nanohydroxyapatite–Sodium Alginate–Polyvinyl Alcohol Composite Scaffold. *Materials Research Innovations* **2010**, *14* (5), 375–380. https://doi.org/10.1179/143307510X12820854748836.

(149) Eghbalifam, N.; Frounchi, M.; Dadbin, S. Antibacterial Silver Nanoparticles in Polyvinyl Alcohol/Sodium Alginate Blend Produced by Gamma Irradiation. *International Journal of Biological Macromolecules* **2015**, *80*, 170–176. https://doi.org/10.1016/j.ijbiomac.2015.06.042.

(150) Nonthasen, K.; Piyatheerawong, W.; Thanonkeo, P. Efficient Entrapment of *Kluyveromyces Marxianus* Dbkkuy-103 in Polyvinyl Alcohol Hydrogel for Ethanol Production from Sweet Sorghum Juice. *Turkish Journal Of Biology* **2015**, *39*, 119–128. https://doi.org/10.3906/biy-1405-43.

(151) Radosavljević, M.; Lević, S.; Belović, M.; Pejin, J.; Djukić-Vuković, A.; Mojović, L.; Nedović, V. Immobilization of *Lactobacillus Rhamnosus* in Polyvinyl Alcohol/Calcium Alginate Matrix for Production of Lactic Acid. *Bioprocess and Biosystems Engineering* **2020**, *43* (2), 315–322. https://doi.org/10.1007/S00449-019-02228-0/TABLES/2.

(152) Hua, X.; Du, G.; Xu, Y. Cost-Practical of Glycolic Acid Bioproduction by Immobilized Whole-Cell Catalysis Accompanied with Compressed Oxygen Supplied to Enhance Mass Transfer. *Bioresource Technology* **2019**, *283*, 326–331. https://doi.org/10.1016/j.biortech.2019.03.094.

(153) Menegatti, T.; Žnidaršič-Plazl, P. Copolymeric Hydrogel-Based Immobilization of Yeast Cells for Continuous Biotransformation of Fumaric Acid in a Microreactor. *Micromachines (Basel)* **2019**, *10* (12), 867. https://doi.org/10.3390/mi10120867.

(154) Lee, J.; Cho, M. H. Removal of Nitrogen in Wastewater by Polyvinyl Alcohol (PVA)-Immobilization of Effective Microorganisms. *Korean Journal of Chemical Engineering* **2010**, *27* (1), 193–197. https://doi.org/10.1007/s11814-009-0330-4.

(155) Chen, W.; Zhang, H.; Zhang, M.; Shen, X.; Zhang, X.; Wu, F.; Hu, J.; Wang, B.; Wang, X. Removal of PAHs at High Concentrations in a Soil Washing Solution Containing TX-100 via Simultaneous Sorption and Biodegradation Processes by Immobilized Degrading Bacteria in PVA-SA Hydrogel Beads. *Journal of Hazardous Materials* **2021**, *410*, 124533. https://doi.org/10.1016/j.jhazmat.2020.124533.

(156) Landreau, M.; You, H.; Stahl, D. A.; Winkler, M. K. H. Immobilization of Active Ammonia-Oxidizing Archaea in Hydrogel Beads. *npj Clean Water* **2021**, *4* (1), 43. https://doi.org/10.1038/s41545-021-00134-1.

(157) Sanjeev Kumar, S.; Kumar, M. S.; Siddavattam, D.; Karegoudar, T. B. Generation of Continuous Packed Bed Reactor with PVA–Alginate Blend Immobilized *Ochrobactrum* Sp. DGVK1 Cells for Effective Removal of N,N-Dimethylformamide from Industrial Effluents. *Journal of Hazardous Materials* **2012**, *199–200*, 58–63. https://doi.org/10.1016/j.jhazmat.2011.10.053.

(158) Wang, P.; Shen, C.; Wang, X.; Liu, S.; Li, L.; Guo, J. Biodegradation of Penicillin G from Industrial Bacteria Residue by Immobilized Cells of *Paracoccus* Sp. KDSPL-02 through Continuous Expanded Bed Adsorption Bioreactor. *J Biol Eng* **2020**, *14* (1), 1–10.

(159) Doria-Serrano, M. C.; Ruiz-Treviño, F. A.; Rios-Arciga, C.; Hernández-Esparza, M.; Santiago, P. Physical Characteristics of Poly(Vinyl Alcohol) and Calcium Alginate Hydrogels for the Immobilization of Activated Sludge. *Biomacromolecules* **2001**, *2* (2), 568–574. https://doi.org/10.1021/bm015514k.

(160) Dave, R.; Madamwar, D. Esterification in Organic Solvents by Lipase Immobilized in Polymer of PVA–Alginate–Boric Acid. *Process Biochemistry* **2006**, *41* (4), 951–955. https://doi.org/10.1016/j.procbio.2005.10.019.

(161) Horzmann, K. A.; Freeman, J. L. Making Waves: New Developments in Toxicology With the Zebrafish. *Toxicological Sciences* **2018**, *163* (1), 5–12. https://doi.org/10.1093/toxsci/kfy044.

(162) Bailey, J.; Oliveri, A.; Levin, E. D. Zebrafish Model Systems for Developmental Neurobehavioral Toxicology. *Birth Defects Research Part C: Embryo Today: Reviews* **2013**, *99* (1), 14–23. https://doi.org/10.1002/bdrc.21027.

(163) Langheinrich, U. Zebrafish: A New Model on the Pharmaceutical Catwalk. *BioEssays* **2003**, *25* (9), 904–912. https://doi.org/10.1002/BIES.10326.

(164) Kimmel, C. B.; Ballard, W. W.; Kimmel, S. R.; Ullmann, B.; Schilling, T. F. Stages of Embryonic Development of the Zebrafish. *Developmental Dynamics* **1995**, *203* (3), 253–310. https://doi.org/10.1002/aja.1002030302.

(165) Brannen, K. C.; Panzica-Kelly, J. M.; Danberry, T. L.; Augustine-Rauch, K. A. Development of a Zebrafish Embryo Teratogenicity Assay and Quantitative Prediction Model. *Birth Defects Res B Dev Reprod Toxicol* **2010**, *89* (1), 66–77. https://doi.org/10.1002/BDRB.20223.

(166) Padilla, S.; Hunter, D. L.; Padnos, B.; Frady, S.; MacPhail, R. C. Assessing Locomotor Activity in Larval Zebrafish: Influence of Extrinsic and Intrinsic Variables. *Neurotoxicol Teratol* **2011**, *33* (6), 624–630. https://doi.org/10.1016/J.NTT.2011.08.005.

(167) Selderslaghs, I. W. T.; van Rompay, A. R.; de Coen, W.; Witters, H. E. Development of a Screening Assay to Identify Teratogenic and Embryotoxic Chemicals Using the Zebrafish Embryo. *Reprod Toxicol* **2009**, *28* (3), 308–320. https://doi.org/10.1016/J.REPROTOX.2009.05.004.

(168) Hurtt, M. E.; Cappon, G. D.; Browning, A. Proposal for a Tiered Approach to Developmental Toxicity Testing for Veterinary Pharmaceutical Products for Food-Producing Animals. *Food and Chemical Toxicology* **2003**, *41* (5), 611–619. https://doi.org/10.1016/S0278-6915(02)00326-5.
(169) Harris, C. Personal Communication Harris, C. 2022.
(170) Truong, L.; Tanguay, R. L. Evaluation of Embryotoxicity Using the Zebrafish Model; Gautier, J.-C., Ed.; Springer New York: New York, NY, 2017; pp 325–333. https://doi.org/10.1007/978-1-4939-7172-5_18.
(171) Köktürk, M.; Çomaklı, S.; Özkaraca, M.; Alak, G.; Atamanalp, M. Teratogenic and Neurotoxic Effects of N-Butanol on Zebrafish Development. *Journal of Aquatic Animal Health* **2021**, *33* (2), 94–106. https://doi.org/10.1002/aah.10123.
(172) Azizian, M. F.; Semprini, L. Aerobic Cometabolism of Chlorinated Solvents and 1,4-Dioxane in Continuous-Flow Columns Packed with Gellan-Gum Hydrogels Coencapsulated with ATCC Strain 21198 and TBOS or T2BOS as Slow-Release Compounds. *ACS ES&T Engineering* **2022**. https://doi.org/10.1021/acsestengg.2c00023.
(173) Vancheeswaran, S.; Halden, R. U.; Williamson, K. J.; Ingle, J. D.; Semprini, L. Abiotic and Biological Transformation of Tetraalkoxysilanes and Trichloroethene/Cis-1,2-Dichloroethene Cometabolism Driven by Tetrabutoxysilane-Degrading Microorganisms. *Environmental Science and Technology* **1999**, *33* (7), 1077–1085. https://doi.org/10.1021/es981021k.

APPENDICES

A.1. Batch Reactor Acetylene Control Results

For the T2BOS gellan gum bead batch reactors, duplicate acetylene controls were created and monitored throughout the incubation period. Acetylene acts to inhibit the monooxygenase enzyme responsible for aerobic cometabolism of dioxane and *c*DCE. The results for these batch reactors are presented in Figure A.1. Dioxane and *c*DCE slightly decreased throughout the incubation period, but the lack of *c*DCE epoxide generation indicated this was likely not due to aerobic cometabolism. Steady oxygen consumption suggested that the 21198 microbial population was still alive in the reactors throughout the incubation period, despite the lack of contaminant transformation.

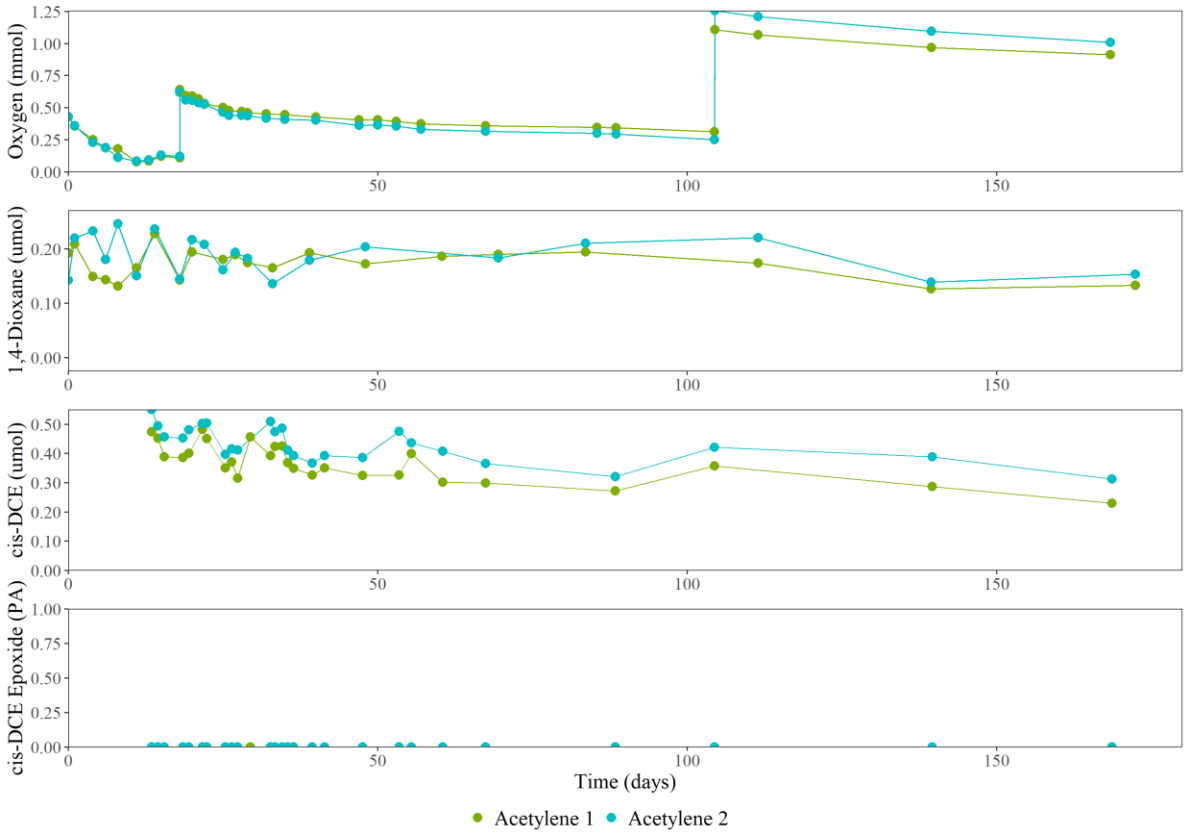

Figure A.1. Oxygen, dioxane, and *c*DCE mass histories and *c*DCE epoxide peak area histories measured in the T2BOS gellan gum acetylene control batch reactors.

The total oxygen consumption for these batch reactors is presented in Figure A.2. Compared to the non-control reactors, oxygen consumption remained significantly more consistent. This suggests that the biomass within the acetylene control reactors was larger in the later stages of incubation than in the non-control reactors. This may have been due to a lack of exposure to *c*DCE epoxide, which is potentially harmful, or due to less exposure to contaminants on a total mass basis.

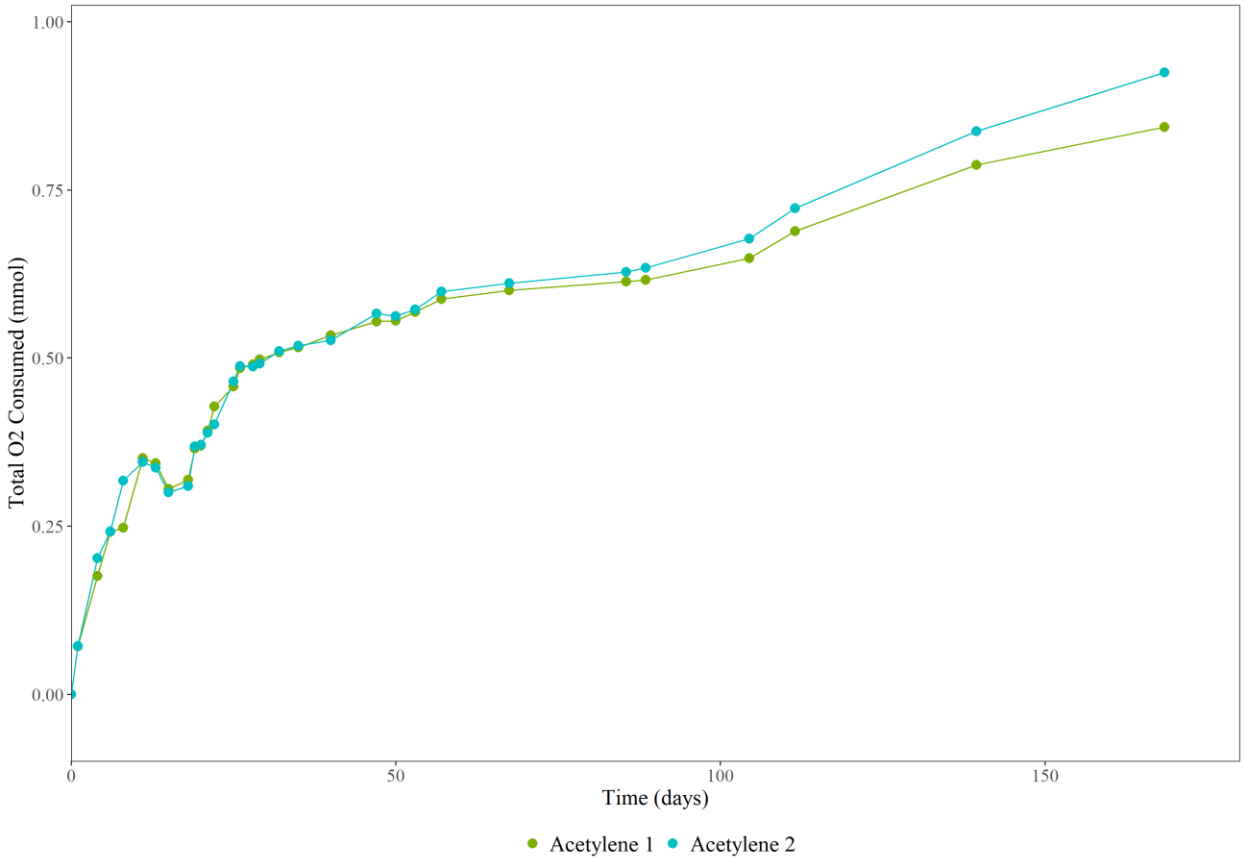

Figure A.2. Total oxygen consumed by the T2BOS gellan gum acetylene control batch reactors over time.

A.2. T2BOS Gellan Gum Bead Column Streak Plating

Due to a darkened spot becoming visible in the later stages of the T2BOS gellan gum bead column operation, liquid sampled from the column influent and column effluent sections was streak plated onto TSGA plates and incubated at 30°C as a way to check for contamination. The results from these streak plates are pictured in Figure A.3. Orange tinted growth is evident, which is indicative of 21198 growth, but the results overall are inconclusive as to whether there was contamination due to a lack of individual colonies.

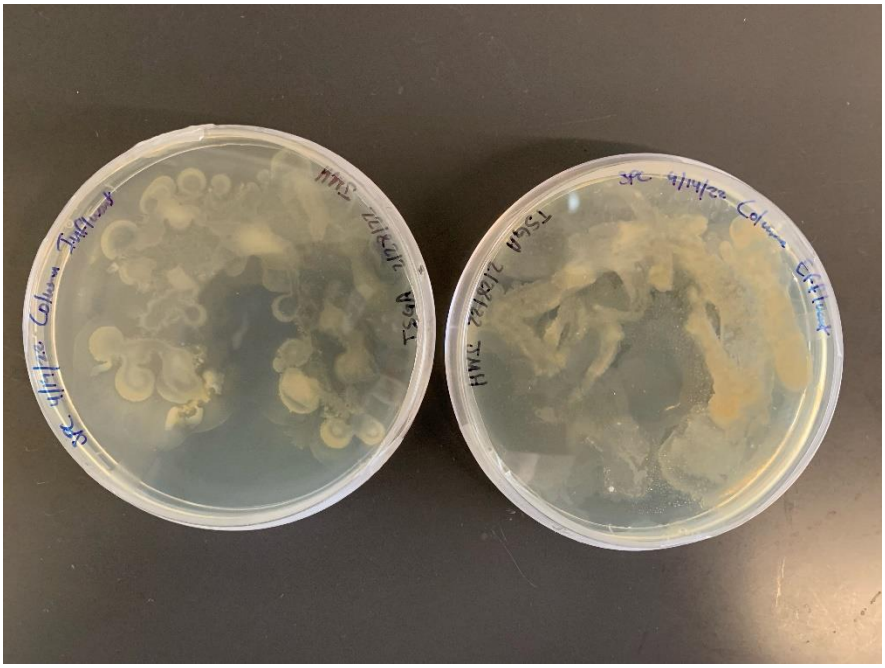

Figure A.3. Pictures of streak plating onto TSGA plates of liquid taken from the column influent section (left) and the column effluent section (right).